Contrails

FOREWORD

This report was prepared by Arthur D. Little, Inc., under USAF Contract No. AF 33(616)-7472. This contract was initiated under Project No. 7350, "Ceramic and Cermet Materials Development", Task No. 735001, "Non-Graphitic". The work was administered under the direction of the Metals and Ceramics Laboratory, Directorate of Materials and Processes, Aeronautical Systems Division, with Mr. Fred W. Vahldiek acting as project engineer.

This report covers work conducted from January through December 1962.

Portions of the work reported herein were carried out under subcontracts with Arthur D. Little, Inc., as acknowledged in the text.

Approved for Public Release

Contrails

Approved for Public Release

Contrails

ABSTRACT

Studies during 1962 are reported on a program to provide the thermodynamic and kinetic data which are required to describe the chemical behavior of the zirconium and hafnium carbides and borides at temperatures to 3000K and in atmospheres of O_2, $O_2 + H_2O$, Cl_2, HF, F_2, H_2, CO, NH_3, and N_2.

Preparation of high purity ZrC, ZrO_2, HfB_2, and HfC are described. Experimental low temperature heat capacity data for ZrC and heat content data for ZrB_2 from 410-1126K are presented. Current status of calorimetric, electron diffraction, equilibria, and spectroscopy studies are reported.

Kinetic studies are described on the oxidation of ZrC from 550-650C at one atmosphere oxygen pressure and from 850-1900C at oxygen pressures of 3-26 Torr, on the oxidation of ZrB_2 for the conditions 1200-1500C and oxygen pressure of 7-38.75 Torr and 945-1256C at oxygen pressures up to one atmosphere, and on the fluorination of ZrC and ZrB_2. The results of metallographic examination of the oxidized ZrC and ZrB_2 samples are discussed. Electrical conductivity studies are reported on pure ZrO_2 from room to 1700C. The oxidation kinetics of molybdenum metal were studied in the temperature range 1400 to 2000K and oxygen pressures of 10^{-5} to 10^{-6} atmospheres using a mass spectrometer with necessary source modifications.

This technical documentary report has been reviewed and is approved.

W. G. RAMKE
Chief, Ceramics and Graphite Branch
Metals and Ceramics Division
Air Force Materials Laboratory

Approved for Public Release

Contrails

TABLE OF CONTENTS

Approved for Public Release

Contrails

TABLE OF CONTENTS (Continued)

Approved for Public Release

Contrails

LIST OF FIGURES

Approved for Public Release

Contrails

LIST OF FIGURES (Continued)

Approved for Public Release

Contrails

LIST OF TABLES

Approved for Public Release

Contrails

LIST OF TABLES (Continued)

Approved for Public Release

Contrails

Approved for Public Release

Contrails

I. INTRODUCTION

There is an increasing demand in our technology today for structural materials to withstand high temperatures, steep temperature gradients, and corrosive atmospheres. The zirconium and hafnium carbides and diborides are among the highest melting point materials known. These materials can be more readily evaluated for specific engineering applications if we have the fundamental thermodynamic and kinetic knowledge which permits predictions of their chemical behavior.

The purpose of this program is to obtain thermodynamic and kinetic information which is necessary for the theoretical considerations on the use of these materials at temperatures to 3000K and in atmospheres of oxygen, oxygen plus water, chlorine, hydrogen fluoride, fluorine, hydrogen, carbon monoxide, ammonia, and nitrogen.

To achieve this purpose, a technical program was developed which can (1) provide all additional thermodynamic data on the carbides and borides of zirconium and hafnium necessary for tabulation of their free energy functions over a temperature range of 3000K; (2) identify gaseous species formed either on vaporization of these carbides and borides or on their interaction with the several atmospheres of interest; (3) provide thermodynamic data for important gaseous species; (4) develop an understanding of the kinetics of the reactions of the carbides and borides with the various atmospheres.

The materials problem and the technical problem were discussed in detail in Technical Documentary Report ASD-TDR-62-204, Part I, which presented work under this contract for the period July 1, 1960, to December 31, 1961.

This report presents the progress and accomplishments of the studies under this program for the period January 1 to December 31, 1962.

Manuscript released by the author May 1963 for publication as an ASD Technical Documentary Report.

Approved for Public Release

Contrails

II. SUMMARY

A. ACCOMPLISHMENTS

1. Materials Preparation

Preparation of high purity macrocrystalline zirconium carbide by the zone-melting technique was completed and samples furnished for the various calorimetric and kinetic studies. Analysis showed the material to be $Zr_{1.00}C_{0.96}$ with the principal contaminants B and N in atom fractions per Zr atom being 0.007 and 0.005 respectively. The principal metallic contaminants are Ti and Fe in atom fractions per Zr atom of 0.0026 and 0.0014 respectively.

Boules of ZrO_2 were prepared for the mass transport studies from powdered ZrO_2 using a modified Verneuil method in an ADL-Strong arc-imaging furnace. The boules resulting from the fusion of the ZrO_2 provided a dense and polycrystalline material from which samples could be cut for the conductivity studies.

High purity macrocrystalline hafnium diboride was prepared by the zone-melting technique. The average formula of the product is indicated by analysis to be $Hf_{1.00}B_{2.02}$ with the principal contaminants in atom fractions per Hf atom being 0.026C, 0.006N, 0.00055Zr, and 0.00032 O. This material is in Professor Westrum's laboratory for low temperature heat capacity measurements and will be distributed to other workers shortly.

Techniques for preparing the desired hafnium carbide samples are being studied. Experimental work with the zone-melting technique and with an arc-melting procedure are discussed.

2. Thermodynamic Studies

The present status of thermodynamic studies completed and in progress on the carbides and borides was reviewed and the existing data evaluated in terms of the objectives of this program.

Low temperature heat capacity measurements from 5 to 350K were completed on ZrC by Professor Westrum at the University of Michigan (see Appendix C). Argonne National Laboratory completed a series of measurements in the fluorine bomb calorimeter on the ZrB_2 sample supplied them from material prepared under this program. This work will be published when final calculations are completed. Under Professor Margrave's direction at the University of Wisconsin (see Appendix B), the heat contents of the high purity ZrB_2 sample have been measured from 410-1126K. These data together with Professor Westrum's low temperature data on the same material were used to select Einstein-Debye functions from which smoothed thermodynamic functions were tabulated for 0-2000K, the data above 1200K representing an extrapolation. Similar heat content measurements from 366 to 1212K were completed on the high purity ZrC material and the data are now being processed.

Approved for Public Release

Contrails

Professor Bauer, Cornell University, attempted to obtain electron diffraction photographs of hafnium tetrachloride and zirconium tetrabromide (see Appendix E). The results were not successful and difficulties may have been due to two factors. Sample purity was much lower than originally believed. Facilities for purification were constructed and the materials purified by repeated sublimations. The second factor was that the MX_4 compounds could not be handled in the existing nozzles. It was necessary to design a new high temperature nozzle suitable for these vapors. It is made of Inconel and platinum, is designed to operate from room temperature to 450C, and can be loaded in a dry box. This device has been vacuum tested and test data are expected shortly.

Professor Robert Freeman's program at Oklahoma State University has as its objective providing thermodynamic data on the subhalides of zirconium and hafnium. Progress is reported (see Appendix A) on development of equipment for study of the disproportionation equilibria. During this year, primary effort was on development of an alternative technique to that originally proposed. Status of this work is presented. Effort was initiated on procurement and preparation of the halides required for the studies. Experiments and apparatus for solution calorimetry were designed.

Professor Otto Schnepp, Technion Institute, continued studies on the applicability of matrix isolation techniques to the spectroscopic studies of high temperature gaseous species (see Appendix D). During this year, the infrared study region was extended to 35 microns by fitting cryostat and spectrometer with CsBr windows and prisms. The infrared spectra of vaporization products of LiF and LiCl trapped in solid argon, krypton, xenon, and nitrogen matrices were studied. From the studies to date, it is concluded that the method is most promising but that some further studies are required before it can be said with certainty that the vapor species can be trapped quantitatively. An electron bombardment furnace using a graphite crucible has been tested and temperatures of 1800C were attained. Some modifications are being made which will enable the furnace to reach temperatures above 2000C. The furnace-crucible system is designed for use with the cryostat for matrix isolation studies and will be used for the study of vapor species over ZrO_2 and HfO_2.

3. Kinetic Studies

Work in progress on the oxidation of ZrC is reported by Dr. Berkowitz-Mattuck in Chapter V and Professor John Margrave in Appendix B. Dr. Joan Berkowitz-Mattuck studied the oxidation over the range of 1126-2165K and 3-26 Torr. She reports that oxidation is linear and nonpreferential with a porous and nonadherent oxide obviously growing down grain boundaries and enveloping individual alloy crystallites. In the experiments reported, the rate was limited for the most part by the rate of oxygen availability and no activation energy could be calculated. Professor Margrave and Dr. Kuriakose report on studies at one atmosphere oxygen pressure. They find that a sample begins to crumble at 700C and breaks up into several pieces at about 850C, so that their kinetic studies were limited to a maximum temperature of about 650C. Studies from 554-652C indicated a linear rate law and an activation energy of 16.7±1.7 kcal/mole.

Approved for Public Release

Contrails

The same workers report on work in progress on the oxidation of ZrB_2. In the oxidation of ZrB_2 they find that the rate of reaction does decrease with time and there is evidence that the oxide film is partially protective.
Dr. Berkowitz-Mattuck reports studies from 1500-1805K and 7-38.75 Torr. She finds that after an initial period of about 40 minutes the data can be fitted to a parabolic rate law. Metallographic examination shows that the oxide grows by inward diffusion of oxide, and it is reasonable to suppose that the diffusion of oxygen in the ZrO_2 is the rate controlling step. An activation energy of 66 ± 9 kcal/mole is obtained from the data. Professor Margrave and Dr. Kuriakose report studies from 945 to 1256C and at pressures up to 1 atmosphere of oxygen. They also find that oxidation follows a parabolic rate law and have observed that boron oxide is present as a molten layer on the surface of the oxide.
Dr. Berkowitz-Mattuck found in x-ray examination of her quenched samples lines for monoclinic ZrO_2 with no evidence of extraneous lines. Margrave and Kuriakose report evidence of boron oxide volatility only at the high temperature end of their studies. They report an activation energy of 19.8 ± 1 kcal. In view of the reportedly different nature of the oxide coating in the two studies the lack of agreement for activation energy is not surprising, however we are concerned that boron oxide volatility may have introduced an error in the value reported here by Margrave and Kuriakose and expect that further studies will be required.

Professor Margrave and Dr. Kuriakose report on studies of the reaction of elemental fluorine with ZrC and ZrB_2. Preliminary examination showed that ZrC burns in fluorine or in an atmosphere rich in fluorine at about 250-300C. On the other hand, ZrB_2 did not catch fire at a pressure of 1 atmosphere, but broke into several bits at about the same temperature. Under low partial pressure of F_2, several runs were made on ZrC at temperatures of 278-410C. A linear rate increase with time was observed. Thick scales of poorly adherent ZrF_4 were observed. An activation energy of 22.1 ± 1.6 kcal/mole was calculated. It was necessary to study the fluorination of ZrB_2 under low partial pressures of F_2 at higher temperatures of 500-900C to obtain measurable weight losses. The reaction obeys a linear rate law with volatile reaction products formed. An interesting point observed was that corrosion rate was a maximum at 800C. This phenomenon may be due to the decomposition of ZrF_4 above 800C, but the few experiments are not decisive and further work is needed before drawing any conclusions.

To increase our understanding of the mechanism of oxidation of the carbides and borides, studies on the defect structure and oxygen transport in ZrO_2 are under way. Experimental results to date of electrical conductivity measurements on ZrO_2 up to 1700C are reported and discussed. The possible effect of carbon, boron, and other impurity content on the defect structure and oxygen diffusion are discussed with relation to the oxidation kinetics of ZrC and ZrB_2.

During this report period available time on the mass spectrometer in our Cambridge laboratories was used to study the oxidation kinetics of molybdenum. This study represents a continuation of work initiated under contract AF 33(616)-6154. Studies were carried out in the temperature range 1400 to 2000K at oxygen pressures of 10^{-5} to 10^{-6} atm. The results obtained prove that a solid oxide film does not form on the molybdenum surface during oxidation although solid MoO_2 is stable at these temperatures and pressures. A reaction mechanism is postulated in which the rate of formation of an adsorbed MoO molecule is rate determining. This study has special significance in that it is providing an understanding of the initial steps in the over-all oxidation reaction.

Approved for Public Release

Contrails

B. FUTURE WORK

1. Materials Preparation

The preparation of HfC samples required for the calorimetric, vapor pressure, and kinetic studies will be completed. Small quantities of carbon deficient ZrC and HfC will be prepared for use in vapor pressure and kinetic studies. Additional samples varying in purity or stoichiometry or duplicating those prepared previously will be prepared as required by the experimental program.

2. Thermodynamic Studies

Under Professor Westrum's direction, low temperature heat capacity measurements on HfB_2 and HfC will be completed. If the high purity Hf metal on order is received by midyear, low temperature heat capacity measurements will be completed by the year's end. Under Professor Margrave's direction, heat content studies will be extended to higher temperatures on the ZrB_2 and ZrC and measurements on HfB_2 and HfC will be carried out over the total temperature range of their apparatus. A HfC sample will be delivered to Dr. K. K. Kelley of the U. S. Bureau of Mines so that it may be incorporated within his program of study on heats of formation of carbides. A similar sample of HfB_2 will be given to Dr. Ward Hubbard of Argonne National Laboratory for inclusion in his program utilizing the fluorine bomb calorimeter for determination of heats of formation.

Completion of the above calorimetric studies will provide an experimental basis for free energy function tabulations to 2000K for the zirconium and hafnium carbides and borides. During the next year under this program, vapor pressure studies of the carbides and borides will be carried out under the direction of Dr. Paul Blackburn. Data from the literature plus data obtained in these studies will provide an experimental basis for extension of the free energy function tabulations of the carbides and borides to 3000K. In addition, we anticipate that the studies completed during the year will provide some knowledge of activity variation over the range of stoichiometry for the carbides and borides. These data can help to relate observed kinetic or equilibria behavior as a function of composition to thermodynamic properties. Existing mass spectrometry studies on TiC and ZrB_2 together with other vaporization studies on the compounds of interest provide convincing evidence that these borides and carbides vaporize to their elements. Therefore, since the vapor species are recognized, we intend to make the studies utilizing a continuous recording microbalance technique. Both Langmuir and Knudsen methods will be utilized as vapor sources as required or warranted by the studies.

Professor S. H. Bauer expects to complete electron diffraction studies under way on ZrF_4, $HfCl_4$, and HfF_4 to establish their structures. The data from this study when combined with other reported structure and spectral data will permit more reliable statistical thermodynamic calculations for the gaseous zirconium and hafnium tetrahalides. Professor R. D. Freeman will continue his program to determine chemical thermodynamic data for the subhalides of zirconium and hafnium. These studies include measurements of disproportionation equilibria, vapor pressures, and heats of solution. These studies of Drs. Bauer and Freeman will provide more reliable thermodynamic information on the zirconium and hafnium halides which are important gaseous products in the reactions of the carbides and borides of these elements with halogen-containing atmospheres.

Approved for Public Release

Contrails

Professor Otto Schnepp will complete studies during the next year on the applicability of matrix isolation techniques to the spectroscopic study of high temperature gaseous species. The technique will be applied to the study of vapor species over ZrO_2 and HfO_2. We can expect such molecules to be important gaseous products in the oxidation of ZrB_2 and ZrC at very high temperatures and these studies will help provide needed thermodynamic data.

3. Kinetic Studies

Kinetic studies on the oxidation of ZrC and ZrB_2 under the direction of Dr. Joan Berkowitz-Mattuck and Professor John Margrave will be completed. Similar studies of HfC and HfB_2 will be carried out during the year. The effect of water vapor on the oxidation reaction will be determined, and, if time permits, the reactions with nitrogen will be explored.

The kinetic studies on the reactions of zirconium and hafnium carbides and borides with elemental fluorine and fluorine-containing atmospheres will be continued under the direction of Professor John Margrave.

Studies on the defect structure and oxygen transport in tetragonal ZrO_2 through electrical conductivity measurements will be completed. The effect of various impurities on oxygen transport will be explored.

Approved for Public Release

Contrails

III. EVALUATION OF THERMOCHEMICAL STUDIES*

One objective of this program is to provide additional data required for free energy function tabulations of the zirconium and hafnium carbides and borides. Thus, in order to direct the program a knowledge and familiarity with the thermodynamic studies on these compounds is required. In this chapter we review and comment on existing and current thermochemical work which may be required in developing and using the free energy function tabulations.

Phase, heat capacity, heat content, heat of formation, vapor pressure and equilibria studies are covered. Free energy function tabulations can be developed from calorimetric heat capacity and heat of transition data. For the use of these data we require standard heats of formation of the compounds. Required thermodynamic data can also be obtained from equilibria studies of processes such as vaporization. The latter approach has been particularly valuable at high temperatures where calorimetric techniques become very difficult. Since the compounds, especially the carbides, exist over a wide range of stoichiometry, we also require knowledge of phase relationships and are interested in activity variations with stoichiometry.

In reading this chapter, one can note the difficulties faced in evaluating the existing data because of the frequent lack of adequate analytical knowledge of the materials which were studied. Note also the difficulties various workers have faced in determining the actual vaporization process being studied.

A. ZIRCONIUM CARBIDE

1. Phase Relationships

Work to 1957 was reviewed by Hansen and Anderko (1958).[1] More recently, E. K Storms (1962)[2] has reviewed the literature data on group 4a carbides and in his review has presented unpublished data from the Los Alamos Laboratory by Farr. Sara and Dolloff (1962)[3] at the Parma Laboratory of National Carbon Company are currently studying the zirconium-carbon system.

ZrC is the only compound in the zirconium-carbon system. Its structure is face-centered-cubic of the NaCl (B1) type. Sara and Dolloff find that the melting point is a maximum at 3420C for a composition of 46 atomic percent carbon. The review of Storms reports that Farr found a maximum melting point at 3400±50C for a composition of 45 atomic percent carbon.

The ZrC phase exists over a range of stoichiometry. Benesovsky and Rudy[4] report a homogeneity range of 35 to 50 atomic percent carbon from studies at 1550. Sara and Dolloff[3] report that the zirconium-rich boundary is located at 38.5 atomic

* - Prepared by L. A. McClaine and John Engelke, Arthur D. Little, Inc.

Approved for Public Release

Contrails

percent carbon and is invariant with temperature in the region 1900 to 3300C. The carbon-rich boundary between the temperatures of 2850-3300C is located at 48.9 atomic percent carbon. Farr is reported[2] to have found the range of homogeneity to be from 35 to 49.1 atomic percent carbon at 2850C and 35 to 49.5 atomic percent at 2400, indicating a closer approach to stoichiometry at lower temperatures. Neither of the last two studies has been published in final form at this time, but the agreement of the data available and the apparent care with which the studies are being made indicate that the phase relationships will be reasonably well established by these studies.

2. Calorimetric Studies

The only low temperature heat capacity study has been that of Westrum as a part of this program (see Appendix C). The material was prepared by George Feick for this program and was 3.5% by weight deficient in carbon as compared to the theoretical content for stoichiometric ZrC. In view of the phase studies discussed above, this is not surprising. The material with its impurity content included corresponded to a formula of $Zr_{.995}(Ti_{.0026}Fe_{.0013})C_{.958}(O_{.00032}N_{.0049}B_{.0067})$. Thus the material is essentially $ZrC_{.96}$ with about .01 atom fraction additional of (N+B) and must represent material very close to if not at the carbon-rich boundary of the ZrC phase region under the high temperature conditions at which it was prepared.

Professor Margrave is currently determining high temperature heat contents on the same material as a part of this program. Margrave reported data from 350-1200K on a ZrC powder supplied by The Carborundum Corporation in Part I of this report published April 1962. No analysis was obtained. Southern Research Institute[5] has recently determined heat contents from 600 to 2900K by a drop calorimeter technique on material supplied by General Electric Company. No analyses were presented. Avco Corporation[6] has recently reported specific heat measurements by a pulse heating technique in the range of 1600 to 2500K. Their sample material contained about 5% by weight of impurities, had a weak x-ray pattern of ZrB_2 in addition to that for ZrC and was reported to contain free carbon. In their report, they compared their specific heat data with values calculated from Margrave and Southern Research Institute studies. Their values appear 50% or more higher than the other studies. Margrave's data are about 10% greater than those of Southern Research Institute. Southern Research Institute and Margrave have exchanged similar samples of ZrB_2 and established that the differences between their work on ZrB_2 are real and must be due to differences in sample material. In view of the lack of analytical data for the samples studied by Margrave and Southern Research Institute and the known high impurity content in the sample studied by Avco Corporation, no real conclusions can be drawn with regard to these studies. The Arthur D. Little, Inc., sample now under study by Professor Margrave under this program has less than 0.4% by weight of impurities and the results should provide more definitive heat content data.

A value for the heat of formation was determined from heat of combustion studies by Mah and Boyle.[7] Their sample analyzed 88.15% Zr and 11.07% C The unaccounted-for remainder was attributed to O and N picked up in preparation and their results were calculated accordingly. This method of obtaining the impurity content by difference is the factor which makes it difficult to assess the accuracy

Approved for Public Release

Contrails

of the derived data. A small error in the Zr content would markedly change the assumed impurity content. In the Arthur D. Little, Inc., sample material, we have attempted to quantitatively determine the impurity content and little reliance has been placed on the zirconium analysis. A portion of the Arthur D. Little, Inc., material has been given to Dr. K. K. Kelley for inclusion in his program as time permits so that a check may be obtained on the existing value of Mah and Boyle.

3. Equilibrium Studies

Prescott[8] in 1927 reported measurements of pressures of CO over ZrO_2, graphite, and ZrC in the temperature range 1880 to 2015K. More recently, Kutsev, Ormont, and Epelbaum[9] carried out a similar study in the range 1814 to 2020K, but obtained pressures approximately half those of Prescott. On the basis of x-ray diffraction examinations and chemical analyses, they concluded that they had been studying the reaction

$$ZrO_2 + 2.63\ C = ZrC_{0.71}\ O_{0.08} + 1.92\ CO$$

If true, definitive data for ZrC can not be obtained from study of this reaction. However, this data may be useful in determining the effect of O substitution on thermodynamic properties of ZrC once good data is available for ZrC as a function of stoichiometry.

4. Vapor Pressure Studies

Several laboratories have reported vapor pressure studies on ZrC. We will discuss these in two groups. In the first group for discussion, an excess of carbon is present and thus the reaction under study is:

$$ZrC(s) = Zr(g) + C(s)$$

Pollock[10] reports a Knudsen cell study of this reaction at three temperatures from 2620 to 2730K. Vidale[11] reports a study at 2740K on spectral absorption in the vapor of this system which checks very well with data from Pollock's study. We have one other reference to work at Pennsylvania University[12] using graphite Knudsen cells which should also contribute data for this reaction, but we have not yet obtained a copy of their report for examination.

The second group of vaporization studies is that using the Langmuir technique in which the stoichiometry of the solid may vary during the study unless a composition of the solid corresponding to congruent vaporization is present. Workers at General Electric[13] have determined vapor pressures of C and Zr over a ZrC sample from 2250 to 2900K. Data of Pollock[10] using a Langmuir technique in studies from 2641 to 2747K agree very well with the data of the General Electric workers. These vapor pressure data are more than an order of magnitude different from those obtained in the Knudsen cell studies. In reviewing these two Langmuir studies, the following points can be made. (1) Both groups found a preferential loss of carbon. Sample analyses showed an increasing variation from stoichiometry with increasing total percent weight loss. (2) At the same time both groups found an increased

Approved for Public Release

Contrails

lattice constant for the sample surface material. On the basis of this data and in the face of the preferential carbon loss, both groups postulated essentially stoichiometric ZrC at the surface and assumed that sample inhomogeneity existed in order to account for the low total carbon content found. (3) In our opinion these assumptions are unrealistic. Studies of lattice constants[2,3] have indicated that the maximum value may be reached at compositions considerably below stoichiometry. Impurities also affect lattice constant value and the observed increase and inhomogeneity in the lattice constant of the sample was more likely due to preferential loss of impurities such as O or N at the surface. (4) It seems unlikely to us that free carbon could still exist after the long heating periods in contact with the extremely carbon deficient carbide phase required by the General Electric workers to interpret their free and combined carbon analyses. In our opinion, it is more likely that all the carbon is combined carbon and on this basis the General Electric samples represent $ZrC_{.93}$. Pollack reported only total carbon, and if we again assume no sample inhomogeneity his samples have a composition of about $ZrC_{.88}$. Without approaching such stoichiometry from a study using initially a lower carbon content sample, it is impossible to say that a congruent vaporization composition has been reached by these workers. In our opinion, these data should be viewed as representing vapor pressures over a sample corresponding to about $ZrC_{.9}$.

Additional Langmuir studies have been reported by Bolgar et al.[14] Pollack[10] reported that their vapor pressures differ by a factor of 1000 from those discussed here, and we have not examined personally this particular reference.

B. HAFNIUM CARBIDE

1. Phase Relationships

The work has not been as extensive as that for ZrC. HfC was included in the recent review by E. K. Storms (1962)[2] who also reports on unpublished work in progress at Los Alamos Laboratory by N. K. Krikorian.

HfC is the only compound in the Hf-C system. Its structure is face-centered-cubic ($NaCl_4$ type). Melting point was reported in 1930 as 3887C. Benesovsky and Rudy (1960)[4] reported the HfC phase limits from studies at 1550C as 37 to 50 atomic percent carbon. Further phase studies on this system are currently under way at Los Alamos Laboratory.

2. Calorimetric Studies

No low temperature heat capacity studies have been reported. Such studies are planned under this program by Professor Westrum on material now being prepared.

Neel et al (1962)[5] at Southern Research Institute have reported heat content studies from 600-2900K on HfC samples from The Carborundum Company. No analytical data were presented. Under this program we expect that Professor Margrave will complete heat content studies on adequately defined HfC material during 1963.

Approved for Public Release

Contrails

No heat of combustion measurements have been reported on HfC. When our material preparation is completed we will be able to supply interested workers with samples for calorimetric studies which can provide heat of formation data.

3. Equilibrium Studies

Zhelankin et al[15] have reported equilibrium studies on the reduction of HfO_2 by carbon.

4. Vapor Pressure Studies

Bolgar and co-workers[14] have reported Langmuir method studies of HfC. Their data for other materials are considerably higher than the accepted values and thus little reliability should be placed on their data for HfC. Langmuir method studies are in progress by the General Electric group which has studied ZrC.[13] We plan some Knudsen cell studies under this program in 1963.

C. ZIRCONIUM DIBORIDE

The current interest in the refractory diborides is reflected by the large number of investigations which are under way and which have been, or soon will be, completed. Zirconium diboride, in particular, has reached the stage where we must evaluate the experimental results and attempt to resolve discrepancies resulting from variations in method, material, or interpretation.

1. Low Temperature Heat Capacity

The only low temperature data available on ZrB_2 are those obtained by Westrum[16] as a part of this program. His careful attention to detail and the use of a high purity fused sample prepared by George Feick[17] are indications that the values of $H^\circ_{298} - H^\circ_o = 1.590$ kcal/mole and $S^\circ_{298} = 8.59$ eu derived from the heat capacity measurements will not soon be replaced.

2. High Temperature Heat Capacity

Several laboratories have recently reported data on the high temperature heat capacity of zirconium diboride. The accuracy of these data and the related thermal functions, $(H^\circ_T - H^\circ_{298})$ and $(F^\circ_T - H^\circ_{298})/T$, have not yet been fully evaluated. Some of the variations in results are undoubtedly due to sample purity, but no information on sample impurity is reported by several investigators. Bender et al[6] at Avco Corporation have measured the heat capacity from 1750K to 2500K on a sample containing about 4% of impurity and a B/Zr ratio of 1.8. The results are unreasonably high. In Appendix B of this report, Margrave et al review the various work and in Table B-3 clearly demonstrate the variation that has been obtained on different samples by different workers. The lower enthalpy values for the Arthur D. Little, Inc., material compared with the earlier University of Wisconsin

Approved for Public Release

Contrails

data as reported by Barnes et al[18] and results of other workers may well be the result of a low impurity content. We believe impurity content to be less than 0.1% by weight for this material.

A recent JANAF Thermochemical Data supplement[19] utilized unpublished results by H. Prophet (Dow Chemical Co., 1962) on ZrB_2 heat capacity between 1300K and 2150K. The tabulated thermal data, however, are based on an unfortunate estimate of S°_{298} and heat capacity to 1300K obtained by comparison with TiB_2.

Kaufman[20] has devised a semi-empirical approach to the evaluation of diboride thermal functions. He assumes that a three parameter, modified Debye theory can adequately represent the heat capacity, viz., the electronic specific heat coefficient, γ , and the Debye Θ's for the individual atoms in the compound. Since the two Θ's are assumed to be related by the square root of the molecular weight ratio, only two parameters are adjustable. Kaufman uses Westrum's[16] heat capacity data on ZrB_2 to evaluate these parameters. The heat capacity measurements of Barnes et al[18] are in agreement with his calculated values, but the more recent results on the Arthur D. Little, Inc., sample reported by Margrave in Appendix B are lower than the calculated values. A result of Kaufman's paper,[20] which will be tentatively useful until reliable thermal functions are tabulated, is that $(\Delta F^\circ_T - \Delta H^\circ_{298}) = 10$ kcal/mole at 2400K for the formation of ZrB_2 from the elements in their standard state. This is certainly to be preferred over the usual Kopp-Neumann assumption that $\Delta C^\circ_p = 0$ (and therefore that $\Delta F^\circ_T = \Delta H^\circ_T = \Delta H^\circ_{298}$).

3. Heat of Formation

The heat of formation, as derived from calorimetric measurements on the one hand and from vaporization studies on the other, has been the focal spot for much of the controversy in thermochemical discussions of the borides in general and zirconium diboride in particular. In addition to the experimental difficulties, problems of interpretation arise in both types of investigation. Combustion calorimetry requires precise information on the state of the combustion products. The fluorine bomb calorimeter is a significant improvement in this regard since the reaction product is BF_3 (gas) rather than an ill-defined B_2O_3 glass.

The ΔH°_{298} as derived from heat of combustion measurements in oxygen are -76.7 ± 1.5[21] and -75.02 3.25 kcal/mole.[22] Recently completed work at Argonne National Laboratory using the fluorine bomb calorimeter[23] on a sample from the same batch of high purity zirconium diboride used by Westrum indicates a value for the heat of formation of -71.5 kcal/mole. However, it should be emphasized that this value is a result of a preliminary reduction of data and may be modified before publication.

Several factors appear to be responsible for the difficulty in deriving heats of formation from the vaporization data. The Kopp-Neumann assumption discussed in the previous section is probably the most serious. Uncertainty in the exact reaction occurring in the vaporization process can also be significant. Although we are confident that vaporization of the borides occurs by decomposition to the elements, the boron to zirconium ratio in the vapor will influence the derived

Approved for Public Release

Contrails

heat of formation. Finally, uncertainties in the heat of vaporization of the elements can be important.

Trulson and Goldstein[24] believe they have compensated for possible instrumental errors in their mass spectrometric study by measuring the vapor pressure of the pure components under conditions similar to those which were used for measurements on zirconium diboride. In this way, they obtain directly a free energy of formation at about 2400K of -59 kcal/mole. The Kopp-Neumann rule would indicate the same value for the heat of formation. On the other hand, by using Kaufman's[20] free energy functions one obtains ΔH^{o}_{f298} = -69 kcal/mole, in fair agreement with the calorimetric values.

Leitnaker, Bowman and Gilles[25] reported on the Knudsen vaporization from material thought to have a constant boiling composition of $ZrB_{1.906}$. The effusion rate of Zr(g) from the tungsten cell was measured over the temperature range 2150 to 2475K and the corresponding zirconium partial pressures were derived for a reference temperature of 2000K. Corrections were made for a slightly enhanced vaporization rate due to residual water vapor in the system and for an apparent orifice size effect. The accepted equilibrium partial pressure for zirconium over the constant boiling composition of zirconium diboride at 2000K is $P_{Zr} = 2.378 \times 10^{-10}$ atm. Based on a vaporizing composition of $ZrB_{1.906}$ the $-R \ln K$ is 129.56 eu. With the aid of the Kopp-Neumann assumption, Leitnaker, Bowman and Gilles calculated $\Delta H^{o}_{o} = 458.3 \pm 2.2$ kcal/mole.

It now appears[26] that the constant boiling composition is close to $ZrB_{1.97}$ since initial analytical difficulties prevented a complete analysis for boron.[27] On the basis of the adjusted composition and the equilibrium pressure adopted above, the value of $-R \ln K$ is 132.3 eu for vaporization at 2000K. Margrave's[28] newly derived free energy function value of 24.71 eu when combined with the corresponding values for the gaseous elements[28] leads to $-(\Delta F^{o}_{T} - \Delta H^{o}_{298})/T$ = 107.9 eu, from which we calculate ΔH^{o}_{298} = 480.4 kcal/mole.

A heat of vaporization for zirconium of 146 kcal/mole[28] is accepted. In spite of increasing mass spectrometric evidence[29] for a value of about 130 kcal/mole for the vaporization of boron, the higher value of ΔH^{o}_{298} = 135 kcal/mole,[28] which considered the classical results as well, will be adopted. Combining these values with the heat of vaporization of 480 kcal/mole leads to a heat of formation of $\Delta H^{o}_{f\ 298}$ = -68 kcal/mole, again in fair agreement with calorimetric results.

The only other reported study of zirconium diboride vaporization is that by Wolff and Alcock[30] in which the weight loss from a hot-pressed cube was measured with a microbalance. The equivalent zirconium pressure for this Langmuir vaporization appears to be from one half to one third of the Leitnaker equilibrium pressure. It should be pointed out that a factor of two in zirconium pressure at 2000K corresponds to a difference of 8 kcal/mole in the derived heats of vaporization or formation. Thus Wolff and Alcock's results indicate a third law heat of vaporization of about 488 kcal/mole while their temperature dependence or second law slope indicates a value of only 459 kcal/mole. The possibility of a temperature dependent

Approved for Public Release

Contrails

evaporation coefficient cannot be excluded. Additional work on zirconium diboride is in progress. Linevsky is attempting to apply the atomic resonance line adsorption method.[31] His results should be quite interesting with respect to relative partial pressures at compositions other than that for constant vaporization. Paul Blackburn of this laboratory will also be examining the effect of composition on the individual partial pressures.

C. HAFNIUM DIBORIDE

The amount of thermochemical work that has been completed to date is considerably less for HfB_2 than it is for ZrB_2. The discrepancies do not exist, in part, because measurements have not been duplicated, but also it appears that the corresponding measurements with zirconium paved the way.

Professor Westrum has completed the experimental aspects of the low temperature heat capacity determination on George Feick's high purity, high density hafnium diboride. This material will now be divided between Professor Margrave for high temperature heat capacity measurements and Ward Hubbard's group for fluorine bomb calorimetry. Krupka[32] has measured the partial pressure of hafnium over $HfB_{1.955}$ with an improved version (ultra-high vacuum) of Leitnaker's equipment. An equilibrium value at 2500K of 3.095×10^{-7} atm $\pm$ 10% is given after correcting for an orifice size effect. The Southern Research Institute[33] has measured the high temperature heat capacity. Reliable free energy functions, however, are not yet available but will probably be generated this year. Tentatively, we may accept Kaufman's[20] conclusion that the Kopp-Neumann rule is approximately correct for hafnium diboride. With this reservation, Krupka's value of $\Delta H^{o} = 477.8$ kcal/mole for the vaporization of $HfB_{1.955}$ can be accepted. The heat of formation can be estimated as approximately -68 kcal/mole if the heat of vaporization of hafnium metal is taken to be 146 kcal/mole[34,35] and 135 kcal/mole is again used for boron. This value for the heat of formation can be compared with -74.2 kcal/mole attributed to Paderno,[36] although the uncertainty associated with this value is not known. Paul Blackburn intends to obtain the individual partial pressures, at least for the two-phase regions.

Approved for Public Release

Contrails

IV. MATERIALS PREPARATION*

Most of the experimental work under this program requires the preparation of dense, well-crystallized samples of highly purified refractory compounds. Prior to this report period, all these samples have been prepared by zone melting in a vertical, induction-heated, floating-zone apparatus operating in an inert gas atmosphere at about one atmosphere pressure. This apparatus and the techniques used have been described in previous reports.

During the present report period, in addition to continued work with zone-refining, we have used a modified Verneuil method for the preparation of ZrO_2 boules and have studied the preparation of HfC by arc-melting.

The materials with which we have been concerned during this period are ZrB_2, ZrC, ZrO_2, Hf, HfB_2, and HfC. These are discussed in detail below.

A. ZIRCONIUM DIBORIDE

The preparation and characterization of ZrB_2 have been previously reported. During the present report period, we have obtained nitrogen analyses on a part of the sample used by Dr. Westrum. Duplicate analyses gave 131 ppm and 137 ppm, average 134 ppm of nitrogen. A hydrogen analysis on the same material gave 1.52 ppm.

In addition to providing a supply of ZrB_2 for work under this contract, we have furnished small samples to various interested parties in other organizations as follows: E. S. Domalski, National Bureau of Standards, for evaluation as calorimetric samples; Dr. Milton Linevsky, General Electric Company, Philadelphia, for vapor pressure measurements; Dr. T. F. Lyon, General Electric Company, Flight Propulsion Laboratory, Cincinnati, for Knudsen cell experiments; Dr. H. Goldstein, Union Carbide Research Institute, Tarrytown, New York, for analytical work; Dr. H. B. Probst, NASA, Cleveland, for hot hardness measurements.

B. ZIRCONIUM CARBIDE

The preparation of zone-refined ZrC and metallographic studies of the product have been previously reported. During the present report period, we have completed the preparation of 200 grams of zone-refined ZrC and have furnished samples to Dr. Westrum and to Dr. Margrave for heat capacity measurements. Analytical data on this material is given below.

We have found that by reducing the rate of zone travel to 1" per hour or less, it is possible to produce ZrC in the form of single crystals about 1/4" in diameter. Attempts to repeat this preparation, however, have been only partially successful and indicate that the conditions required for single crystal growth are difficult to reproduce with our apparatus.

* - Prepared by George Feick, Arthur D. Little, Inc., Cambridge, Mass.

Approved for Public Release

Contrails

Analysis of Bar 264-1 gave the following results:

Carbon	11.20%
Zirconium	89.27
Total	100.47%

Three other samples analyzed for carbon gave:

Bar No.	% Carbon
261-1	11.28
270-1	11.15
272-1	11.25

The average carbon content of these four samples was 11.22%, corresponding to a carbon deficiency of 3.5% of the theoretical 11.63%.

The oxygen content was 0.005% (No. 262-3) and the nitrogen content was 0.067% (No. 273-4).

Quantitative spectrographic analysis of one sample gave:

B	0.07%
Fe	0.07%
Ti	0.12%
Si	0.001%

Semiquantitative spectrographic analysis gave:

Al and Sn	0.01%
Mg	0.001 to 0.01%
Ca, Mn, Cu, Mo, Hf, Pb	0.001%

Samples of ZrC have been furnished to other organizations as follows: E. S. Domalski, National Bureau of Standards, for calorimetric studies; Dr. K. K. Kelley, Bureau of Mines, Berkeley, California, for heat of combustion studies; Dr. V. J. de Santis, General Electric Company, Philadelphia, for emissivity measurements; Dr. R. T. Dolloff, National Carbon Co., Parma, Ohio, for measurements of lattice parameter vs. carbon content.

C. ZIRCONIUM OXIDE

Dense, crystalline samples of pure ZrO_2 are needed for diffusion measurements in connection with studies of the oxidation of metallic zirconium and its compounds. Efforts to procure satisfactory material from outside sources and attempts to prepare samples by hydrothermal methods were not successful. We attempted, therefore, the preparation of fused boules of ZrO_2 by means of an ADL-Strong crystal-growing furnace which was made available to the project.

This apparatus operates on a principle similar to the well-known Verneuil process in that the powdered feed is dropped into a molten pool on the top of the

Approved for Public Release

Contrails

growing boule. In our apparatus, however, heat is furnished by the focused image of a high-intensity (150 to 300 ampere) carbon arc rather than by an oxyhydrogen flame. Continuous operation is obtained by providing two arc sources together with a rapid-switching mirror system. A diagram of the optical system is shown in Figure 1.

Using this sytem, we have made six boules of dense but polycrystalline ZrO_2. Some of the samples cracked on cooling, probably because of the phase transition which takes place at about 1200C.

Two types of zirconium oxide were used for these boules. The first was a high-purity oxide obtained from Wah Chang Corporation. Because of its fine particle size, this material was not free flowing and offered some difficulty in the powder feeder.

A free-flowing oxide was made by oxidizing pure zirconium sponge (also from Wah Chang Corporation) at about 800C for several days. The resulting oxide was ball-milled and screened to minus 100 mesh. The product was somewhat less pure and darker in color than the first oxide. The dark color, however, aided the melting process by increased absorption of radiant energy. Analyses of the two materials are given in Table I.

D. HAFNIUM METAL

Numerous unsuccessful efforts to secure a sample of zirconium-free and otherwise pure hafnium metal have been previously reported. We have now found that Wah Chang Corporation is willing to produce one pound of high-grade hafnium electron-beam ingot containing less than 200 ppm of Zr.

Because of production difficulties, the original delivery date of October 1962 has been postponed. Delivery is now scheduled for January 1963.

E. HAFNIUM DIBORIDE

At the time our previous progress report was written, the purest HfB_2 available was made by The Carborundum Company and contained 6000 ppm of Zr. We considered the possibility of making pure HfB_2 from HfO_2 and B_4C, but concluded that this was not practical. We therefore procured a sample of HfB_2 from The Carborundum Company and produced 200 grams of zone-refined bars.

Analysis of this zone-refined material, however, indicated that it was not suitable for precision calorimetry and other studies because of its impurity content and lack of stoichiometry. The major metallic impurities as found by quantitative spectrographic analysis were:

Columbium	0.52%
Tantalum	0.10
Titanium	0.25
Zirconium	0.44

giving a total of 1.31% of major impurities.

Approved for Public Release

Contrails

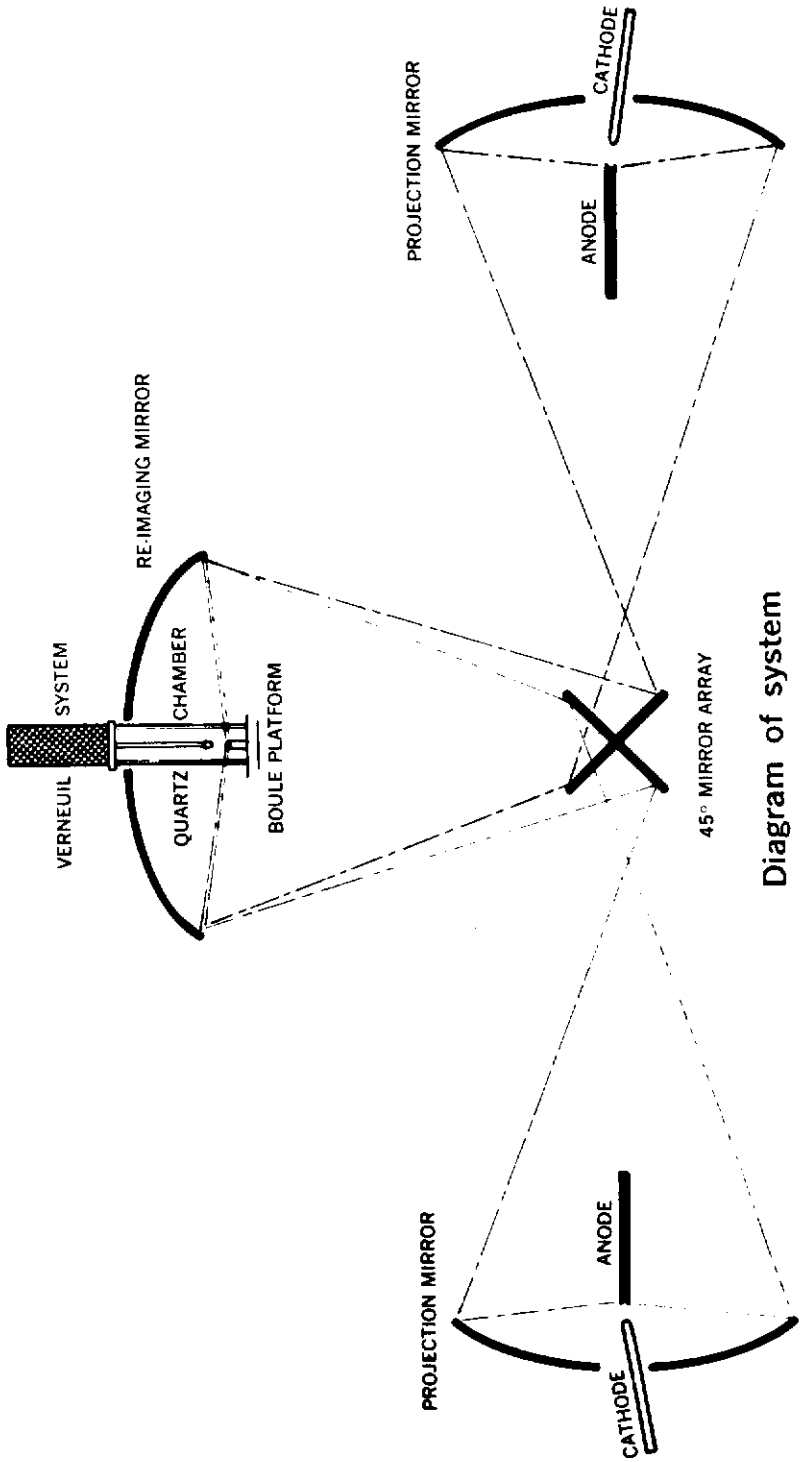

Figure 1. - Optical system of ADL-Strong arc-imaging crystal growing apparatus

Approved for Public Release

Contrails

TABLE I

ZrO_2 ANALYSES

Impurity	Wah Chang ZrO_2 in ppm	ZrO_2 from Metal
Al	125 ppm	.01 to 1.0 %
B	0.2	.001
Cd	0.3	ND
Co	< 5	ND
Cr	<10	.001 to .01
Cu	<25	.001 to .01
Fe	790	.01 to 1.0
Hf	<40	.001 to .01
Mg	30	.001 to .1
Mn	10	.001 to .01
Mo	<10	ND
Ni	< 5	ND
Pb	<5	.001 to .01
Si	40	.01 to .1
Sn	< 10	.001
Ti	52	ND
V	< 5	ND
W	<25	.001 to .01
Zn	<50	ND
Ge	-	.001 to .01
Sr	-	.001 to .01
Ba	-	.001 to .1
Na	-	.001 to .01
Bi	-	.0001

Note: < = less than
ND = not detected

Approved for Public Release

Contrails

Analysis for nonmetallic impurities gave the following results:

H	3.36 ppm
N	101 ppm
O	16 ppm
	22 ppm
Avg.	19 ppm
C	1530 ppm
	1660 ppm
	1670 ppm
	358 ppm
Avg.	1300 ppm

Boron analyses by three different laboratories gave reasonably consistent results of which the following are typical:

HfB_2 Bar No.	Percent Boron
284-5	10.40, 10.67
287-3	10.66, 10.71
304-5A	10.56
304-5B	10.90
310-2	9.48
321-2A	9.70

With the exception of No. 304-5B, the boron content of all these samples is below the theoretical value of 10.81%, despite the fact that a 10% molal excess of boron was added to the sintered bars.

Samples 310-2 and 321-2A were zone refined with the aid of argon jets directed at the bar near the molten zone to control the solidification process. It is evident that the use of these jets has caused excessive evaporation of boron.

After the preparation of this material had been undertaken, we found that Wah Chang Corporation was willing to make a high purity HfB_2, much lower in zirconium and other metallic impurities than the above.

The decision was then made to reject the first lot of HfB_2 and to try to make another lot of bars of improved stoichiometry using this high purity starting material. Three pounds of HfB_2 were therefore procured from Wah Chang Corporation. The suppliers analysis of this material is given in Table II.

In preparing the sintered bars for zone refining, enough pure boron was added to make up the slight deficiency in the starting material and to provide a 10% excess to compensate for evaporation of boron during melting. Approximately 400 grams of selected zone-refined bars were obtained from this lot of material, about 50 grams of which were used for analysis, metallography, etc., and 346 grams were send to Professor E. F. Westrum for heat capacity measurements.

Approved for Public Release

Contrails

TABLE II

HfB_2 ANALYSES

Element	As Received	Zone Refined
Al	<100 ppm	ND*
Cb	<100 ppm	ND
Cd	<100 ppm	ND
Co	<100 ppm	ND
Cr	<100 ppm	.001%
Cu	<100 ppm	.001%
Mg	<100 ppm	.001%
Mn	<100 ppm	ND
Mo	<100 ppm	ND
Ni	<100 ppm	ND
Pb	<100 ppm	ND
Sn	<100 ppm	ND
Ta	<100 ppm	ND
Ti	<100 ppm	30 ppm
V	<100 ppm	ND
W	<100 ppm	ND
Zn	<100 ppm	ND
Zr	450 ppm	0.01 to 0.1%
B	10.6%	See text
C	0.26%	0.16%
N	0.01%	42 ppm
O	0.14%	26 ppm
Fe	0.05%	30 ppm
Si	0.05%	10 ppm

* - ND = not detected

Approved for Public Release

Contrails

The trace impurities in this lot of zone-refined HfB_2 are as shown in Table II. Hafnium and boron analyses are given below:

	#452-3 %	#457-4 %
Hafnium	89.11	89.10
Boron	10.98	10.98
Total	100.09	100.08
B/Hf	2.034	2.035

Since previous experience had led us to expect a boron deficiency, a third sample (#439) was sent to a different laboratory for checking. The results of duplicate analyses were:

	Hf	B	Total
	88.59	10.78	
	88.90	11.11	
Ave.	88.745	10.945	99.69
	B/Hf	2.036	

which is in good agreement with the previous results.

The appearance of the zone-refined bars is illustrated in Figure 2, which shows the surface to be covered with a layer of fine and closely-spaced dendrites. In contrast, the first lot of HfB_2 and the ZrB_2 yielded bars with relatively smooth surfaces. The dendritic surface may be connected with the presence of excess boron.

The HfB_2 bars were prepared for use by rubbing them against one another in order to remove the dendritic layer without introducing extraneous impurities. The abraded bars, which were fairly smooth but slightly pitted, were cleaned in diluted Hf-HNO_3 mixture before use.

Cross sections of a single HfB_2 bar taken at about 1 inch and about 4 inches from the starting point are shown in Figures 3 and 4, respectively. Figure 3 shows a lamellar structure similar to that found in ZrB_2, together with rounded masses of a second phase. In Figure 4 the lamellar structure is less marked and the rounded masses are larger and more numerous. Figure 5 an enlarged view of one of these masses, shows a lamellar structure such as might be expected from the solidifcation of a eutectic liquid or from a eutectoid reaction within the rounded mass. From the chemical analysis, this second phase is expected to be richer in boron than HfB_2.

To our knowledge, the phase diagram of the Hf-B system has not been worked out in detail, hence the identification of this eutectic-like structure is somewhat uncertain. By analogy with the known Zr-B diagram,[37,1] however, we would expect these inclusions to result from solidification of the eutectic between HfB_2 and HfB_{12}.

Since ZrB_{12} is stable only above about 1600C, however, we might expect (again by analogy with the Zr-B system) that the HfB_{12} originally formed may have partially or completely decomposed during cooling into HfB_2 and B.

Approved for Public Release

Contrails

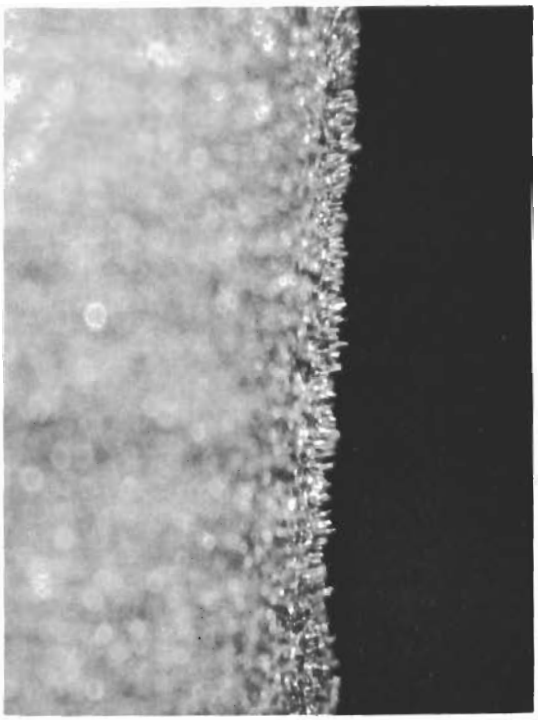

Figure 2

Surface of typical HfB_2 bar showing dendrites. 10X

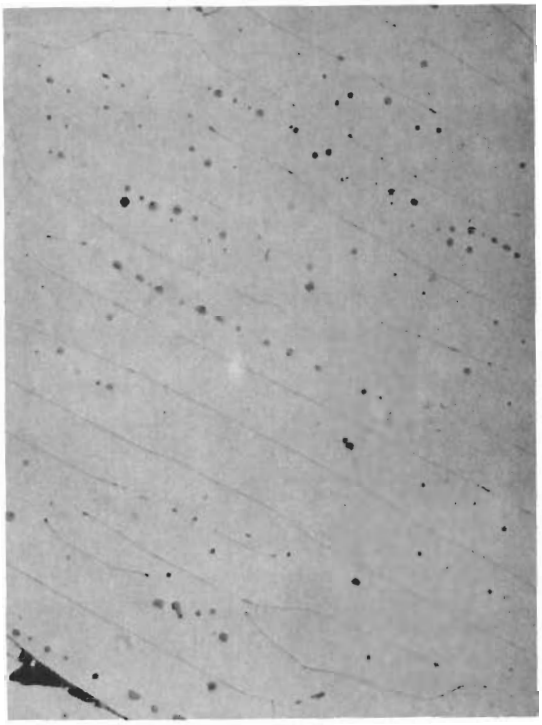

Figure 3

Cross section of HfB_2 bar (#447) at a distance of about 1 inch from the starting point. 100X
As polished.

Approved for Public Release

Contrails

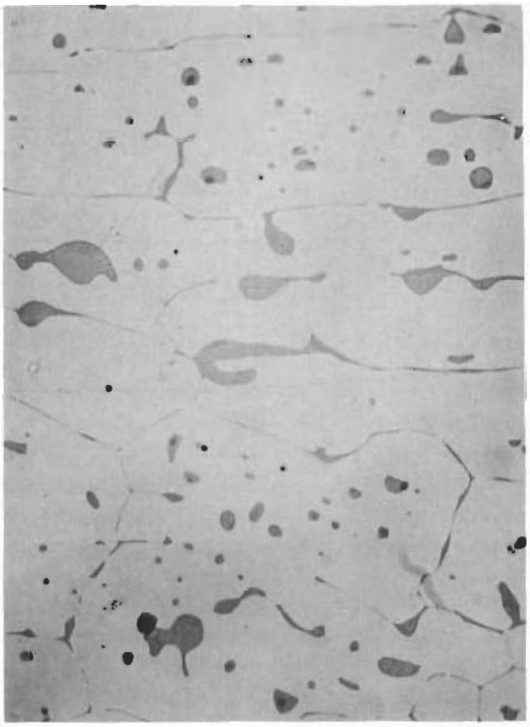

Figure 4

Cross section of HfB_2 bar (#447) at a point about 4 inches from starting point. 200X. As polished.

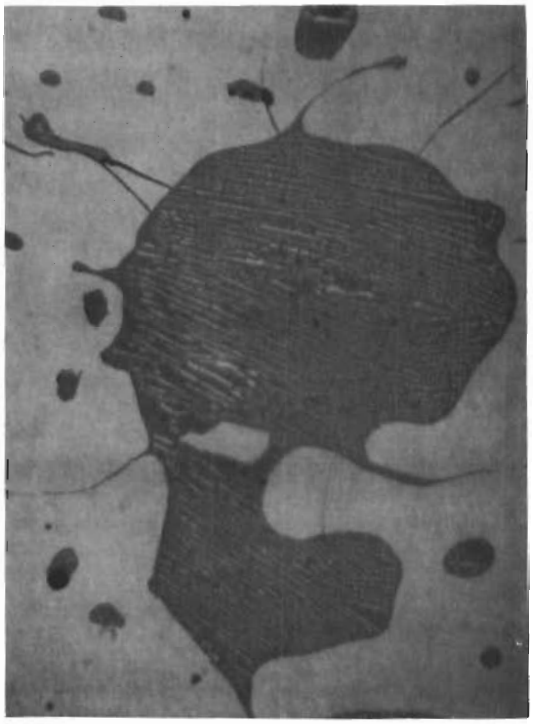

Figure 5

Same cross section as in Figure 4. 400X. Etched with 60% glycerol, 20% HNO_3, 20% HF.

Approved for Public Release

Contrails

It should be noted, on the other hand, that Glaser, Moskowitz, and Post, in their study of the Hf-B system,[38] failed to identify HfB_{12} in a large number of samples, notwithstanding that they were specifically looking for this compound. Because of the uncertainty of this situation, we have investigated the zone-refined HfB_2 in some detail by means of x-ray diffraction and electron beam microanalysis.

A total of twenty-one x-ray diffraction patterns were obtained on seven samples of HfB_2, using filtered copper Kα radiation. All patterns showed sharp, symmetrical peaks corresponding to the indexed values for HfB_2, indicating that the material was of nearly uniform composition. In addition to the HfB_2 peaks, a small peak corresponding to a lattice spacing of about 2.21Å was clearly distinguishable from background in most of the samples.

A more informative pattern was obtained from several "runovers" or drops of the melt which accidentally overflowed during zone-melting and were thus quenched more rapidly than the normal zone-refined material. These runovers showed the 2.21Å line very clearly and two more extraneous lines at about 3.69Å and 4.28Å.

These extraneous lines are compared with the major lines of ZrB_{12} in Table III.

TABLE III

COMPARISON OF

UNKNOWN X-RAY DIFFRACTION LINES WITH THOSE OF ZrB_{12}

ZrB_{12}			
Spacing	Intensity	hkl Plane	Unknown Spacing
2.23	100	311	2.20 to 2.21
3.71	70	200	3.68 to 3.70
4.29	70	111	4.25 to 4.30
2.14*	41	222	Not found
2.62	30	220	Not found
1.70	23	331	Not found
1.514	23	422	Not found

* - This line nearly coincides with a ZrB_2 line and may be masked.

These results provide strong evidence that the hitherto unknown HfB_{12} is present in our HfB_2. This conclusion is supported by the fact that during the course of work under another contract (AF 33(657)-8635) we have observed the presence of ZrB_{12} in bars of ZrB_2 prepared under similar conditions. Using the value of 2.21Å for the strongest line, the lattice constant of HfB_{12} is calculated to be 7.31Å compared to 7.408Å for ZrB_{12}. This shift is in agreement with the known lattice constants of the two monoborides and the two diborides.

Approved for Public Release

Contrails

The sample of bar 447 shown in Figures 4 and 5 was submitted to Advanced Metals Research Corporation, Somerville, Massachusetts, for electron beam microanalysis with the following results:

Phase	Wt. % Hf
Matrix (light gray)	89.2
Average of lamellar areas (as in Figure 5)	43.0±1.0
Dark gray	1.0 or less

These results indicate that the dark gray areas as shown in Figure 5 are nearly pure boron as would be expected from the decomposition of HfB_{12}. This raises the question, however, as to where the HfB_{12} responsible for the x-ray diffraction lines is located. A more careful metallographic examination at high magnification revealed that the dark gray phase shown in Figure 5 in reality consists of two phases, nearly identical in color, but one having a slightly brownish shade and the other a slightly blue or purple shade. The brownish gray material formed the bulk of the dark phase. We conclude, therefore, that all but a trace of the HfB_{12} originally formed has decomposed and that the bulk of the second phase in this sample is nearly pure boron. This conclusion is confirmed by measurements of the back-scattered electron current during the electron beam analysis, which indicate that the dark phase is a material of very low atomic number.

The average composition of the lamellar structure is of interest as a possible indication of the composition of the HfB_2-HfB_{12} eutectic. By analogy with the Zr-B system, we would expect this eutectic to have a composition about 83 atom per cent boron or about 12 weight per cent. The observed value of about 57 weight per cent (by difference) is much higher than expected and corresponds to a composition of about HfB_{22}. This result indicates that much hafnium has probably diffused out of the lamellar region during or after solidification and that the analysis gives no useful information regarding the eutectic composition, if the eutectic is indeed between HfB_2 and HfB_{12}.

F. HAFNIUM CARBIDE

We have obtained 3.5 pounds of high-purity HfO_2 from Wah Chang Corporation which was converted into HfC by The Carborundum Company on a toll basis. The following analysis is reported by The Carborundum Company.

Soluble Hf + Zr	93.52%
Total C	6.25
O_2	0.09
Fe (wet analysis)	0.40
N_2	nil
B	0.001 to 0.005

Approved for Public Release

Contrails

Al, Ca, Co, Ce, Cu, Mg, Mn, Na, Ni, V	< .002
Ti	0.002-0.005
Si, Zr	0.005-0.01
Fe (Spectro)	0.01-0.05

x-ray diffraction showed only single-phase HfC.

The slight carbon deficiency was corrected for by the addition of spectrographic graphite to the sample before sintering.

Preliminary experiments with commercial-grade HfC indicated that the 10 kw, 450 kc power supply, used for the zirconium compounds and HfB_2, was not adequate to melt HfC. The zone-refiner was therefore adapted for use with a 30 kw, 450 kc power supply.

The first difficulty encountered with this apparatus was excessive arcing due to the higher voltages developed by the larger power supply and to the close coil-clearances required to secure good coupling. This trouble was largely overcome by using 25% hydrogen in argon for the zone-refiner atmosphere rather than the 5% hydrogen previously used.

A second difficulty was that the intense thermal radiation from the HfC rod melted the interior face of the copper coil, notwithstanding that the coil was cooled with city water at the full line pressure of about 60 psi. This trouble was remedied by the installation of a gear pump which raised the water pressure to about 100 to 125 psi. At this point, it became possible to produce incipient melting in the sintered HfC bars.

We found, however, that the melting behavior of HfC differed from that of most materials in that melting first took place in the interior of the rod rather than at the surface. Although the high-frequency field generates heat at the greatest rate near the surface of the rod, this effect is apparently overshadowed in the case of HfC by the large flux of radiant energy from the surface. The loss of heat from the surface of HfC at its melting point is very large because of its high melting point (3890C) and the fourth power radiation law. That this effect is a physical one and not due to the chemical constitution of the bar is shown by the fact that tantalum carbide (M.P. = about 3800C) behaves similarly to hafnium carbide.

The result of this interior melting is that the liquid migrates by capillarity to the surface of the bar, forming a hollow tube. This tube is unstable in the RF field, since any thin spot in the wall will become overheated and melt, leaving a hole or crack in the cylinder wall. When this happens, the coupling of the specimen with the RF field becomes much reduced and the specimen quickly cools below the melting point. Figure 6 shows three illustrations of the partial melting behavior of hafnium carbide. The left and center samples show irregular hollow melting with cracked walls. The right-hand sample shows melting in an annular region with the formation of a pattern resembling a cartwheel.

Repeated attempts to modify this melting behavior were not successful. It was thought that the use of a higher frequency would tend to increase the surface

Approved for Public Release

Contrails

Figure 6

Partially melted hafnium carbide bars. Left and center: Hollow cylinders with cracked walls; right: "Cartwheel" formation

Approved for Public Release

Contrails

heating due to the skin effect. Preliminary experiments at 5 megacycles, however, indicated that the voltages required were so high that arcing could not be prevented. The decision was therefore made to postpone efforts to zone refine HfC and to attempt to prepare the samples by arc-melting on a water-cooled copper hearth, using equipment available at Nuclear Metals, Inc.

A preliminary experiment in a helium atmosphere indicated that HfC could readily be arc-melted into a massive macrocrystalline ingot, which was badly cracked because of thermal shock. A black deposit was formed on the walls of the chamber during arc-melting, however, indicating a possible loss of carbon by vaporization. Analysis of this sample showed that not only had substantial carbon loss taken place but that the composition of the bar varied from place to place, probably because the random action of the arc subjected different parts of the bar to a varying degree and duration of heat. Carbon analysis of a typical sample (#279-2) give the following results: 5.17%, 5.82%, 5.88%, 5.17%, 5.73%, 5.71%, 5.88%. The average of these values is 5.62% carbon, but the variation is outside the normal uncertainty range of the analytical method.

A second sample was arc-melted in an atmosphere of 3.14% ethylene, 11.4% hydrogen, balance argon, which is similar to that used by Eckstein and Forman for the carburization of tantalum.[39] The results showed 5.89%, 5.92%, and 6.02% carbon, which represents some improvement but still falls short of the stoichiometric value of 6.3%.

A third sample was melted in an atmosphere containing 1 part of propane with 5 parts of the above mixture in an attempt to increase the carburizing action. This mixture deposited so much carbon on the walls of the arc-melting vessel that the operation was completely obscured within about one second. The product contained free carbon and gave an analysis 6.54%, 6.40%, and 6.26% of total carbon. Because only a small sample was available, free carbon analyses could not be obtained. Because of the deposition of carbon, it was not feasible to use this gas mixture for further experiments.

A fourth sample was mixed with enough pure graphite to give an excess of five atomic per cent and was arc-melted in 3.14% C_2H_4, 11.4% H_2, balance argon. The operation was somewhat difficult because of the deposition of carbon on the walls of the vessel but was considered feasible. Analysis gave 5.63%, 5.57%, and 5.52% carbon or an average of 5.57%.

Because none of the usable gas mixtures gave a product approaching the theoretical value of 6.3% carbon, and because of the lack of uniformity of the arc-melted product, it was decided to try re-carburizing some of this material by heating in contact with graphite.

The first of the recarburization experiments was carried out in a graphite crucible about 1/2" diameter by 3/4" high fitted with a lid having a 1/16" hole for optical pyrometer sighting. The sample was heated by induction for 30 minutes at 2500C in an atmosphere of 5% hydrogen in argon. It was hoped that the hydrogen would react with the walls of the graphite crucible and serve as a carrier of carbon. The starting material gave a carbon analysis of 5.63%, 5.57%, and 5.52% or an

Approved for Public Release

Contrails

average of 5.57%. The recarburized product gave 6.09% and 6.00%, which appeared sufficiently above the statistical variation of the starting material to indicate that a real increase had taken place.

A second experiment was then made with a larger sample (about 15 grams) using a carbon-resistance furnace as the source of heat and an atmosphere of 5% hydrogen in argon. The sample was held at about 2400C for a total of 18 hours, but the heating period was divided into two parts because of failure of the graphite heating element, which was badly attacked by the hydrogen in the atmosphere. After cooling in the furnace, the sample was found to be coated with a layer of pyrolytic graphite about 1/2 mm thick, apparently by transfer of carbon from the crucible wall. The starting material for this experiment was metallographically homogeneous (indicating the absence of free carbon) and gave a carbon analysis of 5.83%. Only one carbon analysis was obtained, but experience with material prepared in the same way leads us to think that this value is within the statistical variation for this material. The recarburized product showed a content of 6.10% total carbon, 0.64% free carbon, and 5.46% combined carbon (by difference). In spite of its thick coating of pyrolytic graphite, therefore, the combined carbon content of this sample appears to have decreased from 5.83% to 5.46% during heating. The result is not conclusive, however, because of the known statistical variations in carbon content of the starting material.

A third recarburization experiment was made as above, but using a pure argon atmosphere. The heating period was about 18 hours at 2500C. The sample after heating was covered only with a thin blue film, the color of which was probably due to optical interference. Total carbon before heating was 5.88% and after heating 5.83%,indicating (again subject to statistical variation) that probably no significant carburization had taken place.

The fourth recarburization experiment was the same as the second except that the crucible and its lid were coated prior to use with a layer of pyrolytic graphite. It was thought that this material might have less tendency than polycrystalline graphite to transfer a great excess of carbon to the sample. The heating period was about 18 hours at 2400C. It was found after heating that the layer of pyrolytic graphite on the surface of the sample appeared much thinner than in the previous case. The starting material contained 5.83% total carbon and was metallographically homogeneous. The product showed 6.31% total carbon, 1.04% free carbon and by difference 5.27% combined carbon; a net decrease of 0.56% combined carbon, subject to the above-mentioned statistical uncertainties. If these changes in combined carbon are real, they appear to indicate that stoichiometric HfC is unstable with respect to free graphite in some temperature range below its melting point.

Because of these difficulties with arc-melted hafnium carbide and especially because of its lack of uniformity, we have decided to re-examine the possibility of zone-refining this material using induction heating. We have now found that a sintered bar of very small diameter (1/4") and containing about 30% of excess carbon can be zone-melted, and we are examining the product. If this material appears satisfactory and if the production rate is not too slow, we plan to prepare several hundred grams of HfC by this method.

Approved for Public Release

Contrails

V. OXIDATION STUDIES OF ZIRCONIUM CARBIDE AND DIBORIDE ABOVE 1000C*

A. ZIRCONIUM DIBORIDE

1. Background

The oxidation of ZrB_2 was studied by F. H. Brown, Jr., in 1955 in the temperature range 649-1315C in pure oxygen, and moist dry air.[40] Since Brown worked with porous compacts of the diboride, his initial surface areas are unknown, and undoubtedly changed during the course of exposure at high temperatures. His qualitative conclusions that ZrB_2 is oxidized more rapidly in oxygen than in dry air, and much more rapidly in moist air than in dry, may have some validity.

Samsonov[41] oxidized ZrB_2 in air at 1000C and measured a depth of corrosion of 0.45 mm after 150 hours. For material of theoretical density, this would correspond to stoichiometric oxidation of 0.274 g/cm^2 of the alloy or to a total oxygen consumption of 0.0873 g/cm^2. The net weight change cannot be computed since an unknown portion of the $B_2O_3(l)$ must certainly have evaporated during the experiment. From metallographic examination of the oxide scale, Samsonov postulated the existence of ZrO(s) immediately adjacent to the alloy and a molten layer of B_2O_3 at the surface of the oxidized specimen. He assumed that with increasing time of exposure oxygen would diffuse through the $B_2O_3(l)$ to the alloy and react with ZrO(s) to form $ZrO_2(s)$, while at the same time B_2O_3 would gradually vaporize.

The present work was undertaken to obtain much needed quantitative data on the oxidation of ZrB_2 over a wider temperature and pressure range than that covered in previous studies. The materials used are described in Chapter IV of this report and in Part I issued in April 1962; they were zone-refined specimens of ZrB_2, large grained polycrystals of near theoretical density. The samples were heated inductively in the 1200-1530C range and exposed to oxygen partial pressures of 8-39 Torr in a helium stream at a total pressure of 760 Torr. The rate of oxygen consumption was monitored continuously with a thermal conductivity apparatus; weight change was measured before and after each experiment; oxide films were characterized by both x-ray and metallographic examination.

2. Experimental Rate Data

The experimental technique was described in adequate detail in a previous report.[42] The only essential change necessitated in the work with borides was the substitution of platinum wire support rods for the ceramic fingers, which tended to react with the product B_2O_3.

A summary of the experimental data is given in Table IV. The initial weights listed are weights taken after degassing the samples in pure helium at about 1870K until the signal from the thermal conductivity bridge dropped to zero (approximately 30 minutes). Weight changes during this period were in every case less than

* - Prepared by Joan Berkowitz-Mattuck, Arthur D. Little, Inc., Cambridge, Mass.

Approved for Public Release

Contrails

TABLE IV

SUMMARY OF EXPERIMENTAL RATE DATA ON ZrB_2

(at a flow rate of 95 cc/min)

Pellet	Initial Weight (g)	Area $(cm)^2$	Density (g/cc)	Temp (^oK)	O_2 Pressure (Torr)	Exposure Time (min)	Weight Change (g/cm^2)	Total O_2 Consumed (g/cm^2)	k_p (*)
XIV-5	0.6880	1.4355	5.875	1540	16.5	121	0.0023	0.00976	0.102
XIV-18	0.6804	1.529	5.56	1556	38.75	120	0.00439	0.01654	0.262
XIV-20	0.7240	1.602	5.57	1556	27.0	120	0.00424	0.01552	0.255
XIV-1	0.7068	1.5155	-	1560	11.3	130	0.00324	0.01698	0.259
XIII-47	0.7586	1.6097	5.82	1550	19.9	117	0.00267	0.01342	0.230
XIII-49	0.7715	1.6368	5.78	1562	8.5	133	0.0030	0.01518	0.272
XIII-45	0.8033	1.6452	5.98	1604	19.9	135	0.00546	0.0296	1.057
XI-48	0.6627	1.453	5.80	1633	9.9	130	0.0095	0.0509	2.89
XIII-2	0.7403	1.5536	5.91	1654	8.25	118	0.00572	0.0362	2.13
XIII-6	0.7080	1.5172	5.84	1656	10.1	120	0.00686	0.0350	1.74
XIII-16	0.6963	1.5038	5.82	1687	7.0	128	0.00671	0.0302	1.53
XIII-42	0.7623	1.5864	5.94	1711	19.9	120	0.0204	0.0403	1.912
XIII-4	0.7597	1.5782	5.96	1729	8.0	144	0.00984	0.0519	4.0
XIII-8	0.7578	1.5738	5.97	1759	13.2	120	0.01282	0.0709	7.34
XIII-40	0.7688	1.5994	5.93	1805	19.9	114	0.01452	0.0798	7.83
XIV-12	0.8293	1.674	6.04	1550	19.9	-	-	-	0.407
				1657					1.26
				1701					2.04
XIV-8	0.6761	1.454	5.88	1557	27.0	-	-	-	-
					16.5				0.187

* - g^2/cm^4-min x 10^5

Approved for Public Release

Contrails

2×10^{-4} g. The sample surface areas (A) were calculated from the gross physical dimensions of the specimens. It will be shown below that this may introduce considerable uncertainty in the calculated absolute rates, since oxidation along the length of cracks seems to proceed just as it does on the outer sample surface. The densities (ρ) are simply initial sample weights divided by geometric sample volumes. The range of densities, computed in this crude way, is from 5.56 to 6.04, with an average value of 5.86±0.11 g/cc. The average is to be compared to a theoretical x-ray density for ZrB_2 of 6.09 g/cc. The temperatures (T^{o},K) are measured pyrometer temperatures read during the oxidation runs, corrected for sample emissivity (assumed equal to 0.6) and the measured transmission characteristics of the optical system. Temperatures can usually be held to ± 5°C during the course of heating. The oxygen pressures, P_{O_2}, are partial pressures in helium; all work was done at a total pressure of one atmosphere. The carrier gas flow rate of 95 ml/min corresponds to a linear flow velocity in the neighborhood of the sample pellet of about 3.1 cm/sec. The exposure times indicate the duration of each oxidation experiment from the time the induction unit is turned on until it is turned off. The net weight changes are simply the differences in weight of each pellet before and after oxidation, divided by initial geometric surface area. In some cases, the net weight changes are only approximate, due to flaking of the oxide, slight sticking of the pellet on the platinum fingers, or some ambiguity about whether a particular glassy product fragment should be weighed or not. The total oxygen consumed is computed from the area under the thermal conductivity curve, and represents the amount of oxygen in all of the product oxides formed during the oxidation experiment.

Experimental curves of total oxygen consumption per unit area (W_{O_2}/A) vs time (t) are given in Figures 7-20; the same data are plotted as $(W_{O_2}/A)^2$ vs t in Figures 21-34. It is clear that the rate of oxidation of ZrB_2 decreases with time over the temperature and pressure range investigated, and that the material therefore has some potential for structural applications in oxidizing environments at temperatures above 1200C. Quantitatively, the data can be fitted to a parabolic rate law after an initial period of about 40 minutes. The parabolic rate constants k_p obtained from the slopes of the lines in Figures 21-34 are listed in Table IV for each experiment, and are plotted as log k_p vs 1/T in Figure 35. The least squares straight line through the plotted points is shown, and gives an activation energy of 66±9 kcal/mole for the oxidation process. There are several reasons for the large standard deviation. First, since the activation energy is high, small errors in temperature measurement or small fluctuations in temperature during a run will result in large uncertainties in measured oxidation rates. The Arrhenius equation for the parabolic rate constant as a function of temperature is:

$$k_p = A\, e^{-\Delta E/RT}$$

where A is a constant, ΔE measured activation energy, and R is the gas constant. If the temperature during an experiment was measured with an accuracy $\pm \Delta T$, then the corresponding error Δk_p in k_p is given by:

$$\frac{\Delta k_p}{k_p} = \frac{\Delta E}{RT^2} \Delta T$$

Approved for Public Release

Contrails

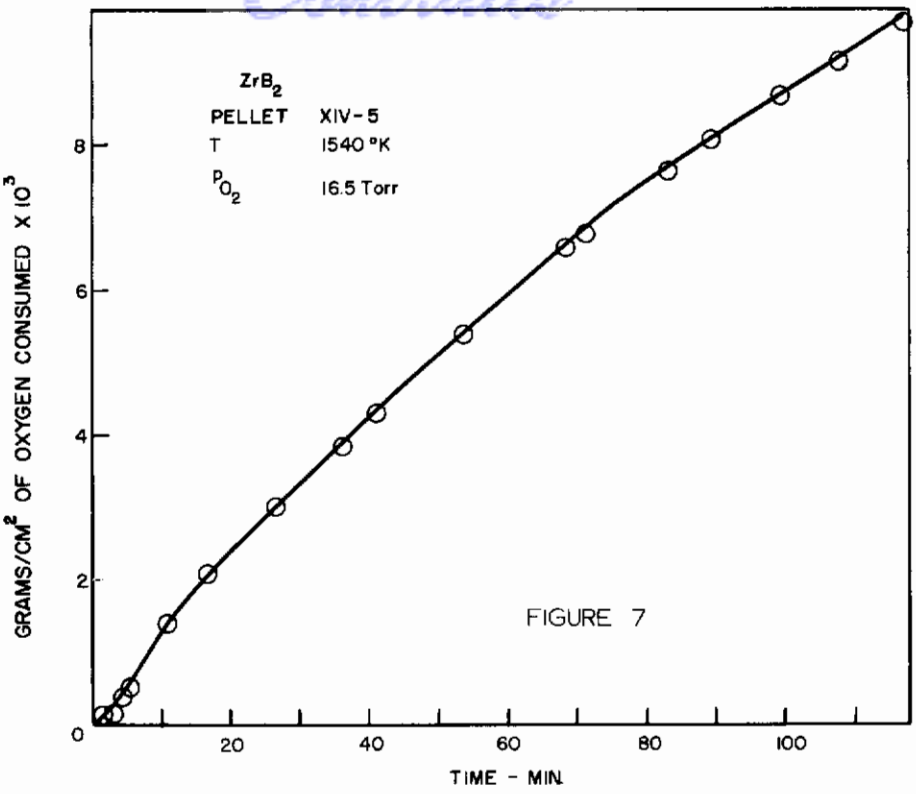

FIGURE 7

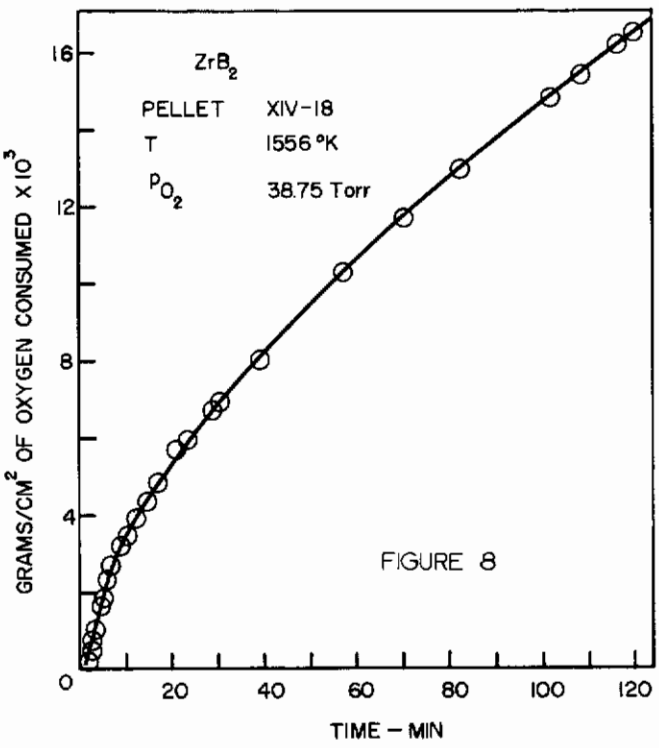

FIGURE 8

Figures 7-8: Linear plots of ZrB_2 oxidation data.

Approved for Public Release

Contrails

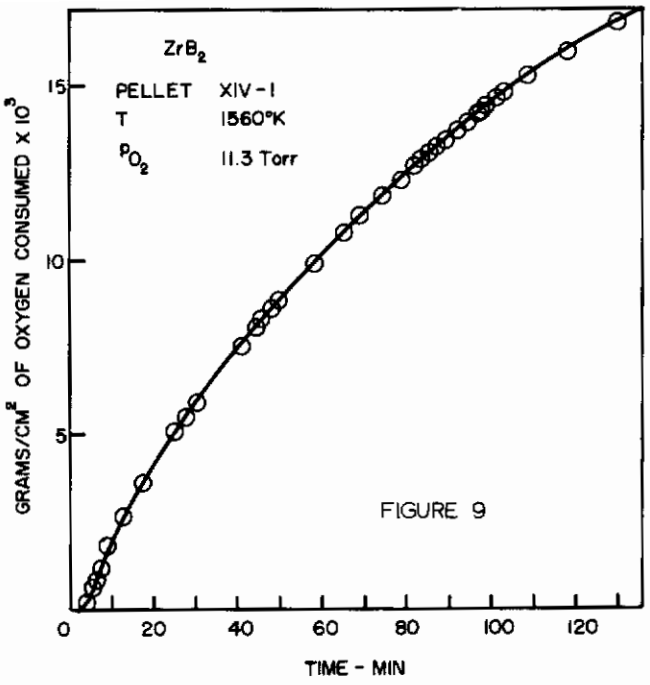

FIGURE 9

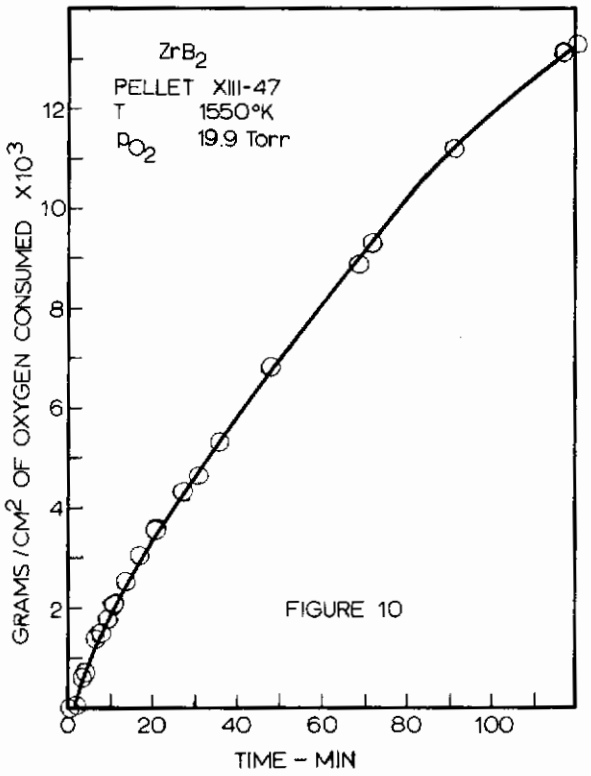

FIGURE 10

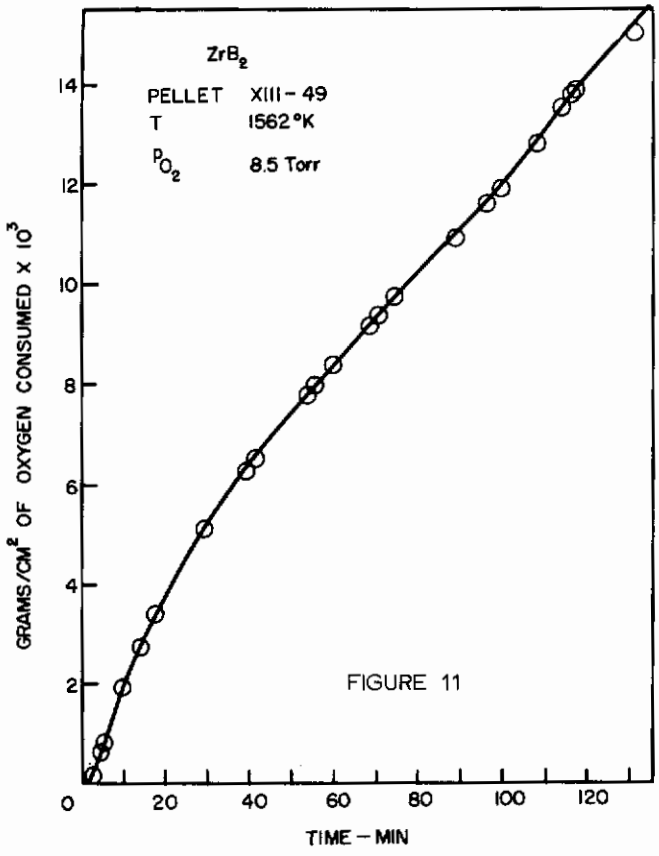

FIGURE 11

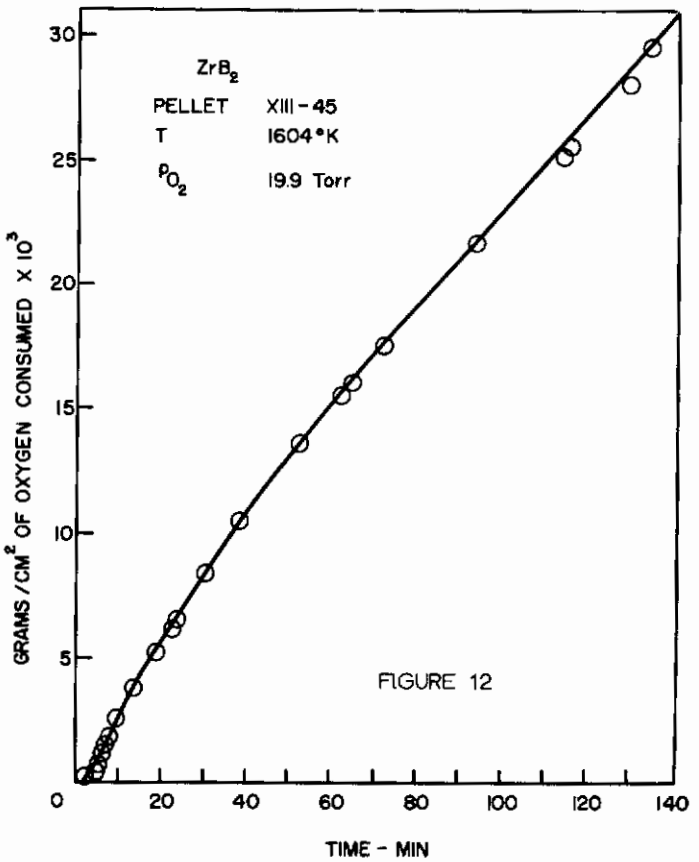

FIGURE 12

Figures 9-12: Linear plots of ZrB_2 oxidation data.

Approved for Public Release

Contrails

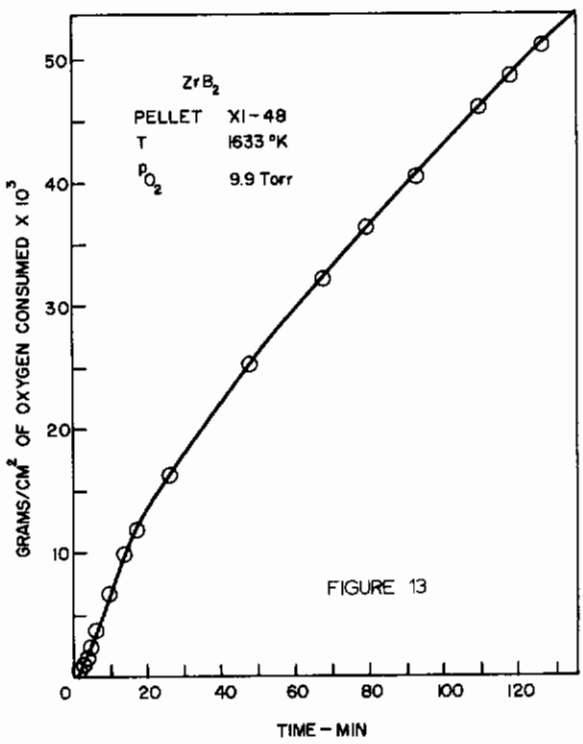

FIGURE 13

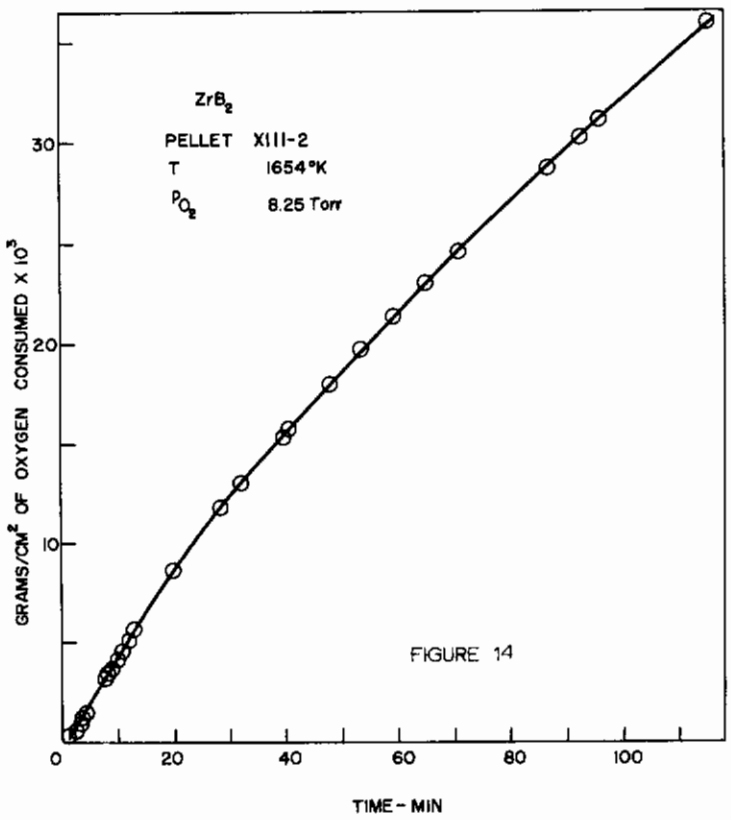

FIGURE 14

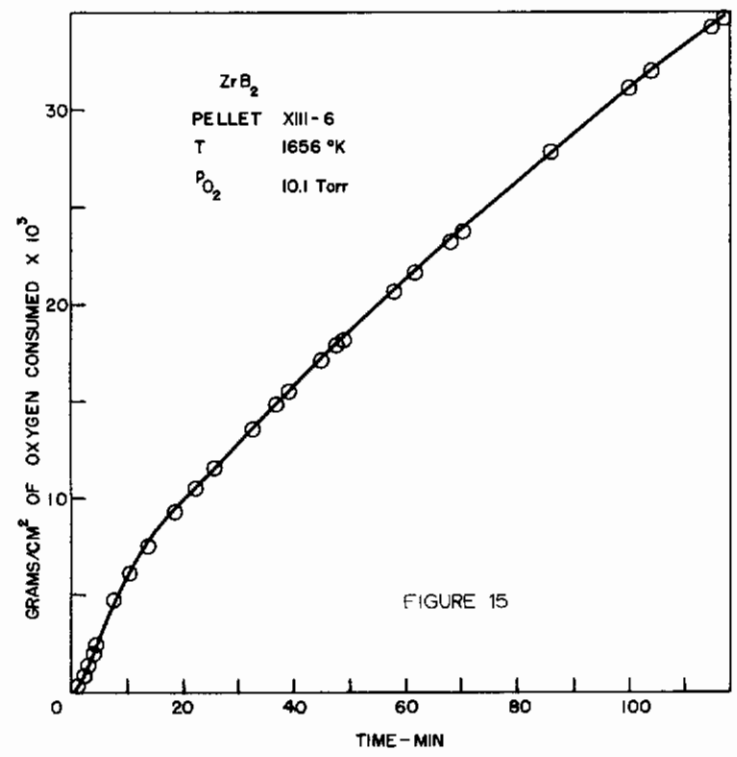

FIGURE 15

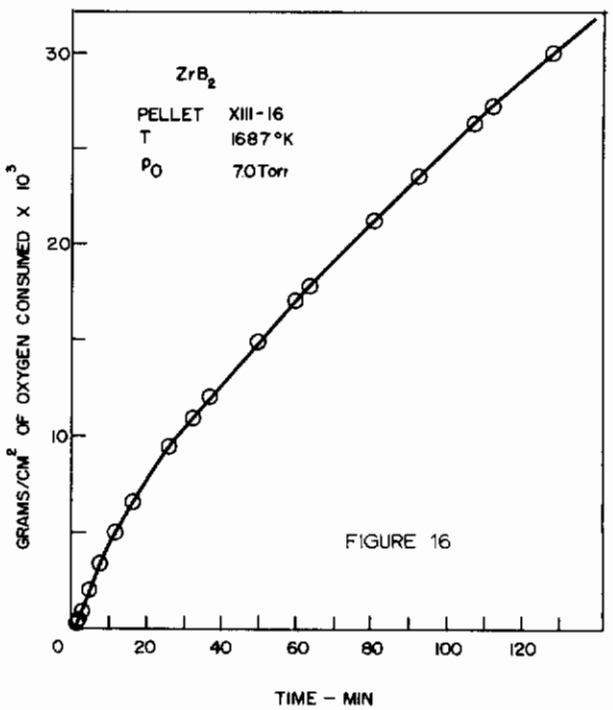

FIGURE 16

Figures 13-16: Linear plots of ZrB_2 oxidation data.

Approved for Public Release

Contrails

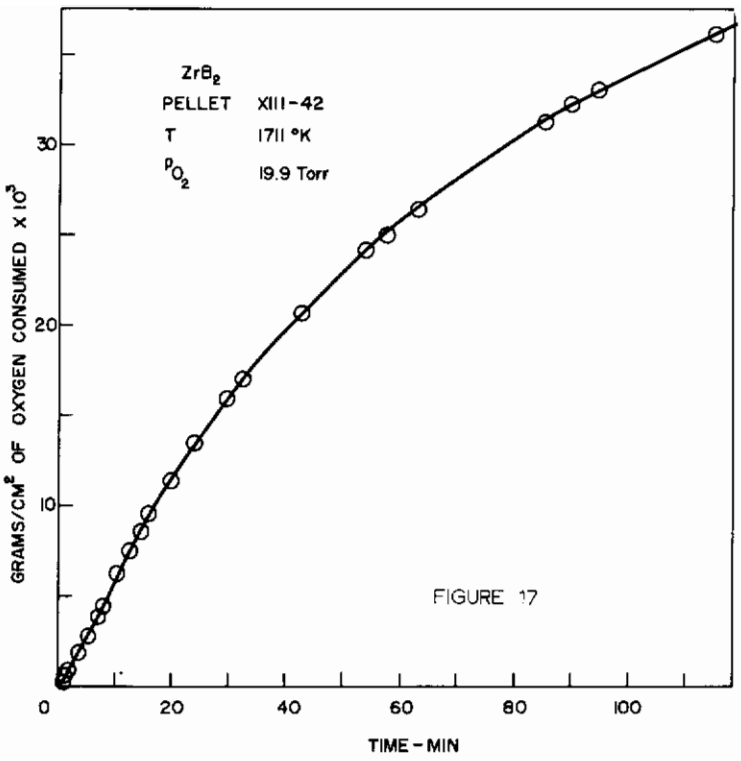

FIGURE 17

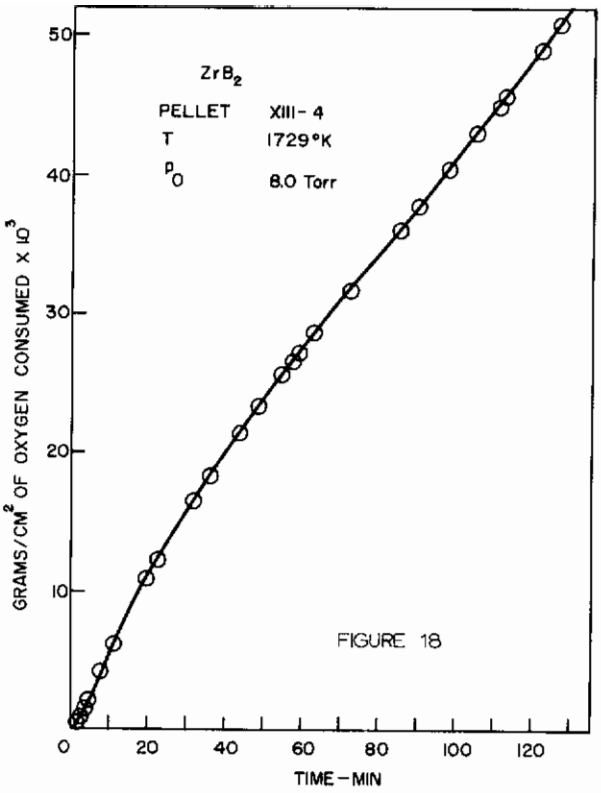

FIGURE 18

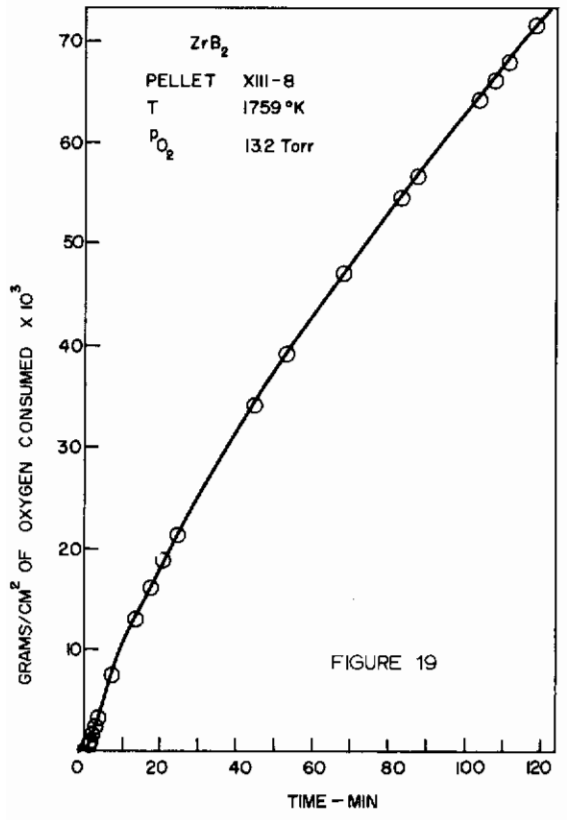

FIGURE 19

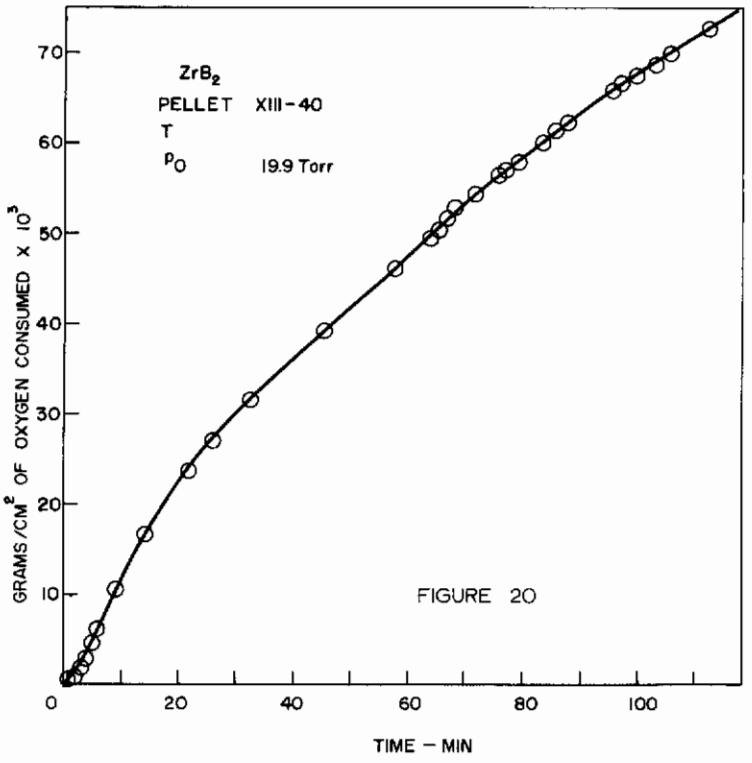

FIGURE 20

Figures 17-20: Linear plots of ZrB_2 oxidation data.

Approved for Public Release

Contrails

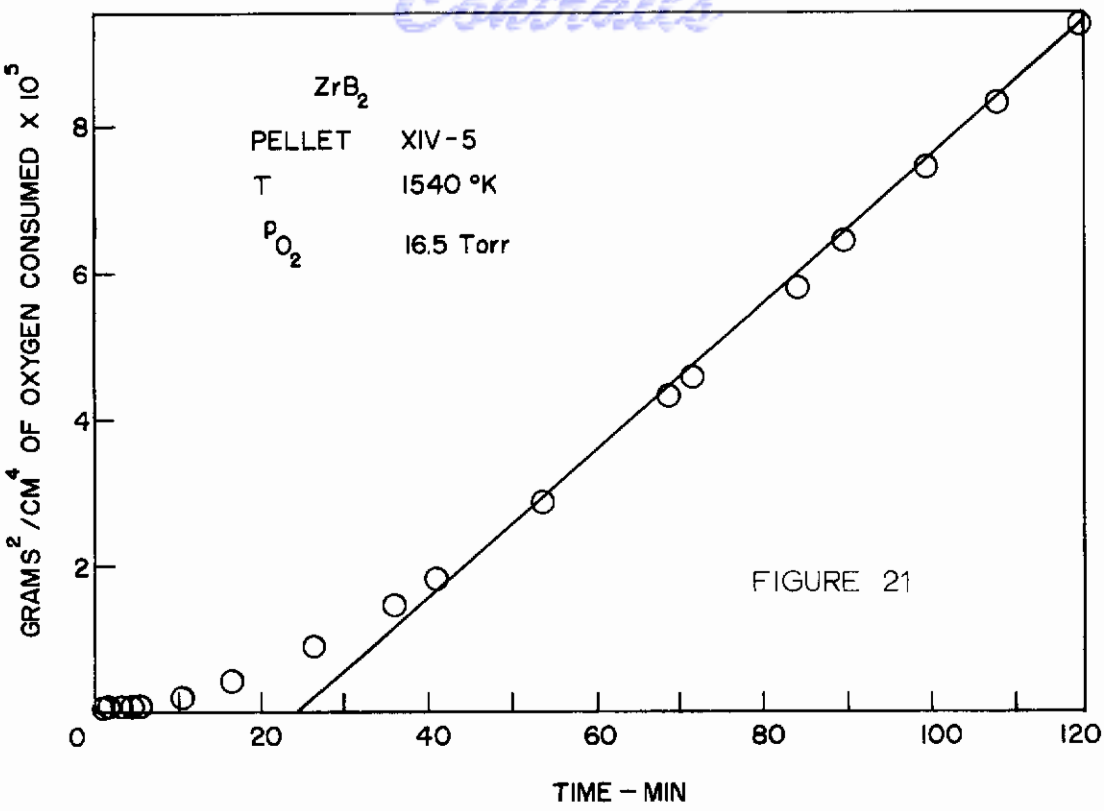

FIGURE 21

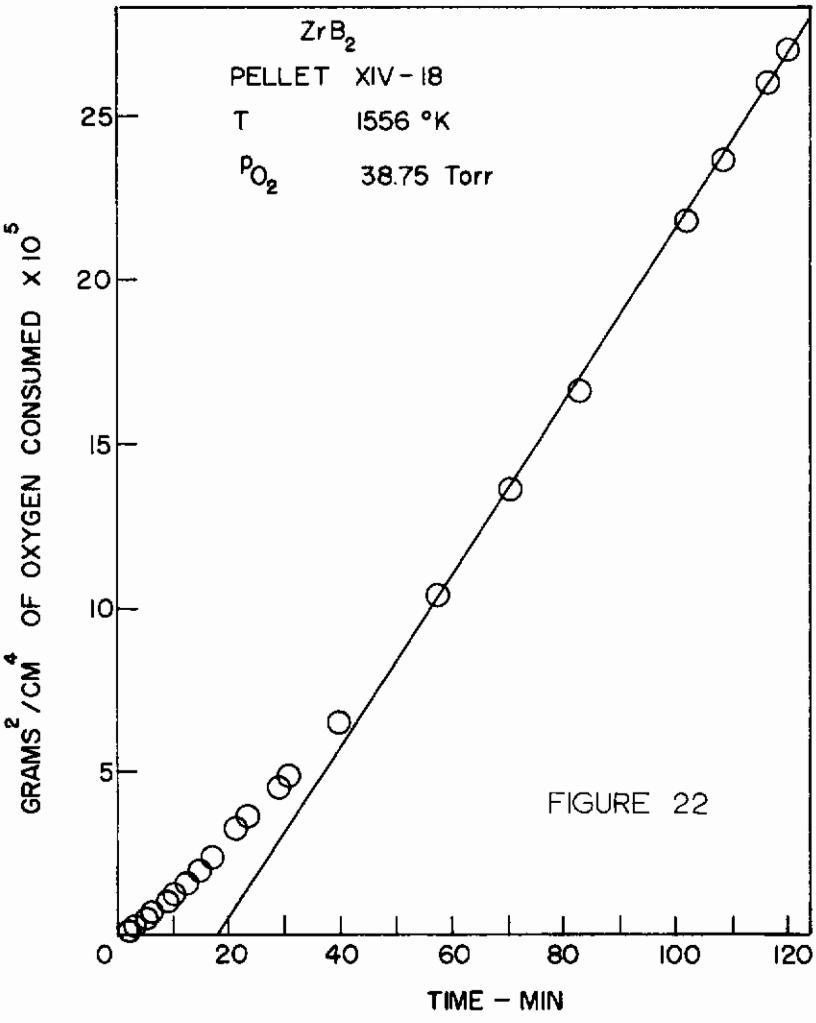

FIGURE 22

Figures 21-22: Parabolic plots of ZrB_2 oxidation data.

Approved for Public Release

Contrails

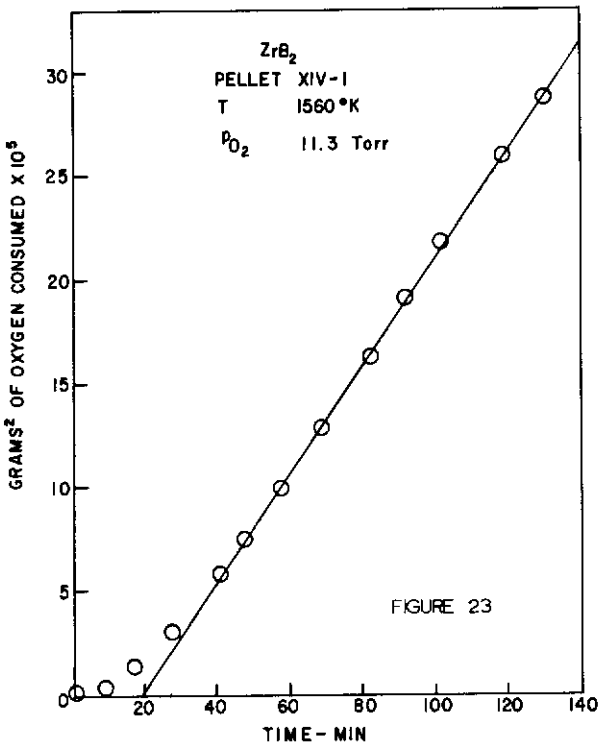

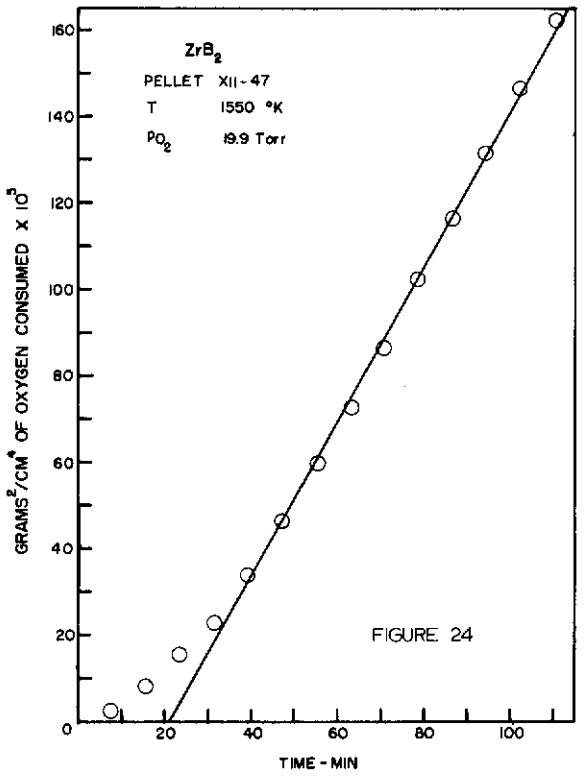

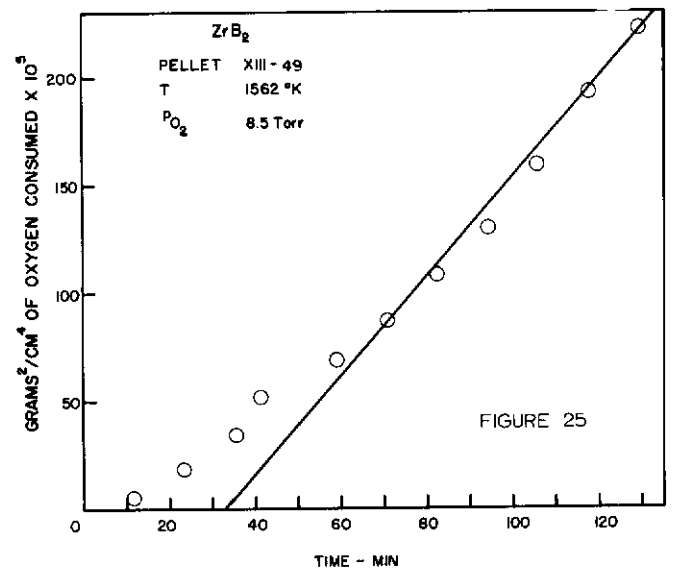

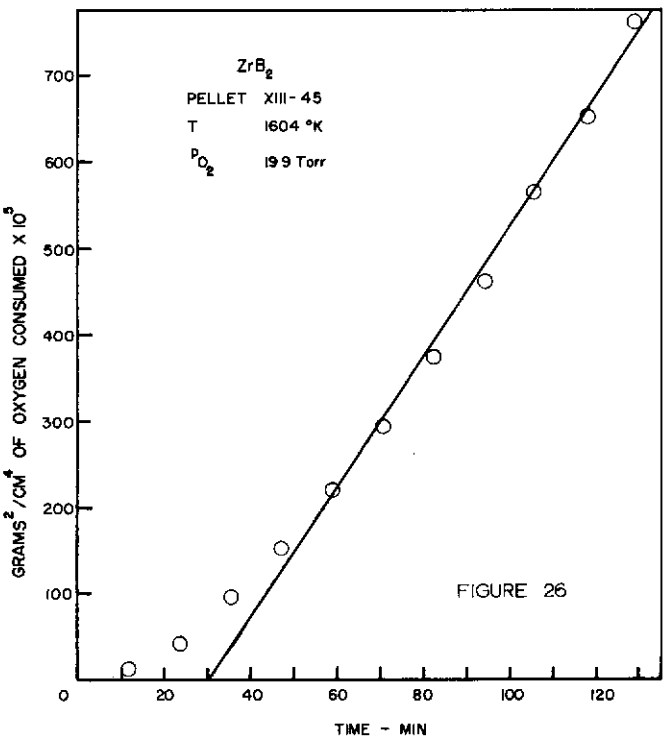

Figures 23-26: Parabolic plots of ZrB_2 oxidation data.

Approved for Public Release

Contrails

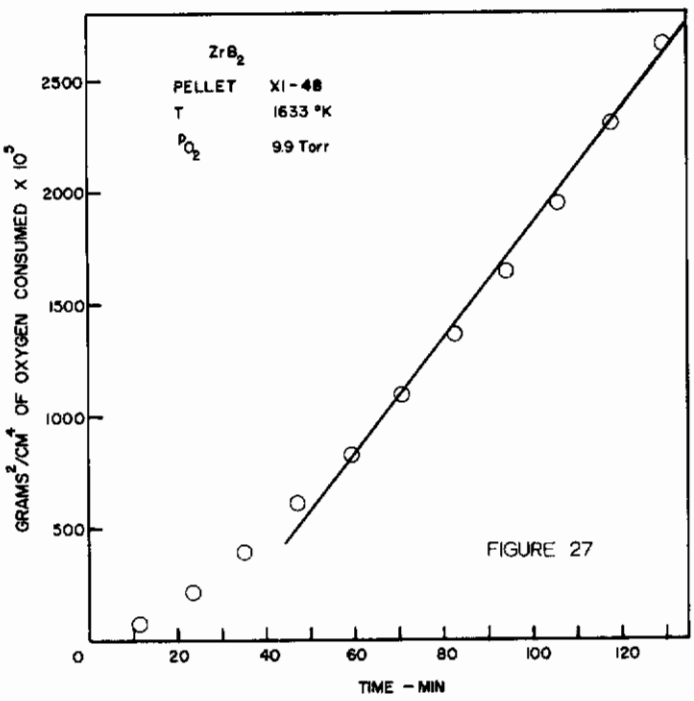

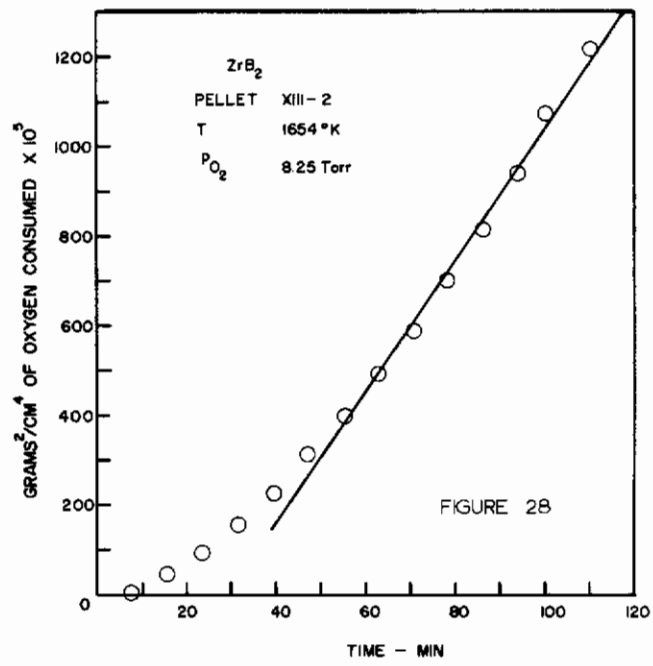

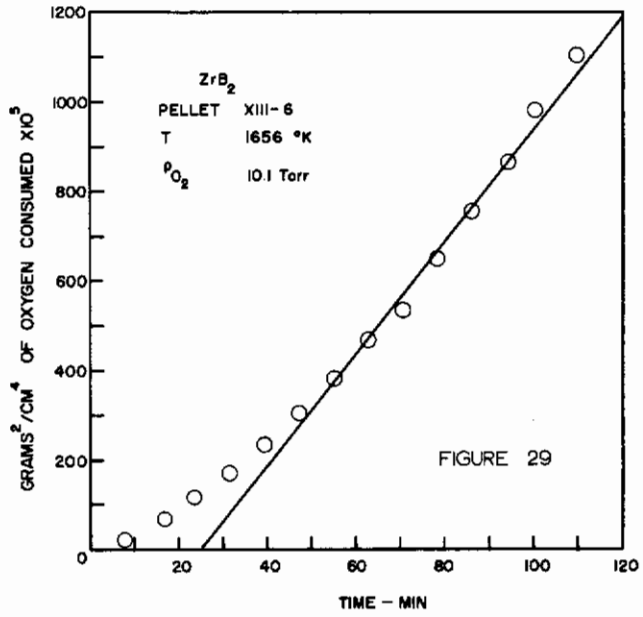

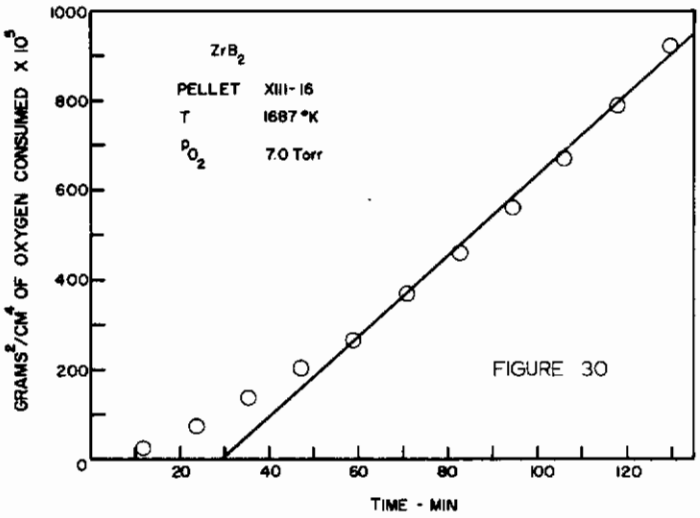

Figures 27-30: Parabolic plots of ZrB_2 oxidation data.

Approved for Public Release

Contrails

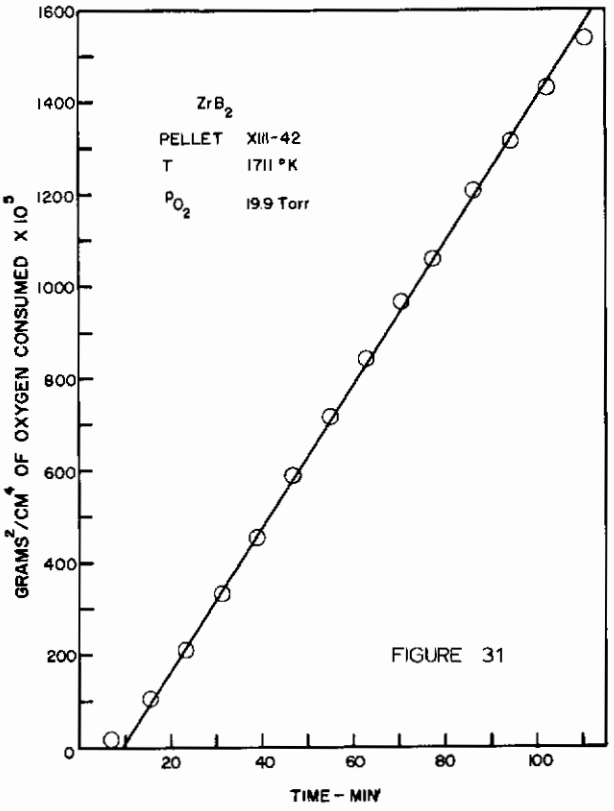

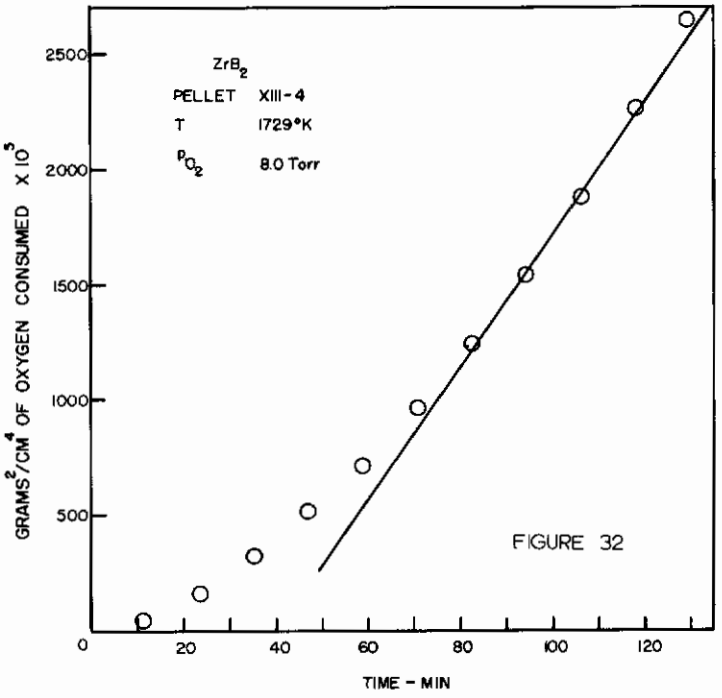

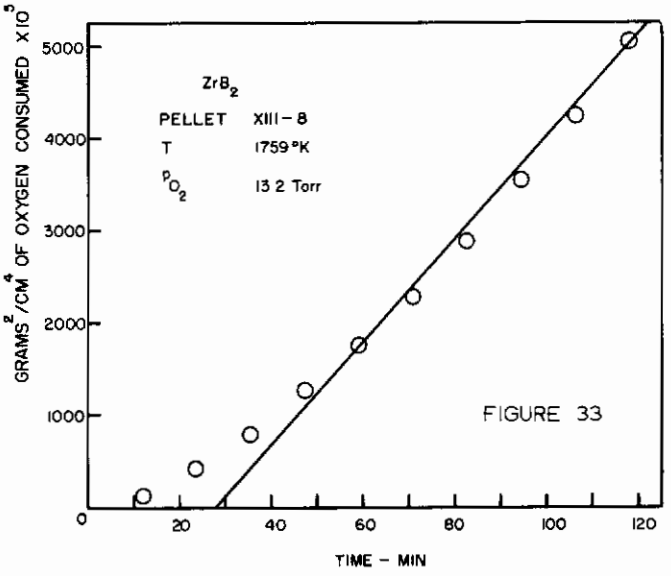

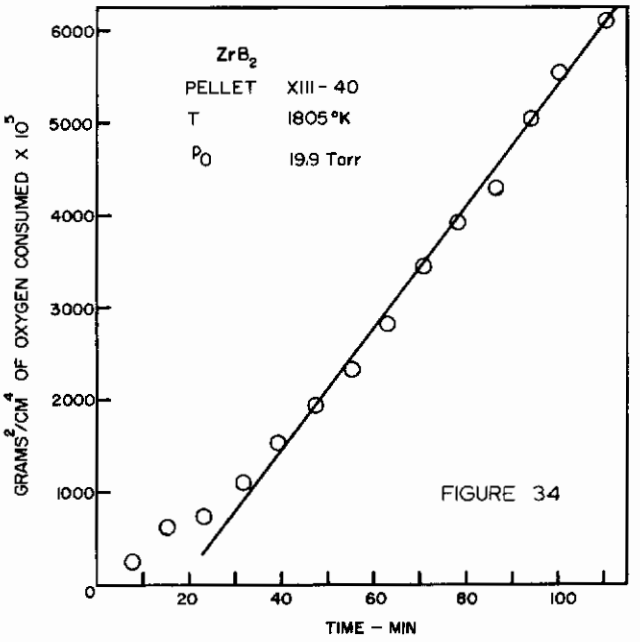

Figures 31-34: Parabolic plots of ZrB_2 oxidation data.

Approved for Public Release

Contrails

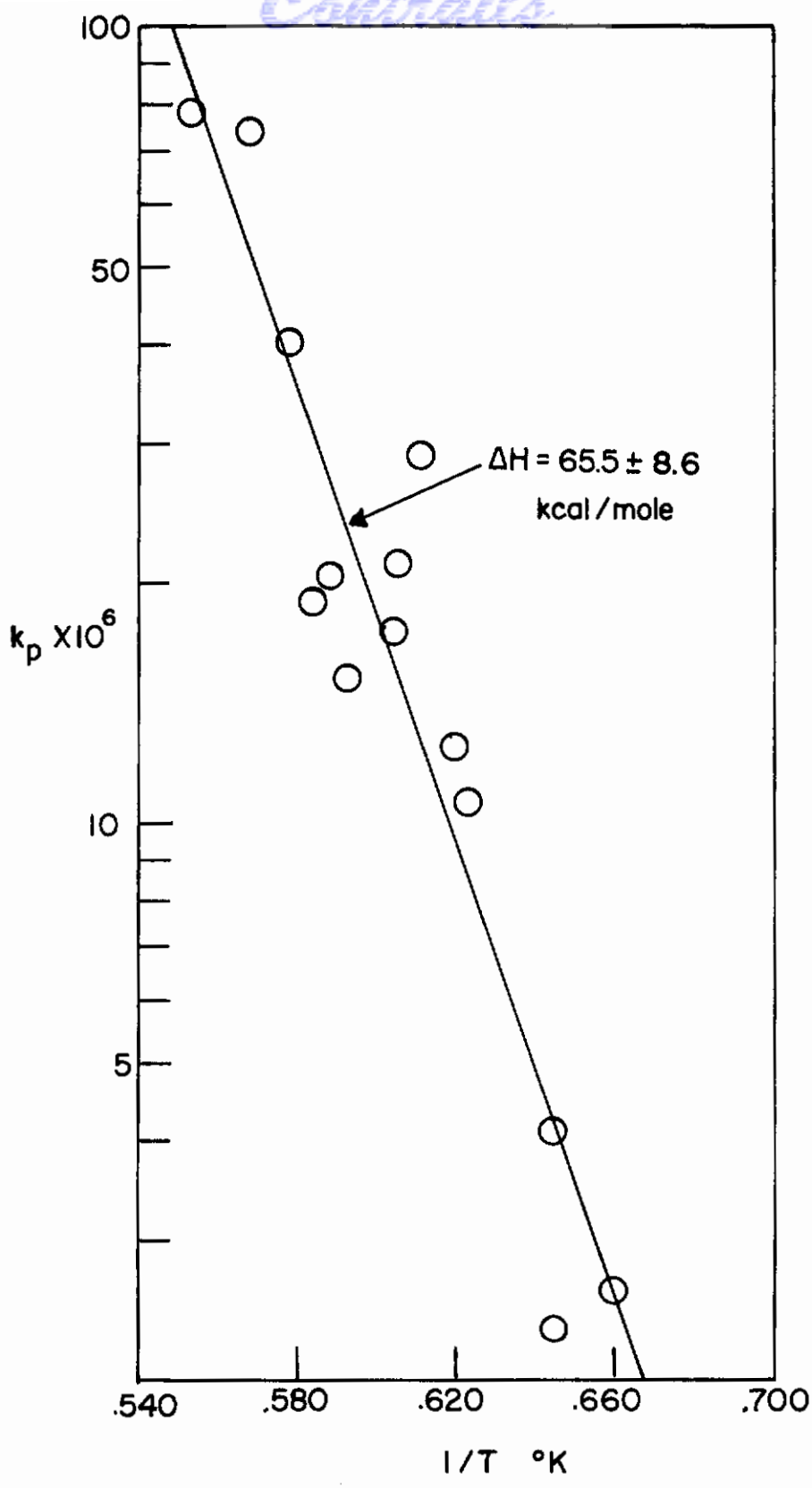

Figure 35. - Logarithm of parabolic rate constant vs reciprocal temperature.

Approved for Public Release

Contrails

For an activation energy of 66 kcal/mole, and an average experimental temperature of 1200C, an error 10° in T (typical temperature fluctuation during run) will be reflected in a 15% error in k_p ($\frac{\Delta k_p}{k_p} = 0.15$).

Second, the materials as received normally have cracks in them, introduced during the zone-refining process. It will be shown below that the surface of a crack that extends into the bulk specimen is oxidized just as if it were external surface. Since the number of cracks is certainly not constant from one sample to another, the area used in computing k_p should really be the sum of gross geometric surface area and surface areas of cracks. The use of the former alone can introduce the observed scatter in the data.

Finally, the oxidation rate may be slightly dependent upon oxygen partial pressure. Our results suggest this, although the pressure coefficient of reaction rate is certainly far less than the temperature coefficient. Quantitative measurements of the pressure dependence, however, have been hampered by temperature fluctuations during a single run.

3. Metallography

Pellet XIII-40 was mounted and polished for metallographic examination after it had been oxidized for 114 minutes at a temperature of 1805K and an oxygen partial pressure of 19.9 Torr. Figure 36a, taken at a magnification of about 90X, shows clearly both the grain structure of the bulk material and the dense columnar oxide which forms on the surface during oxidation. The oxidation rate does not seem to change significantly with grain orientation. Figure 36b is similar, but shows a region with an extensive crack running parallel to the ZrB_2 surface. Figure 36c at a magnification of about 450X focuses on the oxide within such a crack. The product is very similar to that on the surface of the refractory and appears to grow into the bulk material at certain preferred growth sites. Figures 36d, e, f, and g show the surface oxide once more at higher magnifications than Figure 36a. The oxide is seen to be crystalline in nature, with the grains running for the most part perpendicular to the ZrB_2 surface. The oxide-metal interface is clearly not smooth, but the points of maximum growth rate do not seem to be related in an obvious way to the structure of the substrate. The interesting photomicrograph in Figure 36h at a magnification of 35X (and the same area at 90X magnification in Figure 36i) shows the oxidation behavior of ZrB_2 in the neighborhood of a crack that intersects the surface. The surface of the crack as seen in these pictures is almost certainly the surface of the original alloy. Therefore, the oxide must grow by inward diffusion of oxygen. The columns of oxide are seen to run perpendicular to the outer surface of the ZrB_2 and, in like manner, are seen to run perpendicular to the surface of the crack (parallel to the sample surface). A crack then effectively increases the surface area of the alloy above that of the outer surface area. Furthermore, the oxide on ZrB_2 does not have the "self-healing" character which is desirable for all high temperature protective coatings. The oxide on $MoSi_2$ would bridge over a crack, partially fill it in; the oxide on ZrB_2 simply grows from the surface of the crack into the bulk alloy.

Approved for Public Release

Contrails

36a 90X

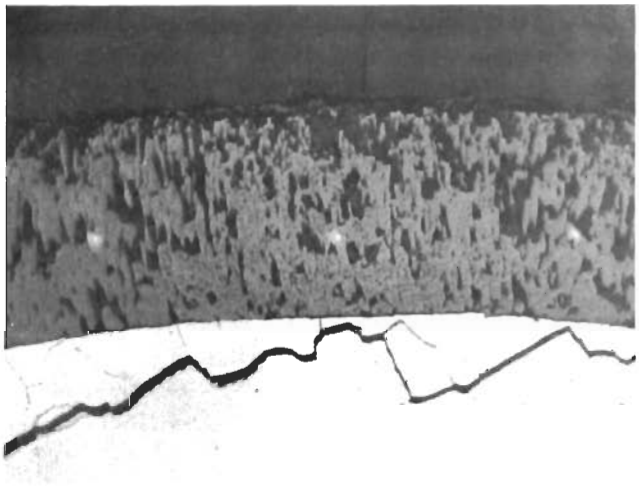

36b 90X

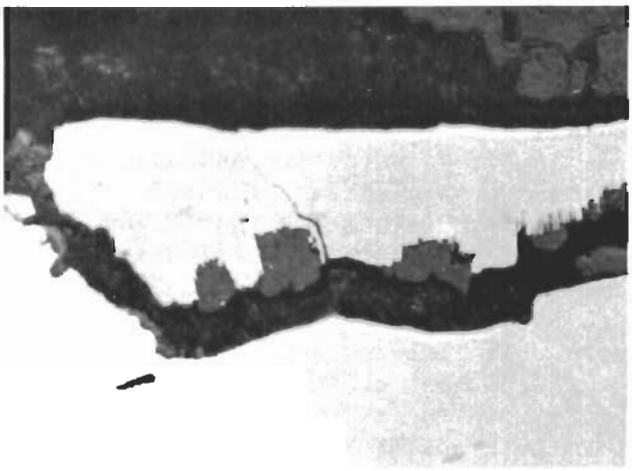

36c 450X

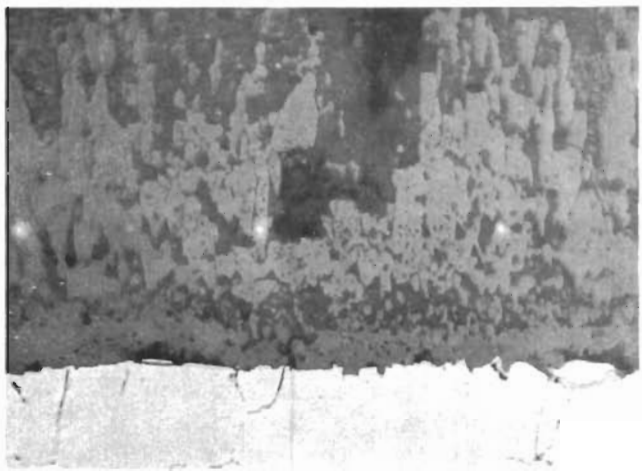

36d 170X

Figure 36 a-d

Photomicrographs of oxidized ZrB_2 (Pellet XIII-40).

T = 1805K, P_{O_2} = 19.9 Torr

Approved for Public Release

Contrails

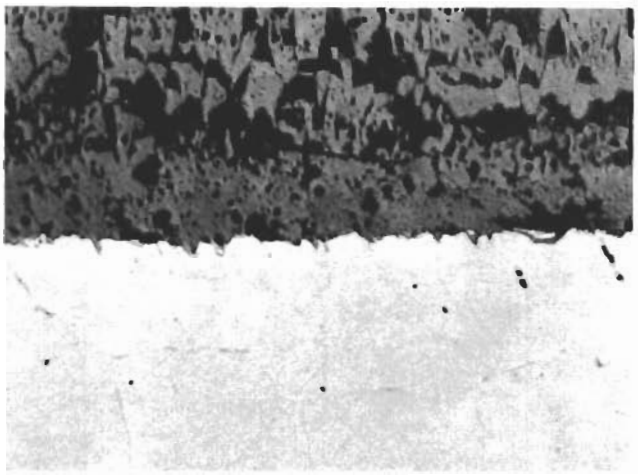

36e 240X

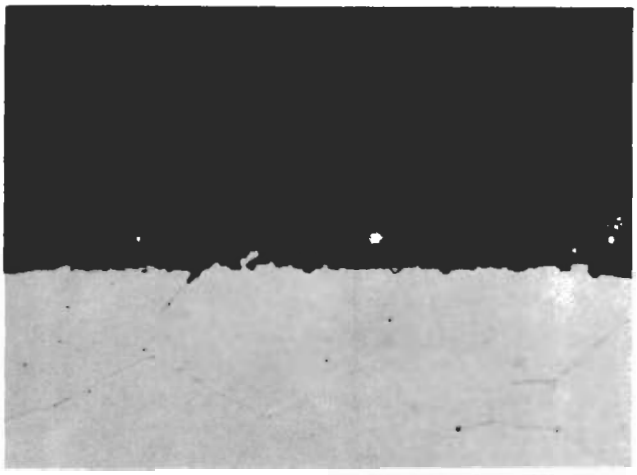

36f 240X

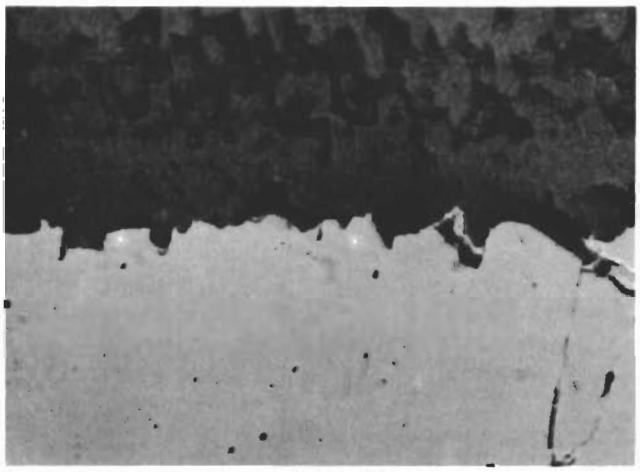

36g 450X

Figure 36 e-g

Photomicrographs of oxidized ZrB_2 (Pellet XIII-40).
T = 1805K, P_{O_2} = 19.9 Torr

Approved for Public Release

Contrails

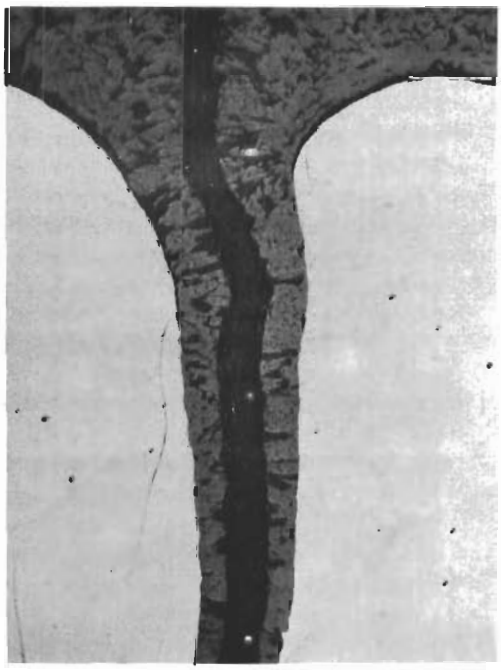

36h 30X 36i 90X

Figure 36 h and i

Photomicrographs of oxidized ZrB_2 (Pellet XIII-40).
T = 1805K, P_{O_2} = 19.9 Torr

Approved for Public Release

Contrails

X-ray analysis of the oxidized surfaces of all of the ZrB_2 samples showed lines for monoclinic ZrO_2 and no extraneous lines. Analysis was, of course, performed on quenched samples and, therefore, does not necessarily reflect accurately the structure of the high temperature oxide. Evidence was not found in either the photomicrographs or in x-ray for the existence of a lower oxide adjacent to alloy substrate.

Since the oxidation of ZrB_2 is parabolic, and the oxide was shown by metallographic examination to grow by inward diffusion of oxygen, it is reasonable to assume that diffusion of oxygen in ZrO_2 is the rate controlling step in the oxidation process. Unfortunately, independent diffusion measurements on ZrO_2 are not available to check this hypothesis. The measurements by Kingery, Pappis, Doty and Hill[43] on the mobility of oxygen ions in stabilized cubic $Zr_{0.85}Ca_{0.15}O_{1.85}$ are obviously not applicable to the present problem.

B. ZIRCONIUM CARBIDE

In the oxidation of zirconium diboride, there is evidence that the rate of reaction decreases with time of exposure and that the oxide film is, therefore, partially protective. In the oxidation of zirconium carbide, on the other hand, the rate of reaction is independent of time, probably because of poor adherence betweeen oxide and substrate.

A general survey of the oxidation of Group IV-A, V-A, and VI-A carbides has been given in a previous report.[42] For the sake of completeness, some of the information pertinent to ZrC will be repeated and extended here.

1. Background

The most recent study of the oxidation behavior of ZrC is contained in the doctoral dissertation of R. W. Bartlett.[44] He measured the rate of weight gain of sized powders in air, oxygen, and oxygen-helium mixtures in the temperature range 450-580C and oxygen pressure range 60 -6.8 atm. Semiquantitative data were obtained at temperatures up to 900C, at oxygen pressures below 4 mm. Net weight changes were monitored with a spring balance and results were interpreted on the bases of stoichiometric non-preferential oxidation of ZrC to ZrO_2 and CO_2. No attempt was made to analyze the gaseous products separately, or to check that the solid phase composition does remain constant during oxidation. In the 450-580C range the weight gain vs time curves showed an initially curved part, when oxidation was very rapid, followed by a straight line section for the remainder of the reaction. Runs lasted from 50-900 minutes, with the longer runs being made at lower temperatures. The oxidation product was found to be cubic ZrO_2 in every case, a phase normally thought to be unstable, but which might be stabilized by small amounts of carbon. At oxygen pressures between 0.1 and 1 atm., the reaction rates appeared to be independent of pressure. Between 1 and 6.8 atm., the rate decreased slightly with increasing pressure. Below 4 Torr, oxidation rates were linear from zero time (i.e., the weight gain curves failed to show an initially curved portion) and were directly proportional to oxygen pressure. The activation energy for oxidation in the 450-580C range computed from the final linear portions of the weight gain curves

Approved for Public Release

Contrails

was found to be 45.7 kcal/mole. In the 580-900C range, at pressures below 4 mm, the oxidation rate was found to be proportional to oxygen pressure, but virtually independent of temperature. The reason for this may be that under the experimental conditions, the reaction was controlled by the rate of arrival of oxygen at the refractory surface. While some monoclinic ZrO_2 was detected in the product oxide at the higher temperatures, cubic ZrO_2 still seemed to be the major product. In contrast to zirconium metal, which follows a cubic rate law between 575 and 950C, the oxidation of ZrC is linear in the same range.

Watt, Cockett, and Hall[45] made a single weight change measurement of 49.8 mg/cm^2 in a solid sample of ZrC of density 6.20 g/cc and 4.8% porosity, exposed to a stream of dry air flowing at 5.3 cm/sec, for 30 minutes at 800C. Zirconium metal under the same conditions would have shown a weight gain of 1.75 mg/cm^2. ZrB_2, by extrapolation of the data in the previous section, would have picked up 0.1 mg/cm^2 of oxygen.

2. Experimental Rate Data

The oxidation of ZrC was studied at temperatures of 1126 to 2165K and oxygen partial pressures of 3-26 Torr. The oxidation appears to be linear and non-preferential, i.e., zirconium is oxidized at the same rate as carbon. Both CO(g) and CO_2(g) are formed as reaction products. The solid oxide gave x-ray lines for monoclinic ZrO_2 only.

The data obtained are summarized in Table V. The first column identifies each sample pellet. The second column gives the weight of each pellet after it had been degassed at 2200K in pure helium until the signal from the thermal conductivity cell indicated that no permanent gases were being evolved. The third column gives geometric surface areas, calculated from micrometer measurements of the height and diameter of the cylindrical pellets. The fourth column records sample densities, computed from weights after degassing and pellet dimensions. Columns 5, 6, and 7 record the pellet temperature, assuming an emissivity of 0.7, oxygen partial pressure, and carrier gas flow rate, respectively, for each oxidation run. The duration of the experiment is given in column 11, and the net weight change, total CO(g) produced, and total CO_2(g) produced in this time are given in columns 8, 9, and 10, respectively.

From the measured quantities in columns 8-10, the derived quantities, total carbon consumed and total zirconium consumed, in columns 12-14 can be computed if the nature of the oxidation products is assumed. From the observed weight changes in the Ascarite bulbs, it is known that both CO(g) and CO_2(g) form during oxidation. In addition, a white nonadherent oxide, with the x-ray pattern of ZrO_2(s), is visible on the surface of the sample pellets after reaction. If it is assumed that the only oxidation products are CO_2(g), CO(g), and ZrO_2(s), then the total carbon consumed, c, is calculated from the measured weights w_{CO_2} and w_{CO} of CO_2(g) and CO(g), respectively.

$$c = \frac{(C)}{(CO_2)} \; w_{CO_2} + \frac{(C)}{(CO)} \; w_{CO}$$

where the symbols in brackets represent molecular weights. The total weight of zirconium, z, that has been converted to oxide is calculated from the measured

Approved for Public Release

TABLE V

SUMMARY OF EXPERIMENTAL RATE DATA ON ZrC

(1) Pellet	(2) Weight after Degassing, g	(3) Surface Area, cm^2	(4) Density, g/cc	(5) Temp., ^oK	(6) Oxygen Pressure, Torr	(7) Flow Rate, cc/min	(8) Wt. Change, g(w_o)	(9) CO Formed, g(w_{CO_2})	(10) CO_2 Formed, g(w_{CO_2})	(11) Time, min	(12) (c) C Consumed, g	(13) (z) Zr Consumed, g	(14) $\frac{Zr}{C}$	(15) Wt. Change, g/cm^2-min x 10^{-4}
XII-8	0.4446	1.1031	5.72	1126	22.9	58.6	-	0.0001	0.0611	51	-	-	-	-
XII-5	0.5645	1.3942	5.29	1259	20.4	58.6	-	-	0.0709	128	-	-	-	-
XII-3	0.6963	1.4926	5.89	1559	21.2	58.6	-	0.0289	0.0399	62	-	-	-	-
X-31	0.5864	1.310	5.89	1857	9.1	58.6	0.0402	0.0438	0.0220	129	0.0248	0.1852	7.47	2.38
X-29	0.7073	1.450	6.19	1944	8.1	58.6	0.0366	0.0405	0.0145	120	0.0214	0.1652	7.72	2.10
XII-1	0.7051	1.500	5.05	1969	25.9	58.6	0.0851	0.0968	0.0356	112	0.0510	0.388	7.60	5.06
X-27	0.6361	1.252	6.71	2066	8.5	58.6	0.0389	0.0464	0.0175	124	0.0236	0.1780	7.55	2.50
X-16	0.6840	1.388	6.33	2066	8.5	58.6	0.0402	0.0540	0.0073	119	0.0252	0.1862	7.39	2.44
VII-37	0.6643	1.528	5.41	2098	3.0	51.5	0.0207	0.0242	0.0079	180	0.0126	0.0949	7.54	0.754
X-25	0.6812	1.371	6.40	2165	8.9	58.6	0.0356	0.0523	0.0072	120	0.1710	0.0244	7.01	2.16

Approved for Public Release

Confidential

Contrails

weight change, w_o, and the derived carbon consumption:

$$z = \frac{(Zr)}{2(O)} \quad (w_o + c)$$

The ratio of the number of grams of zirconium consumed to the number of grams of carbon consumed during oxidation is given in column 14 of Table V. The ratio is seen to have an approximately constant value of 7.5 ± 0.2. Since the corresponding ratio in the ZrC starting material is 7.6, it would appear that the oxidation of ZrC is stoichiometric. That is, for each zirconium atom converted to oxide, a single carbon atom is also converted to oxide. In column 15, the rate of oxidation is seen to be highest for pellet XII-1. In all of the other runs where weight data is given, more than 90% of the oxygen passed over the refractory pellet reacted with it, and the reaction was probably controlled, therefore, by the rate of arrival of oxygen gas at the sample surface. For XII-1, the supply of oxygen was sufficient to permit a significant determination of oxidation rate.

Weight change data is not given for pellets XII-8, XII-5, and XII-3 because at these relatively low temperatures the pellets were broken apart by the oxidation process. At the end of each experiment, the grain boundaries of the ZrC were seen to be outlined by a white material, probably ZrO_2. The growth of the oxide in pre-existing cracks and grain boundaries of ZrC undoubtedly creates enough stress to fracture the carbide.

3. Metallography

Pellet XII-1, which had been exposed for 112 minutes at a temperature of 1969K and oxygen partial pressure of 25.9 Torr in helium, was mounted and polished for metallographic examination. The photomicrographs are reproduced in Figure 37, in order of increasing magnification. After oxidation, the ZrC pellet was supported in plastic and polished down to the metallic surface of the alloy. Figure 31a shows the prepared oxidized specimen, at a magnification of 7X. The gray outer rim is the oxide and the inner bright circular area is the surface of carbide. To the naked eye, the outer oxide coating looks white and chalky and the inner surface, from which the oxide coating was polished off, looks bright and metallic. A mottled rim is clearly visible along the oxide-alloy interface and most of the remaining pictures will focus on portions of this interface. Figure 37b, at a magnification of 60X, is the first of the series. The oxide fills the entire upper half of the photograph and the alloy the lower. The oxide is obviously growing down grain boundaries in the carbide and enveloping individual alloy crystallites, a phenomenon not previously observed with any system studied in this laboratory. The structure of the bulk oxide is very different from that on ZrB_2 (Figure 36), although both show only the x-ray lines for monoclinic ZrO_2. On ZrB_2, the oxide was seen to grow in a columnar structure; on ZrC, the ZrO_2 assumes a grain structure very similar to that of the original alloy. Figures 37c and 37d show the oxide alloy interface at a still

Approved for Public Release

Contrails

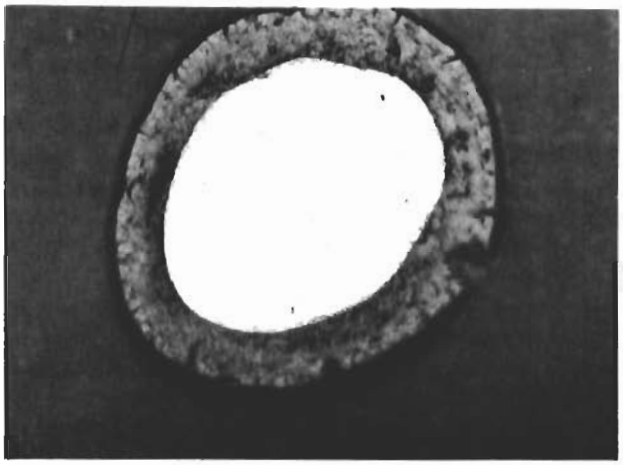

37a 7X

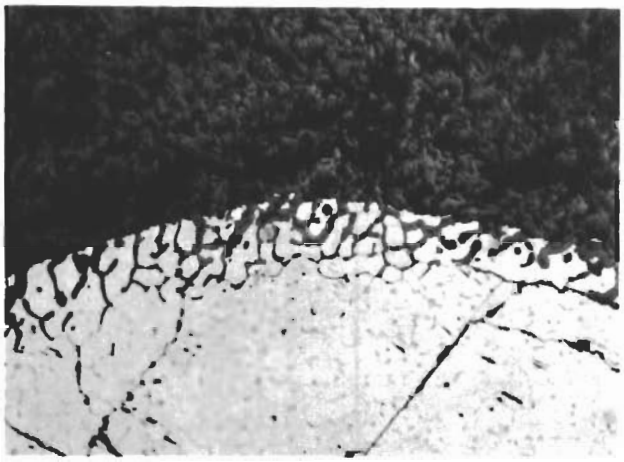

37b 60X

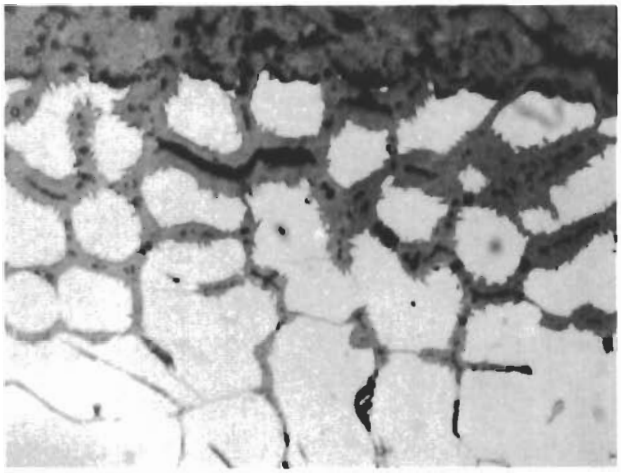

37c 390X

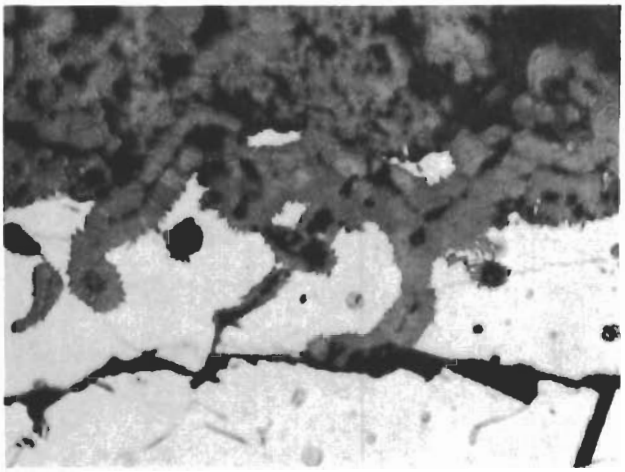

37d 390X

Figure 37 a-d

Photomicrographs of oxidized ZrC (Pellet XII-1).

T = 1969K, P_{O_2} = 25.9 Torr

Approved for Public Release

Contrails

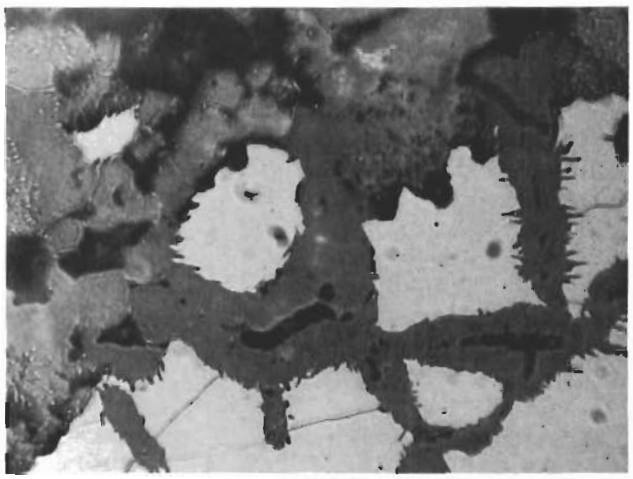

37e 690X

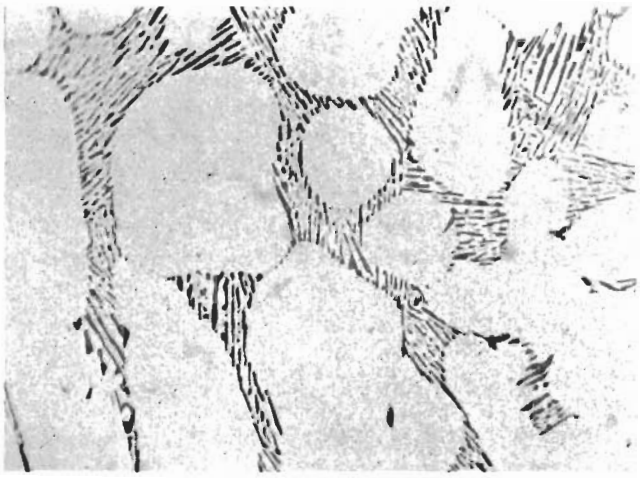

37f 690X

Figure 37 e and f

Photomicrographs of oxidized ZrC (Pellet XII-1).

T = 1969K, P_{O_2} = 25.9 Torr

Approved for Public Release

Contrails

higher magnification, 390X, and one sees even more clearly the preferential oxidation of grain boundaries and the lateral fingerlike growth of oxide from the boundaries into the crystallite bulk. This would appear to be the mechanism of oxide growth on ZrC at high temperatures--rapid attack at grain boundaries and slow oxidation of the alloy from the grain boundary surface inward. Figure 37e, at a magnification of 680X, shows portions of the alloy completely enveloped by oxide. Finally, Figure 37f is a view of the alloy surface at a magnification of 680X. This surface had been covered with a dense oxide prior to polishing, and one sees here the penetration of the oxide into grain boundaries of the alloy. Between 1126 and 1559K, the grain boundary attack results in intergranular fracture of the alloy. Above 1580K, there is apparently enough plasticity in either alloy, oxide, or both so that the sample remains intact during oxidation.

Approved for Public Release

Contrails

VI. MASS TRANSPORT STUDIES*

A. INTRODUCTION

In the oxidation of the zirconium and hafnium carbides and borides, coatings of oxide will form; providing that these are adherent and nonporous, the rate of oxidation may be limited by the rate of diffusion through these oxide coatings.

Our objectives in the Air Force program are to present data on the over-all rates of oxidation of pure materials and to determine and understand, as far as possible, the mechanisms of oxidation so that one can design carbide or boride structural bodies which will have maximum service life in oxidizing atmospheres.

The rates of diffusion through oxides are determined by the defect structure of these materials. There is also a possibility that the defect structure may be a factor in whether an adherent and nonporous coating is formed. Thus, a knowledge of transport processes and defect structure in the zirconium and hafnium oxides and the degree to which these can be controlled can be important in understanding observed kinetic behavior and in "engineering" ceramic bodies for specific applications.

We have undertaken the study of mass transport in zirconium dioxide and its relationship to the defect structure. The proposed program of electrical conductivity, ion transport, and isotope tracer studies was discussed in Part I of this report.

We present here the results obtained during this report period on the program. These consisted of the preparation of suitable samples and the measurement of their electrical conductivity. The results are discussed in relationship to other work which has recently become available. In the discussion, we have also considered the defect structure of the oxide and its relationship to the observed oxidation kinetics.

B. EXPERIMENTAL WORK

During this report period, sample material was prepared by fusing powdered ZrO_2 in an ADL-Strong arc-imaging furnace into boules about one cm diameter and three centimeters long. Two sources of powder were used in preparation of the boules. One was a spectrographic grade ZrO_2 powder from Wah Chang Corporation and the second was a powder which we prepared by oxidation of pure zirconium sponge obtained from Wah Chang Corporation. The details of preparation and the analyses

---

* - Prepared by L. A. McClaine, Arthur D. Little, San Francisco, California.

Approved for Public Release

Contrails

are presented in Chapter IV of this report. Density measurements indicate that material prepared in this manner is at least 99% of theoretical density. A semi-quantitative spectrographic analysis of a wafer cut from a fused boule, when compared to an analysis of the powder, indicated no significant change in composition arising from the fusion operation.

Resistance measurements were made on wafers cut from the boules in a temperature range from ambient to 1900K and in atmospheres of air or oxygen at one atmosphere pressure. A platinum-wound tube furnace was used and most temperature measurements were made by sighting an optical pyrometer on the sample through a small hole in the furnace tube. The resistance was measured at one kc with a General Radio Type 1650-A Impedance Bridge. The sample heating or cooling rate was usually about $1^{\circ}C$/min.

For measurements presented in this report a sample holder providing a constant pressure contact to the samples was used. A representation of this holder is given in Figure 38. The holder was cut from a low-density alumina block in the manner shown to minimize parallel conduction paths. Small platinum electrodes were vacuum plated onto the samples to insure good electrical contact. One side of the sample rested on a platinum foil to which the lower electrical lead was welded. The other contact was made through a bead on the end of the upper platinum lead. The bottom portion of the holder was fixed in place and the upper contact maintained with a fixed pressure as determined by the weight of the upper portion of the holder. Ceramic disks for the purposes of centering the holder and minimizing radiation losses were mounted above and below the sample position.

Using this sample holder, we have obtained good reproducibility in the rate of change of resistance with temperature, but aboslute resistance values vary from run to run and are easily affected by mechanical disturbance of the holder system. Thus we developed, toward the end of this report period, a technique for attaching electrical leads directly to the sample faces. We have found that if we vapor plate a platinum coating we can then sinter an electrical lead to this face by using a "platinum black" paint and firing the assembly. If we do not first put down a vapor coating, we find that the platinum black paint will simply ball up when fired and will not wet the sample surface. This technique, as opposed to the holder described above, should permit absolute resistance measurements and further minimize the possibility of short circuiting the sample.

C. RESULTS

Samples were cut from boules made from both sources of ZrO_2. Resistance was measured as a function of temperature and the sample was cycled repeatedly either up and down through the monoclinic-tetragonal transition or within the tetragonal region.

Figure 39 (for Sample #6, Run #3) shows the type of data obtained on a run up and down through the monoclinic-tetragonal phase transition. A hysteresis loop is observed with sharp breaks followed by a long nonequilibrium period. The transition separates two difference crystallographic structures and probably different conduction mechanisms. For this run, calculations from the slopes of the linear portions of the curves yield values of activation energy of 0.606 ev in the tetragonal region and 1.14 ev in the monoclinic region.

Approved for Public Release

Contrails

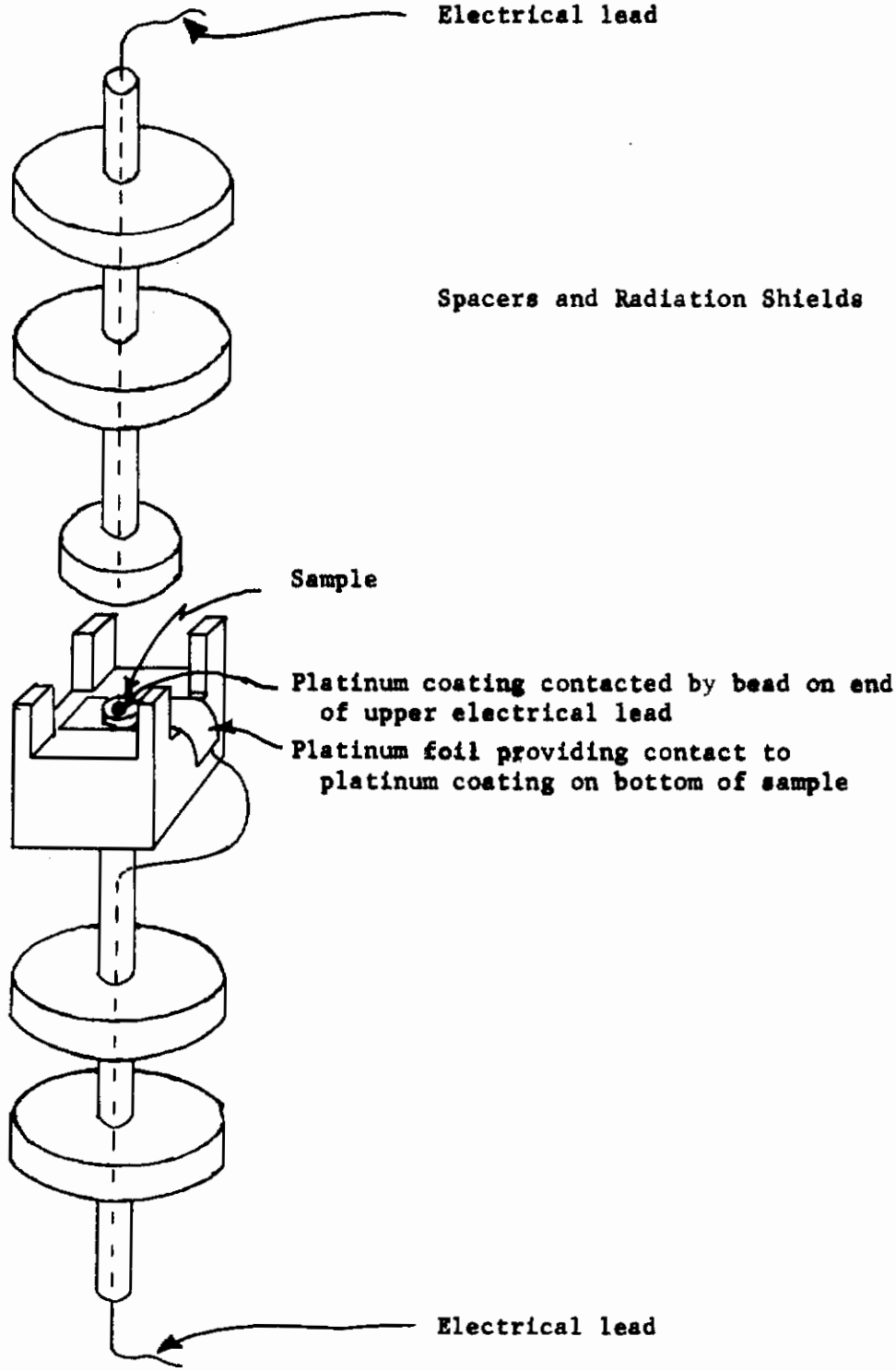

Figure 38. - Sample holder for electrical resistance measurements.

Approved for Public Release

Contrails

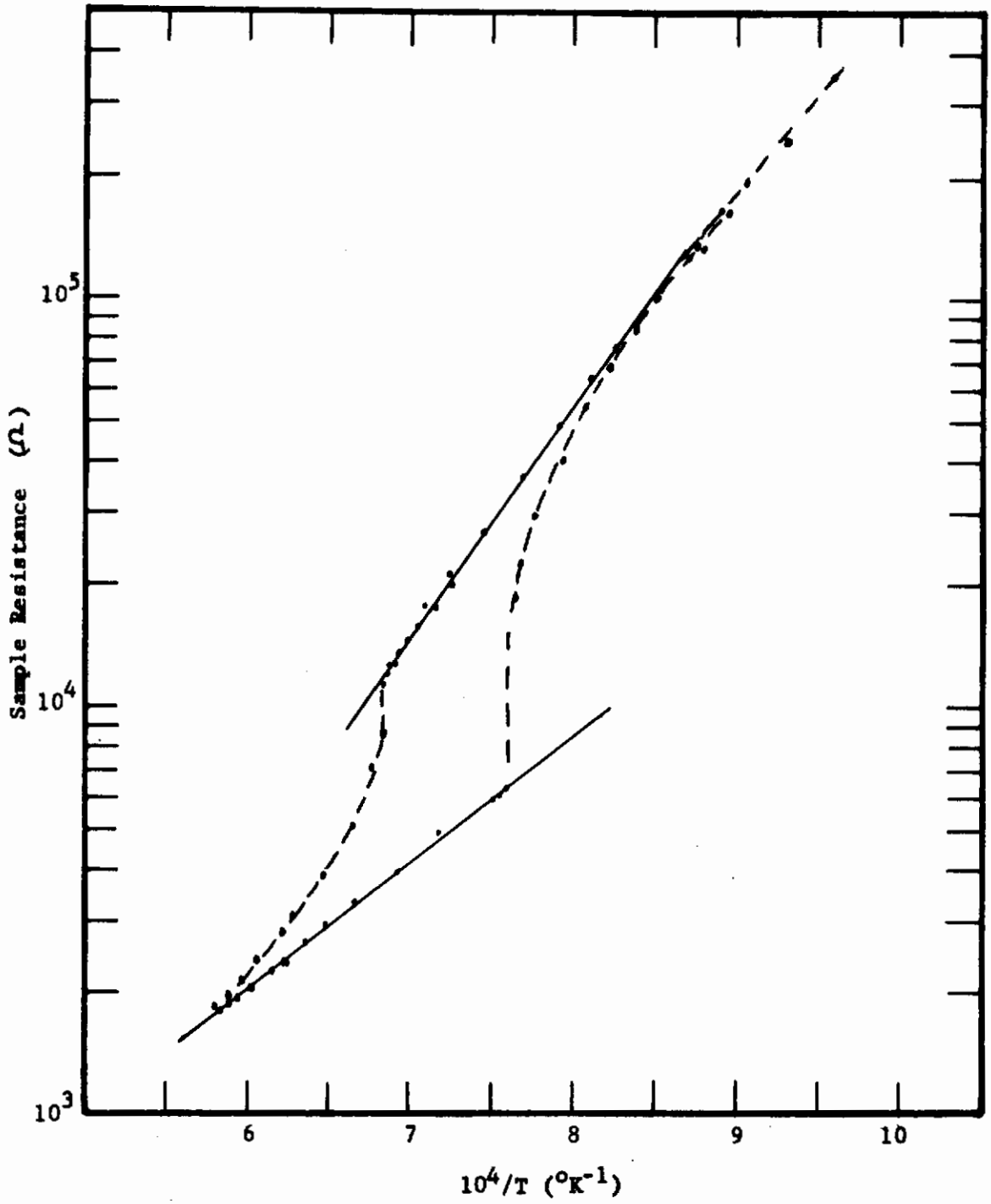

Figure 39. - Electrical resistance of fused ZrO_2 cycled through the monoclinic-tetragonal phase transition.

Approved for Public Release

Contrails

Figure 40 presents data obtained on repeated cycling in the tetragonal region of Sample #7 under two different oxygen pressures. Also included is one set of data points from Sample #4, for which sample the highest temperatures were reached in any runs. This run resulted in the burn out of the furnace and subsequent runs were limited to lower temperatures. The best straight line fit to these data in the region 1100 to 1400C gives an activation energy of 0.548 and 0.595. It is not known whether there is any significance to this slight difference in activation energy for the different oxygen pressures. There does appear to be a break in these curves for Sample #7 at the high temperature end and the data for Sample #4, which extends to higher temperatures, also shows this much greater slope. If true, and not due to experimental procedures, this must indicate a change in conduction mechanism.

D. DISCUSSION

Kingery et al[43] have reported on oxygen ion mobility in cubic $Zr_{0.85}Ca_{0.15}O_{1.85}$ determined directly by isotope exchange measurements. Their electrical conductivity measurements indicate that the conductivity for this material is wholly ionic. Hund[46] has reported conductivity data for the same composition of lime-stabilized zirconia. The activation energy calculated from Hund's data is in good agreement with Kingery's study, but the absolute conductivity data are smaller.

Kauer[47] has reported on conductivity measurements in the ZrO_2-MgO system. His samples contained between .03 and .55 mole percent of impurity and he studied conductivity in both monoclinic and tetragonal phase. The purest sample had an activation energy of 0.580 ev in the tetragonal region. Thermoelectric power measurements were carried out and in all cases positive current carriers were indicated. Kauer interpreted his studies as indicating that the conductivity was due to mobility of oxygen vacancies. In view of the much higher activation energy determined for oxygen ion mobility in Kingery's study, this conclusion appears to be in error. Activation energies from our data on pure ZrO_2 in the same region do agree with Kauer's study rather than Kingery's, but must be attributed to electronic rather than ionic conductivity.

Several current studies were discussed at the recent meeting on Research-in-Progress on ZrO_2.[48] R. W. Vest working at ARL has studied high purity ZrO_2 up to 1300C. Work in progress indicates an activation energy in the tetragonal region of 0.61 ev. His results at 1300C indicate p-type conduction above 10^{-3} oxygen pressure and n-type below. No study had been completed on the proportions of ionic and electronic conductivity. M. Hoch and A. Iyer at the University of Cincinnati are studying the effect on electrical conductivity of varying the ratio of CaO to ZrO_2 from 15 to 30%. Their preliminary findings show a decrease in conductivity with increase in CaO content, which may indicate that increasing defect concentration favors a clustering action. D. L. Douglass of General Electric Company[56] reported on diffusion studies on $ZrO_{1.995}$ between 950 and 1250C which yielded the expression $D = 0.55\ e^{-33,500 \pm 3,000/RT}\ cm^2/sec.$

Approved for Public Release

Contrails

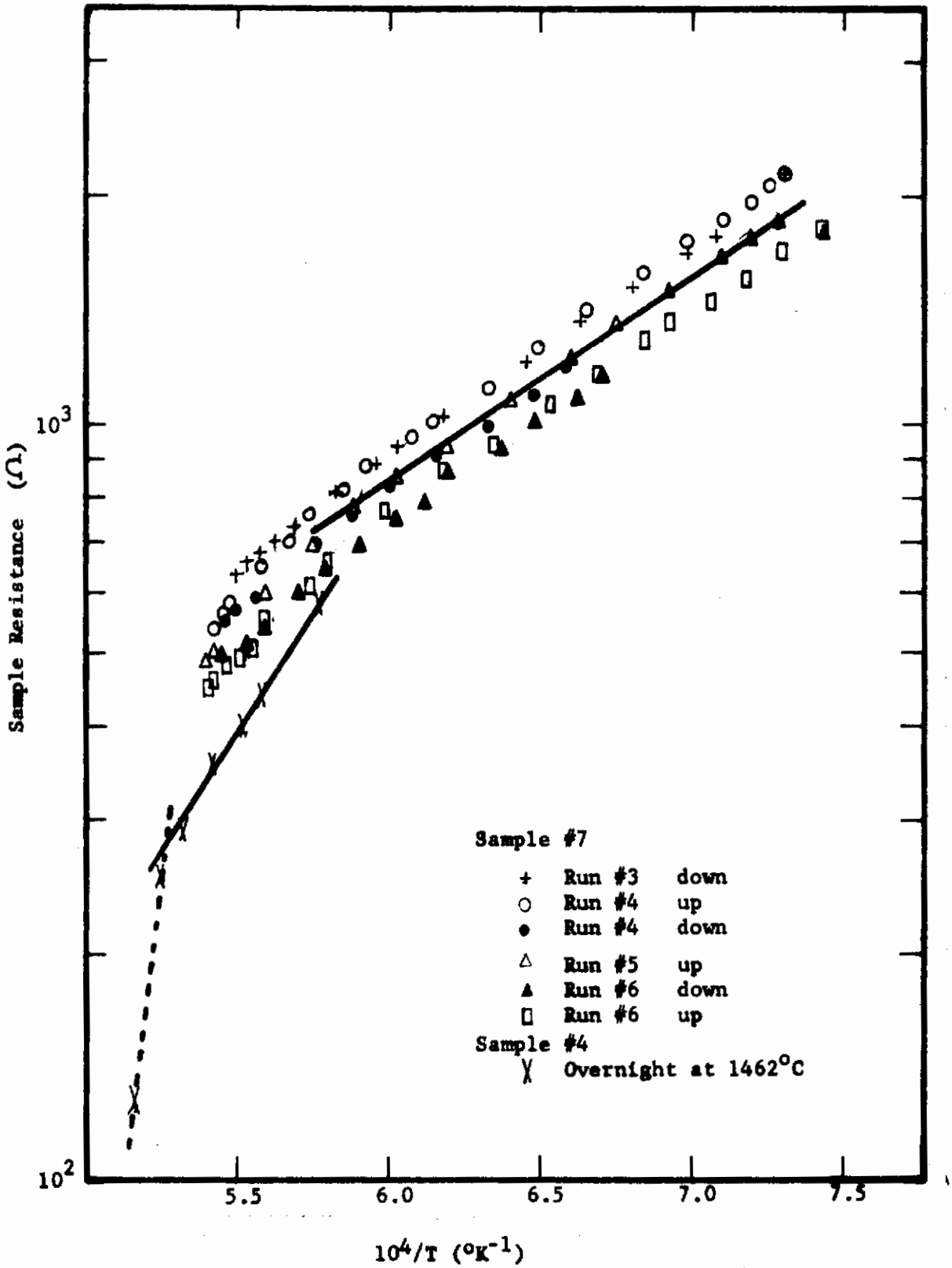

Figure 40. - Electrical resistance measurements on fused ZrO_2 in the tetragonal phase region

Approved for Public Release

Contrails

On Figure 41 we show the diffusion data of Kingery for $Zr_{0.85}Ca_{0.15}O_{1.85}$ and that of Douglass for $ZrO_{1.995}$; these correspond to vacancy contents of 42×10^{20} V_O per cc and 1.4×10^{20} V_O per cc, respectively. On the basis of difference in vacancy content, we would expect a thirty-fold difference in D. The results for the two studies check quite well.

We also show on this figure an estimated curve for diffusion corresponding to intrinsic oxygen vacancy defects, assuming the energy of formation for an oxygen vacancy of 2 ev. This estimate is made assuming that

$$\left[V_O \right] = N_O e^{-\frac{2}{kt}}$$

where N_O is the number of oxygen atoms per cc and $e^{-\frac{2}{kt}}$ is the fraction with sufficient energy to move into surface sites leaving a vacancy. By this means we calculate $\left[V_O \right]$ at 1250K equals about 10^{15} per cc. Since D is proportional to the number of vacancies, we can locate D for intrinsic diffusion with respect to the experimental curves on Figure 41. The slope of the curve of D vs 1/T for intrinsic vacancy content will be equal to the sum of the energy for formation of a vacancy (which we have assumed is 2 ev) plus that for motion of the vacancy which the experimental curves indicate are on the order of 1.25 ev.

The activation energy of about 0.6 ev found in our conductivity studies in the tetragonal region up to 1700K must be for an electronic conduction mechanism. We have observed a tendency for a break in these conduction curves of Sample #7 and a higher slope for Sample #4, which may be evidence for a change in the controlling conduction mechanism. The data are limited, but do indicate an activation energy of 1.38 ev above 1700K. This would correspond to that found by Kingery and by Douglass for oxygen transport and could indicate that ionic conductivity becomes more important than electronic in this region. We can expect that trace impurities in the ZrO_2 will produce a short region of impurity-controlled conduction followed by a further break to an intrinsic conduction region. The last point obtained on Sample #4 at 1930K does indicate a sharp break and may be the onset of the intrinsic conduction region. More data is needed to confirm this interpretation.

The diffusivity, D, is proportional to both the probability that a diffusing ion is next to a vacant site and the probability that the ion has the energy to surmount the energy barrier between its site and the vacant site. As a result, the activation energy for diffusion in a pure material is the sum of the energy required for motion and that required for formation of a vacancy. Using our value of 1.38 for motion plus our estimate of 2 ev for formation, we have a total of 3.38 ev or about 77 kcal as the estimated energy of activation for diffusion in ZrO_2. Joan Berkowitz-Mattuck has reported in Chapter V of this report an activation energy for the observed parabolic oxidation behavior of ZrB_2. Since her data indicate that diffusion through the ZrO_2 coating is the rate limiting step, this value obtained from the kinetic studies should correspond to the activation energy for diffusion in ZrO_2. She finds a value of 66±9 kcals, i.e., in close agreement with our estimate.

Approved for Public Release

Contrails

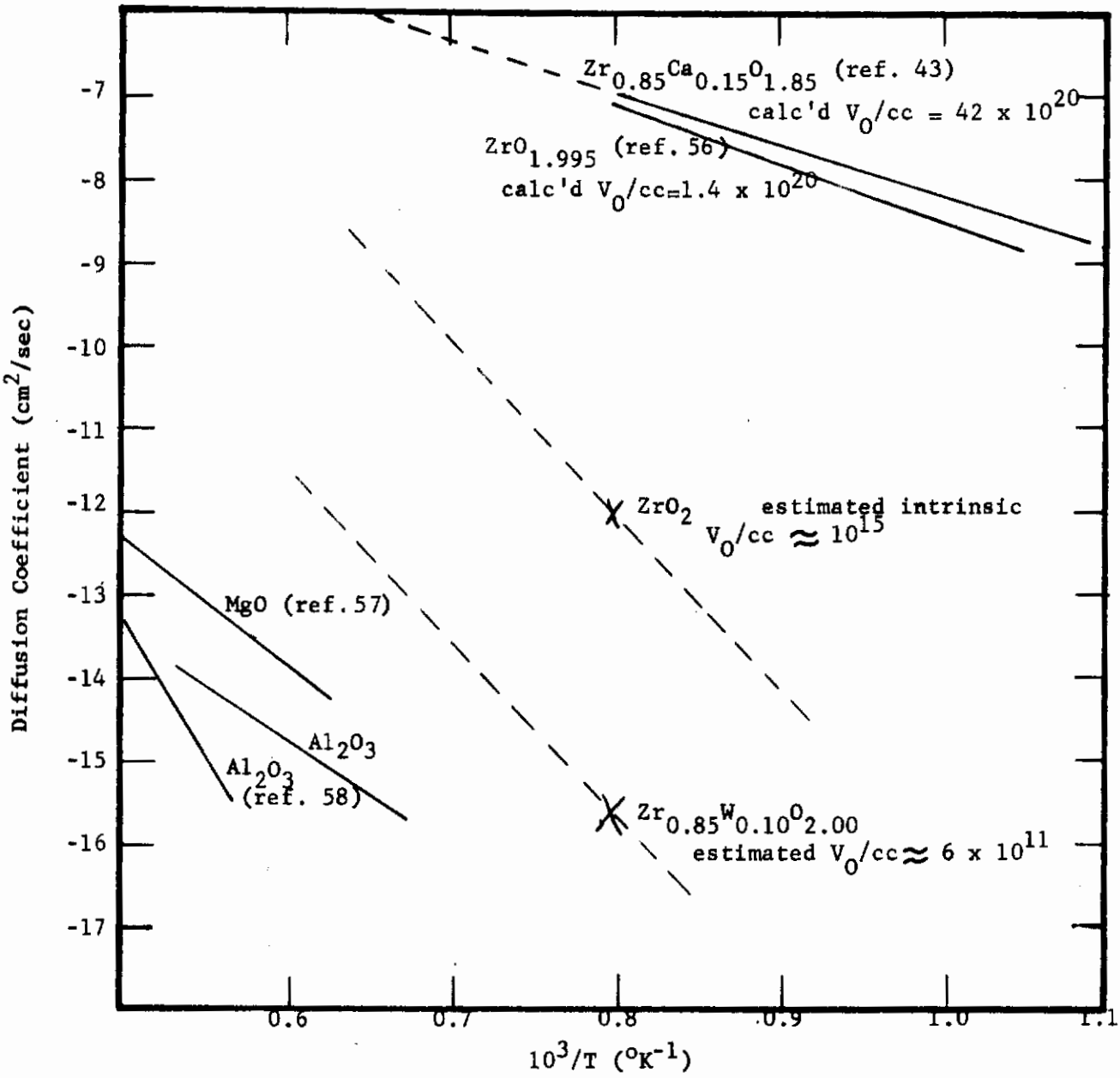

Figure 41. - Diffusivity vs reciprocal temperature for O_2 in selected oxides. Experimental and estimated curves.

Approved for Public Release

Contrails

It is instructive to consider controlling vacancy content by addition of higher valent cations. For addition of WO_3 to a ZrO_2 lattice, we can write an equation

$$2WO_3 \text{ (in } ZrO_2) = 2W_{Zr} + 6O_O + V_{Zr}$$

indicating that $\left[V_{Zr}\right] = \frac{1}{2}\left[W_{Zr}\right]$. We also know that for intrinsic vacancy formation $\left[V_{Zr}\right]\left[V_O\right]^2 = K_i(T)$. Thus, with WO_3 present in ZrO_2

$$\left[V_O\right] = \frac{\sqrt{2}\ K_i^{1/2}}{\left[W_{Zr}\right]^{1/2}}$$

We have previously calculated that $\left[V_O\right] \cong 10^{15}$ per cc in pure ZrO_2 at 1250K. Thus, assuming equal activation energy for formation of zirconium vacancies, $K_i = 1/2 \times 10^{45}$ at 1250K. If we assume we can incorporate 3 atom percent of W in ZrO_2 and that it behaves as we have indicated, we can estimate that

$$\left[V_O\right] = \frac{(10^{45})^{1/2}}{(25 \times 10^{20})^{1/2}} = .6 \times 10^{12} \text{ per cc}$$

Looking again at Figure 41 and recalling that D is proportional to the number of vacancy sites, we can visualize that D for oxygen diffusion will be reduced 1000-fold if tungsten will build into ZrO_2 in this manner. If oxygen diffusion in ZrO_2 is the rate determining step in oxidation of ZrB_2, we can expect reductions in the rates of oxidation if tungsten is a part of the original ZrB_2 body and will build into the ZrO_2 coating in this manner.

It is interesting to speculate on the effect which defect structure of the oxide might have on the adherence and porosity of an oxide coating. As reported in Chapter V of this report, the oxide coating found on oxidation of ZrB_2 is dense and adherent, while that on ZrC is porous and nonadherent. ZrB_2 exhibits behavior characteristic of a diffusion-controlled reaction, whereas ZrC does not. We can expect that B and C may exist as impurities in the ZrO_2. Lets consider the addition of boron and carbon to ZrO_2 and their effect on its defect structure.

Because of the position of C on the electronegativity scale, about equidistant between Zr and O, we would guess that its size would be controlling and that it would enter the ZrO_2 lattice on O sites. Assuming that it would ionize to a greater extent than O, this would have the effect of forming oxygen vacancies. B, however, is much closer to Zr than to O on the electronegativity scale. In addition, its size is very small and thus we would guess that it would enter the ZrO_2 lattice as positively charged interstitials. This could have the effect of decreasing the oxygen vacancy content. In addition to this impurity effect which can control

Approved for Public Release

Contrails

vacancy content, there is a control due to the oxygen activity in accordance with the reaction:

$$ZrO_2 = ZO_{2-\delta} + \delta V_O + \frac{\delta}{2} O_2(g)$$

The zirconium oxide structure is known over a range of $ZrO_{1.90}$ to ZrO_2, a low oxygen activity at equilibrium favoring the oxygen deficiency. Oxide forming at the carbide or boride interface we would expect to be at the oxygen deficient end. Thus, we can expect a variation in vacancy content from this effect from the carbide-oxide (or boride-oxide) interface to the oxide-atmosphere interface. The vacancy content from this effect will be on the order of a few atom percent at the carbide-oxide interface and negligible at the oxide-atmosphere interface. The carbon content of TiO_2 coatings on TiC has been reported as a few tenths of a percent, and assuming a similar content in ZrO_2 the vacancy content at the carbide-oxide interface from carbon impurity affect alone could be a few tenths atom percent and only slightly lower at the oxide-atmosphere interface. Thus, at the oxide-atmosphere interface the C content would control the vacancy content while at the carbide-oxide interface the stoichiometry determined by the oxygen activity would control. Both effects tend to increase the vacancy content over the intrinsic level. In the case of boride, B in the ZrO_2 will probably tend to reduce the level below the intrinsic level and oppose the oxygen activity affect.

We conclude that a ZrO_2 coating with B impurity such as we would expect on ZrB_2 should be more protective than a ZrO_2 coating with C impurity such as we would expect on ZrC. Thus the observed behavior is not counter to our expectations from a consideration of the defect structure of the oxide. It is very likely that the magnitude and the way in which vacancy content varies across the ZrO_2 coatings plays a part in the different adherence and porosity behavior observed in the oxidations of the carbide and boride of zirconium.

Approved for Public Release

Contrails

VII. MASS SPECTROMETRIC INVESTIGATION OF THE KINETICS OF OXIDATION OF MOLYBDENUM*

A. SUMMARY

A mass spectrometer has been used to study the oxidation kinetics of molybdenum in the temperature range of 1400 to 2000K and oxygen pressures of 10^{-5} to 10^{-6} atm. Under these conditions, oxidation occurs primarily by the vaporization of MoO_2 and MoO_3 gaseous species. Between 1400 and about 1700K, MoO_3 is the predominant vaporizing species. Above 1700K, the vaporization rate of MoO_3 decreases while the rate of MoO_2 vaporization continues to increase. The vaporization curves cross at about 1700K with the temperature of the cross-over point increasing slowly with increasing oxygen pressure. By contrast, mass spectrometer studies of the equilibrium vaporization from $MoO_2(s)$[49] show a much stronger temperature dependence, with MoO_3 the predominant vaporizing species over the entire temperature range. This proves that a solid oxide film does not form on the molybdenum surface during the oxidation studies, although thermodynamically $MoO_2(s)$ would be stable.

The rate of arrival of oxygen at the surface is determined by the kinetics of molecular flow since the mean free path for gas molecules is large compared with the distance from the reaction site to the mass spectrometer entrance slit. The rate of arrival of oxygen at the surface is about 400 times the rate of consumption at 1700K and is not, therefore, the rate controlling step. The oxidation rate is first order in oxygen pressure.

The rate of formation of an active precursor at the molybdenum-oxygen interface appears to be rate determining and a stepwise mechanism is postulated. A rapid equilibration between adsorbed MoO_2 and MoO_3 species is shown to be in agreement with the experimental results. The observed oxidation rate of molybdenum was 0.1 microgram/cm^2 sec at 1700K and 10^{-6} atm of oxygen.

B. INTRODUCTION

The purpose of this work is to provide an insight into the oxidation of metals at high temperatures, under conditions for which the formation of gaseous oxides becomes a significant part of the over-all process. The essential steps in the oxidation of metals are (1) chemical reaction at an interface, and once an oxide layer has been built up (2) mass transport of oxygen or metal through that layer. The work on metal oxidation over the last 30 years has dealt primarily with the latter step.

More recently, attention has been paid to interface reactions, but again principally from the point of view of the structure of the condensed phase. While it was

---

* - Work by Alfred Buchler, Joan Berkowitz-Mattuck, and John L. Engelke, Arthur D. Little, Inc., Cambridge, Massachusetts.

Approved for Public Release

Contrails

established quite early that formation of volatile oxides constitute an important part of the high temperature oxidation of some metals, such as molybdenum and tungsten, means were lacking until recently to establish reliably their chemical formulas. This situation has been changed radically by the development of high temperature mass spectrometric techniques.

In the experiments to be described, oxygen at low pressures impinges on a sheet of molybdenum heated to temperatures between 1200-1700C. The gaseous molybdenum oxides form at the gas-solid interface, then reach the mass spectrometer slits without making collisions with other gas phase molecules. The mass spectrometer thus provides an accurate sampling of the gaseous reaction products formed at the molybdenum-oxygen interface. It is particularly interesting to compare the results obtained in this fashion with those obtained from equilibrium vaporization studies of molybdenum dioxide. It is immediately obvious that no condensed oxide film is formed in the present experiment even though the effective oxygen pressure is considerably higher than that in equilibrium with molybdenum dioxide. At the same time, the results suggest that thermodynamic equilibrium is established between MoO_2 and MoO_3 molecules on the surface before they evaporate, and that a prior interface reaction controls the rate of over-all oxidation.

C. EXPERIMENTAL DETAILS

1. Sample Preparation

The 1.8 cm x 1.5 cm plate used in these experiments was cut from a 0.010 in. thick sheet of rolled molybdenum. After mechanical polishing, the polycrystalline sample was electropolished for one minute at 20C in a solution of 5% H_2SO_4 and 1.25% HF in methanol. A rapid flow of electrolyte was maintained parallel to the surface and a potential of 60 volts used. A highly polished, microscopically smooth surface was obtained.

Although an x-ray Laue pattern indicates an initial preferred orientation, heat treatment during the preliminary vacuum degassing in the mass spectrometer (ca. 1800C) caused recrystallization and grain growth which destroyed any orientation effects. The surface density expected for low index planes on molybdenum is about 1×10^{15} atoms/cm^2.

2. Apparatus

A Nuclide Analysis Associates 12-in. radius, 60°-sector, direction-focusing mass spectrometer was used for this work. The modification of the reaction chamber for kinetic studies was previously described.[50] The molybdenum plate is mounted on tungsten support rods at a 45° angle to the beam-defining slits of the mass spectrometer and is heated from behind by electron bombardment from a rhenium filament. Oxygen is introduced through a 10-in. length of 0.083-in. I.D. nickel tubing which is bent as shown in Figure 42. A 2-in. length of 0.147-in. I.D. seamless molybdenum tubing, capped with a molybdenum plug containing a 0.0135-in. diam by 0.125-in. long channeled orifice is pressure fit to the end of the delivery tube.

Approved for Public Release

Contrails

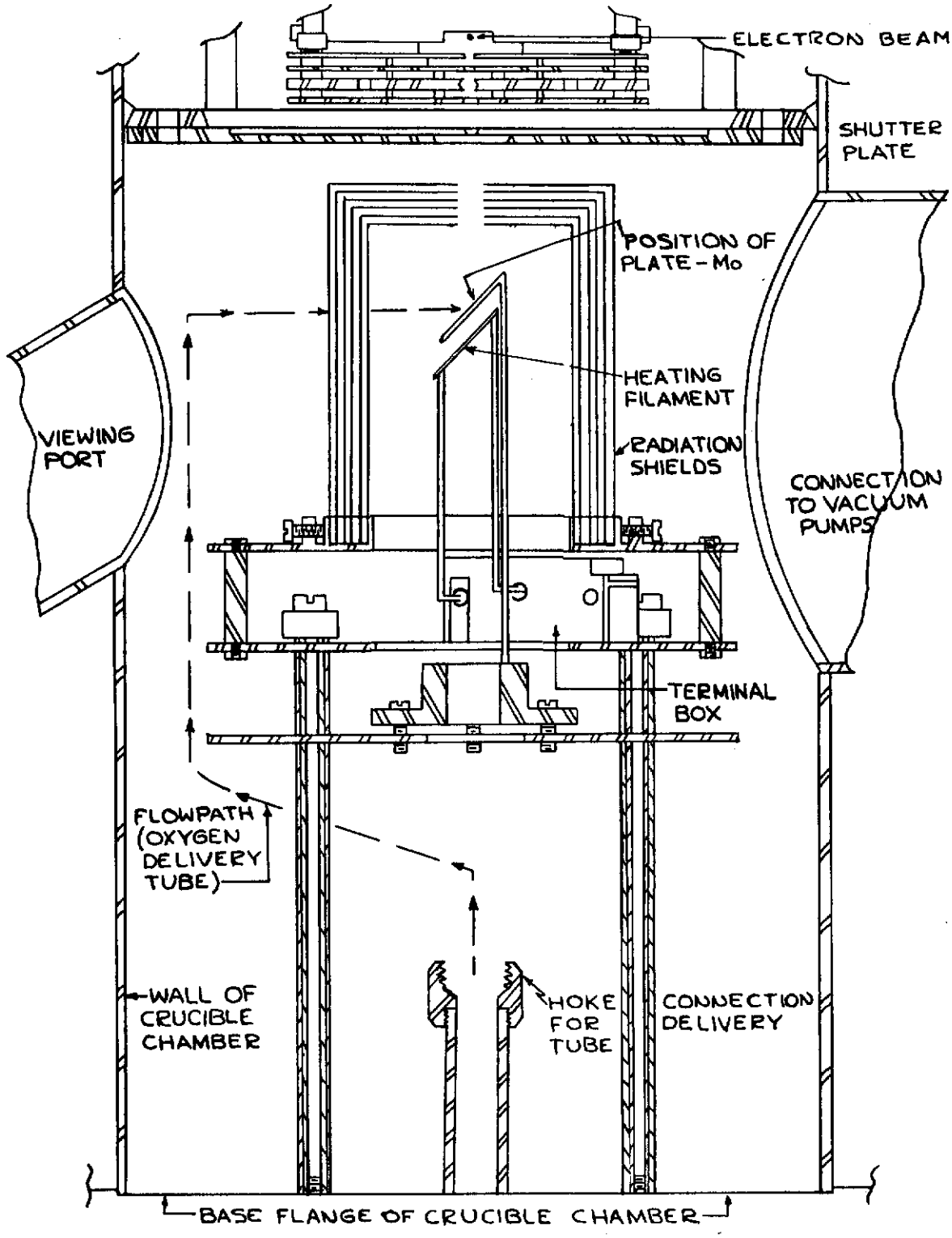

Figure 42. - Mass spectrometer modification for oxidation studies.

Approved for Public Release

Contrails

A set of six coaxial tantalum radiation shields surrounds the molybdenum plate. The shield chamber thus formed has a rectangular opening along one side through which oxygen can escape. The temperature of the plate is measured by sighting the optical pyrometer through this opening, essentially parallel to the delivery tube. A set of holes in the end of the cylindrical chamber are aligned with the beam-defining slits of the mass spectrometer. Between these slits and the molybdenum plate is a sylphon-bellows-operated shutter which can be positioned to block the passage of molecules vaporizing from the plate. In this way, a correction for the background intensity at any mass number is obtained.

Commercial oxygen, after drying, is maintained at 15 cm Hg pressure, in a 2-liter ballast flask. The line connecting the flask to the delivery tube includes a Hoke 281 series needle valve for pressure reduction and regulation of the oxygen flow. A thermocouple gauge measures the pressure at the inlet to the delivery tube.

In the experiments to be described, two configurations are employed-- a direct-beam configuration in which the beam axis intersects the normal to the center of the molybdenum plate at 45^{o} and a deflected-beam configuration in which the beam merely supplies oxygen to maintain an ambient pressure in the shield chamber. In the directed beam experiments, the orifice is one centimeter from the center of the plate. The pumping speed from the shield chamber is such that the ambient oxygen contributed approximately the same flux density to the plate as does the direct molecular beam.

3. Procedure

The experimental procedure for both the directed beam and ambient oxygen runs is as follows. The mass spectrometer is pumped down and baked overnight. The rhenium filament is heated to 2000-2500C and about 1000 volts is applied to the molybdenum plate. The resulting electron bombardment heats the plate to about 2100K. The system is degassed for at least an hour at this temperature during which time the pressure in the crucible chamber drops to about 10^{-6} mm. The intensity of the mass spectrometer signal for the molybdenum isotope, Mo^{98} (relative abundance, 23.75%) is then measured. This serves as a calibration for the intensities of the molybdenum oxides.

The mass spectrometer sensitivity is obtained by assuming that the molybdenum intensity with the plate at 2100K corresponds to the equilibrium pressure of 1.90×10^{-9} atm [51] and that the relative ionization cross section for Mo, MoO_2, and MoO_3 are 52.5, 59.1, and 62.4, [49] respectively. The intensities measured for Mo^{98} at the start of four runs gave calibration factors which agreed within a factor of two.

The plate is then cooled; the desired flow of oxygen is established and its intensity is measured at mass 34, which corresponds to the oxygen species $O^{16}O^{18}$ present to the extent of 0.41% in natural oxygen. The intensity for oxygen at mass 32 was too high to measure conveniently. The plate is again heated to various temperatures in the range 1400-2000K and the mass spectrometer signals for $MoO_2(g)$ and $MoO_3(g)$ are measured at mass 130 ($Mo^{98}O_2$) and

Approved for Public Release

Contrails

146 ($Mo^{98}O_3$) respectively. About ten minutes is allowed at each point for steady state conditions to be reached. The rate of approach to steady state has an exponential time constant of 40 sec. A desorption peak is generally observed with an increase in plate temperature and, conversely, adsorption is evident on cooling.

D. RESULTS

The results for five runs at various oxygen levels are plotted in Figures 43 and 44. Runs 1 and 3 are for the beam deflected configuration in which only the oxygen ambient in the shield chamber provides the oxygen flux to the plate. Runs 2, 4, and 5 include the additional contribution of the direct flux from the oxygen beam. The plotted flux values are proportional to the experimentally measured intensities and are obtained by adjusting the mass spectrometer sensitivity to an average temperature of 1700K. The equivalent pressures in atmospheres can be obtained by multiplying these flux values by $1.08 \times 10^{-26}T$ and $1.03 \times 10^{-26}T$ for MoO_2 and MoO_3 respectively, where T is the temperature in degrees Kelvin.

The important features to be noted in the curves of Figures 43 and 44 are the relatively small changes in intensity with temperature and the crossing of the MoO_3 and MoO_2 curves. Below about 1700K, MoO_3 is the predominant vaporizing species just as it is for the entire temperature range in the equilibrium vaporization from $MoO_2(s)$. Above 1700K, however, the MoO_3 intensity drops off while that for MoO_2 continues to increase. The temperature of the crossover point increases slowly with increasing oxygen pressure.

While the absolute values for the oxygen pressure may be in error by as much as an order of magnitude, relative values at 1700K are probably within $\pm$20% as evidenced by the proportionality of the MoO_2 and MoO_3 vaporization rates to the calculated oxygen pressures. The oxygen pressures in the delivery tube during the runs were too high for the thermocouple gauge to be used. The calibration procedure, therefore, was as follows. The ratio of the oxygen flux leaving the orifice to the oxygen signal at mass 34 was determined at a reduced inlet pressure. This ratio was then used to calculate the flux values for the various runs. Thus, with an inlet pressure of 82 microns, as measured by the thermocouple gauge, a calculated pressure drop of 18 microns for the delivery tube, and a Clausing factor of 0.12, an oxygen flux of 0.26×10^{16} molecules/sec was determined.

From the proportionality of the flux to the intensity at mass 34, the corresponding values for the five runs given in Table VI were calculated. The area of the plate contributing to the mass spectrometer signal is about 1/3 cm^2 and it is estimated that about 70% of the flux from the channeled orifice impinges on this area. On this basis, the flux density due to the beam alone is calculated for the three directed beam experiments.

Approved for Public Release

Contrails

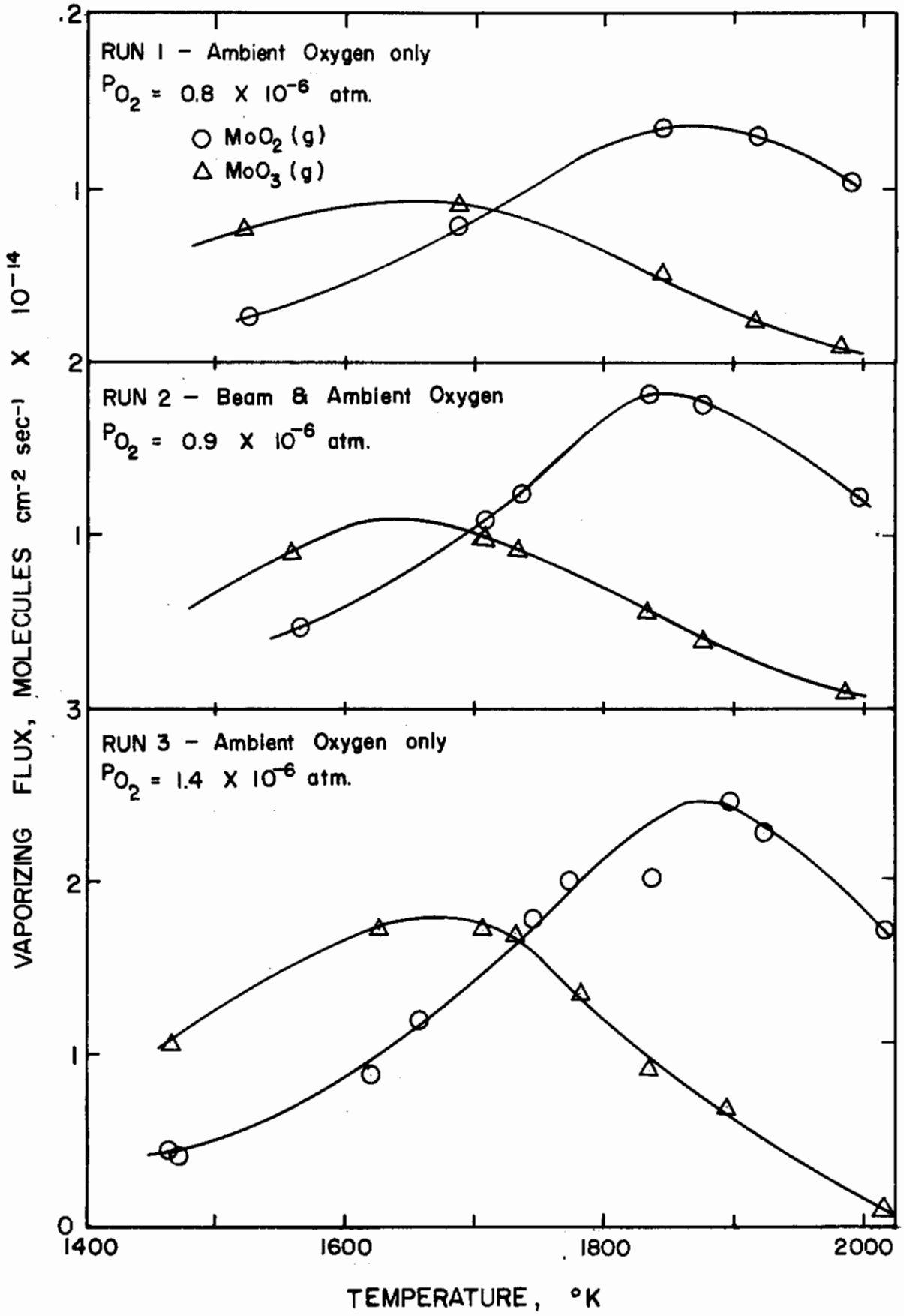

Figure 43. - Steady state flux of molybdenum oxides vs temperature, Runs 1-3.

Approved for Public Release

Contrails

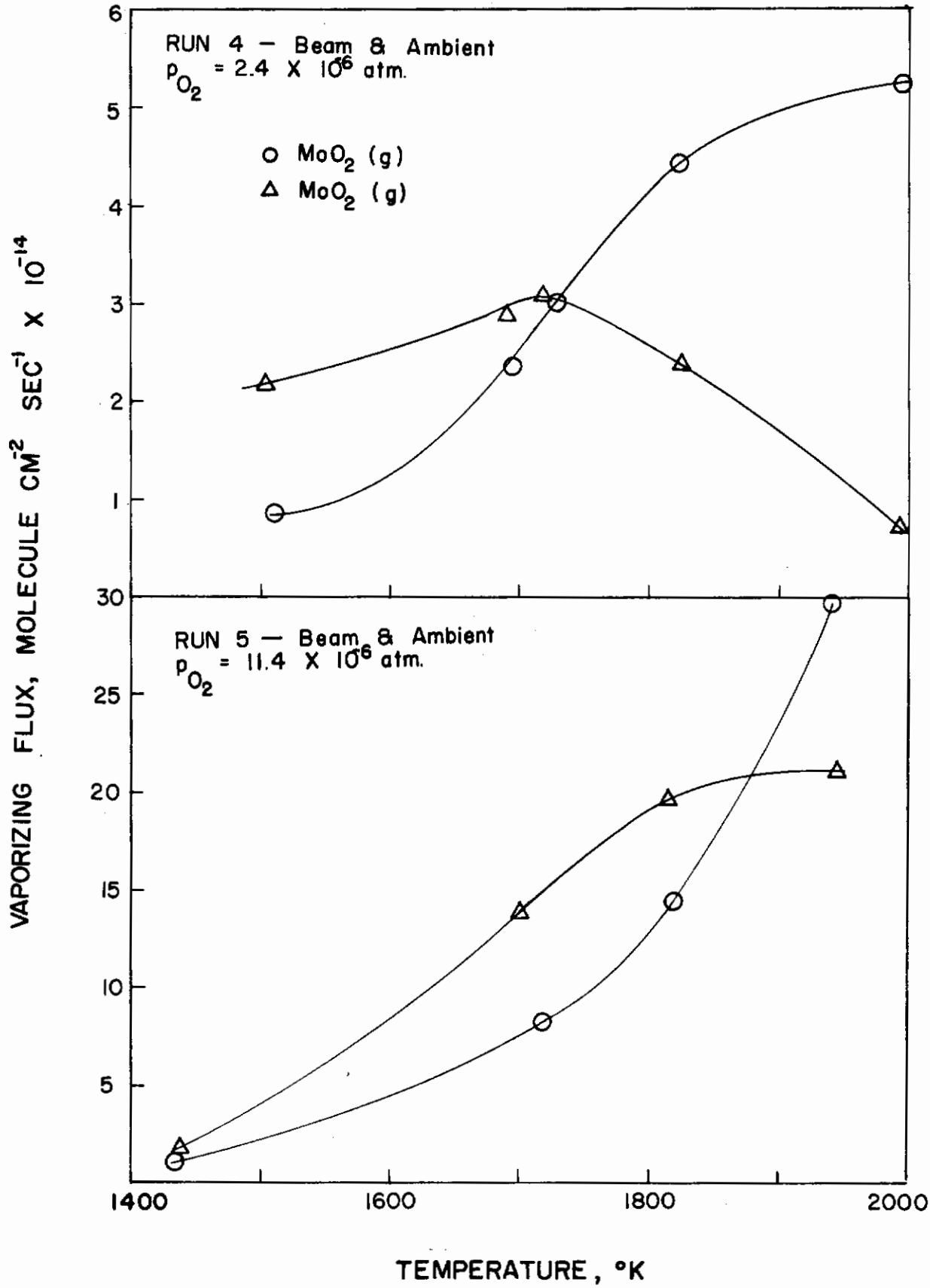

Figure 44. - Steady state flux of molybdenum oxides vs temperature, Runs 4 and 5.

Approved for Public Release

Contrails

TABLE VI

FLUX, FLUX DENSITY AND EQUIVALENT PRESSURE

OF OXYGEN FOR THE VARIOUS RUNS

Run No.	Flux 10^{16} Molecules/sec	Flux Density at Plate, 10^{16} Molecules/cm^2 sec			Equiv. Oxygen Pressure at 1700K, atm
		Beam Only	Ambient	Total	
1	3.2	-	9.0	9.0	0.8×10^{-6}
2	2.1	4.3	5.9	10.2	0.9
3	5.6	-	15.7	15.7	1.4
4	5.6	11.6	15.7	27.3	2.4
5	26.5	54.8	74.2	129.0	11.4

A comparison of runs 3 and 4, for which the flux is comparable, indicate that the contribution from the ambient oxygen alone is about 1.35 times the contribution from the beam alone at 1700K. This factor and the proportionality between the ambient pressure and the flux were used to calculate the ambient flux densities given in Table VI. Finally, the combined flux densities were used to calculate the equivalent oxygen pressures for the average temperature of the experiments, i.e., 1700K.

In addition to the uncertainties involved in this calibration, there is evidence that the ambient pressure varied with temperature. It is estimated that the ambient flux is about twice the value of the beam alone at 1500K and only about one half the value at 2000K.

Since bombardment energies of 60 ev. were used to ionize the molecules entering the mass spectrometer source, it was necessary to check that the ions were not fragmentation products. Ionization efficiency curves indicate that MoO_2^+ and MoO_3^+ are, in fact, produced primarily by direct ionization of the corresponding neutral molecules. Quite apart from this, the independent variation of MoO_2 and MoO_3 intensities and the drastic change in their relative contribution with plate temperature prove that fragmentation cannot be a significant factor. A mass scan to mass 800 gave detectable intensities for the ions $Mo_2O_6^+$, $Mo_2O_5^+$, $Mo_2O_4^+$, and $Mo_3O_9^+$ in decreasing order of importance. After correcting for isotope ratios and ionization cross sections, the total contribution of these species corresponds to less than 10% of the MoO_2 and MoO_3 flux values.

Approved for Public Release

Contrails

E. DISCUSSION

The oxidation of molybdenum in the temperature range of 1400 to 2000K and with oxygen pressures of 10^{-5} to 10^{-6} atm occurs predominantly according to the over-all reactions, $Mo\ (s) + O_2 \longrightarrow MoO_2\ (g)$ (1)
and $Mo\ (s) + 3/2\ O_2 \longrightarrow MoO_3\ (g)$ (2)

The relative contribution of reactions 1 and 2 is a function of both temperature and pressure. Below about 1700K, reaction 2 predominates and has only a small temperature dependence (ca. 15 kcal/mol). At about 1700K, the rate of MoO_3 vaporization reaches a maximum and above this temperature is observed to decrease. The vaporization rate of MoO_2 is less than that of MoO_3 below 1700K, but has a slightly greater temperature dependence (ca. 27 kcal/mol). The rate of MoO_2 vaporization continues to increase with temperature up to at least 1850K, so that reaction 1 predominates above 1700K.

A comparison of the oxidation results with the equilibrium vaporization of MoO_2 (s) will be made which shows that although thermodynamically stable, an oxide film does not form on the molybdenum surface. Further, it will be shown that the results are consistent with a rapid equilibration of MoO_2 and MoO_3 molecules on the surface, the rate determining step being the formation of an active precursor on the surface.

1. Equilibrium Considerations

The minimum oxidative conditions for the formation of a condensed molybdenum oxide are determined by the invariant 3-phase system, Mo(s) - MoO_2(s) - gas.* The equilibrium partial pressures for this system have been calculated and are given in Table VII for the temperature extremes of the experiment.

TABLE VII

EQUILIBRIUM PARTIAL PRESSURES

FOR THE Mo (s) - MoO_2 (s) SYSTEM**

Temperature °K	Logarithm of the Partial Pressure in Atmospheres			
	Mo(g)	O_2	MoO_2(g)	MoO_3(g)
1400	-16.8	-12.7	-10.9	-9.4
2000	-9.5	-6.3	-4.6	-3.9

* - A suboxide Mo_3O is known to form slowly at lower temperatures,[52] but is not stable at the temperatures of this experiment.

** - Thermodynamic data are from King,[51] Christensen, and Weller;[53] Brewer and Rosenblatt;[54] and Stull and Sinke.[55] Free energy functions for MoO_3 (g) were obtained from DeMaria et al.

Approved for Public Release

Contrails

It should be noted again that under equilibrium conditions $MoO_3(g)$ is the predominant species evaporating from $MoO_2(s)$ in this temperature range. It is evident that the experimental oxygen pressures are more than sufficient for the formation of $MoO_2(s)$ if they are maintained in a closed isothermal container. It is also evident that kinetic factors have prevented the formation of an oxide film since the experimental vaporization behavior deviates both qualitatively and quantitatively from that of MoO_2 (s). This may be readily seen in Figure 45 where equilibrium vapor pressures over MoO_2 (s), as determined by the mass spectrometric studies of Burns et al,[49] are plotted as a function of 1/T in the same diagram as the oxidation results from run 3. For both MoO_2 and MoO_3, the temperature dependence of the kinetic curves is much less than that of the equilibrium curves. Even more strikingly, the MoO_3 concentration reaches a maximum and then decreases so that above the crossover point at 1700K the relative importance of MoO_2 and MoO_3 in the kinetic case is actually the reverse of that in the equilibrium case. In order to maintain, in the face of this evidence, that a solid MoO_2 film exists on the surface, one would have to postulate an irregular decrease in the evaporation coefficient of MoO_3 (g) from about unity at 1400K to less than 10^{-6} at 2000K. A crude Langmuir evaporation of MoO_2 (s) in the mass spectrometer shows that such an effect does not occur. It is concluded, therefore, that no more than two or three chemisorbed layers can be present on the surface of the molybdenum plate during the high temperature oxidation experiments, since otherwise the vaporization behavior of the bulk oxide would be manifest. In fact, the surface coverage may be less than a monolayer. The activation energies suggested by the straight line portion of the oxidation curves in Figure 45 are 15 kcal/mol for $MoO_3(g)$ and 27 kcal/mol for $MoO_2(g)$ compared with the equilibrium enthalpies of vaporization from $MoO_2(s)$ of 122 and 134 kcal/mol, respectively.

Equilibrium consideration may also be used to investigate the possibility that a series of rapid equilibration steps occurs among the adsorbed species on the molybdenum surface. The assumption is made that rates of vaporization of $MoO_2(g)$ and $MoO_3(g)$ are proportional to the surface concentrations of the respective adsorbed species, and that the equilibrium among the latter is given by the reaction.

$$Mo(s) + 2MoO_3\ (ads) = 3MoO_2\ (ads) \qquad (3)$$

The logarithm of the equilibrium constant for reaction 3 was determined from the equivalent $MoO_2(g)$ and $MoO_3(g)$ pressures calculated for 100° intervals from the smoother curves in Figures 43 and 44. These constants are plotted vs 1/T in Figure 46.

The data appear to obey a linear relation within reasonable limits. The precise value of the equilibrium constant seems to depend on the oxygen pressure and whether the beam directed or beam deflected configurations were used, but, in general, the higher oxygen pressure emphasizes the MoO_2 vaporization. This may be due to a reduction in the molybdenum activity at the surface or may be a kinetic effect.

The measured slope of 110 kcal/mol in Figure 46 is to be compared with the gas phase value determined by Burns et al[49] of 160 kcal/mol. The difference could easily be due to the values of the heats of adsorption of MoO_2 and MoO_3 on molybdenum. It is interesting to note that the equilibrium constant calculated

Approved for Public Release

Contrails

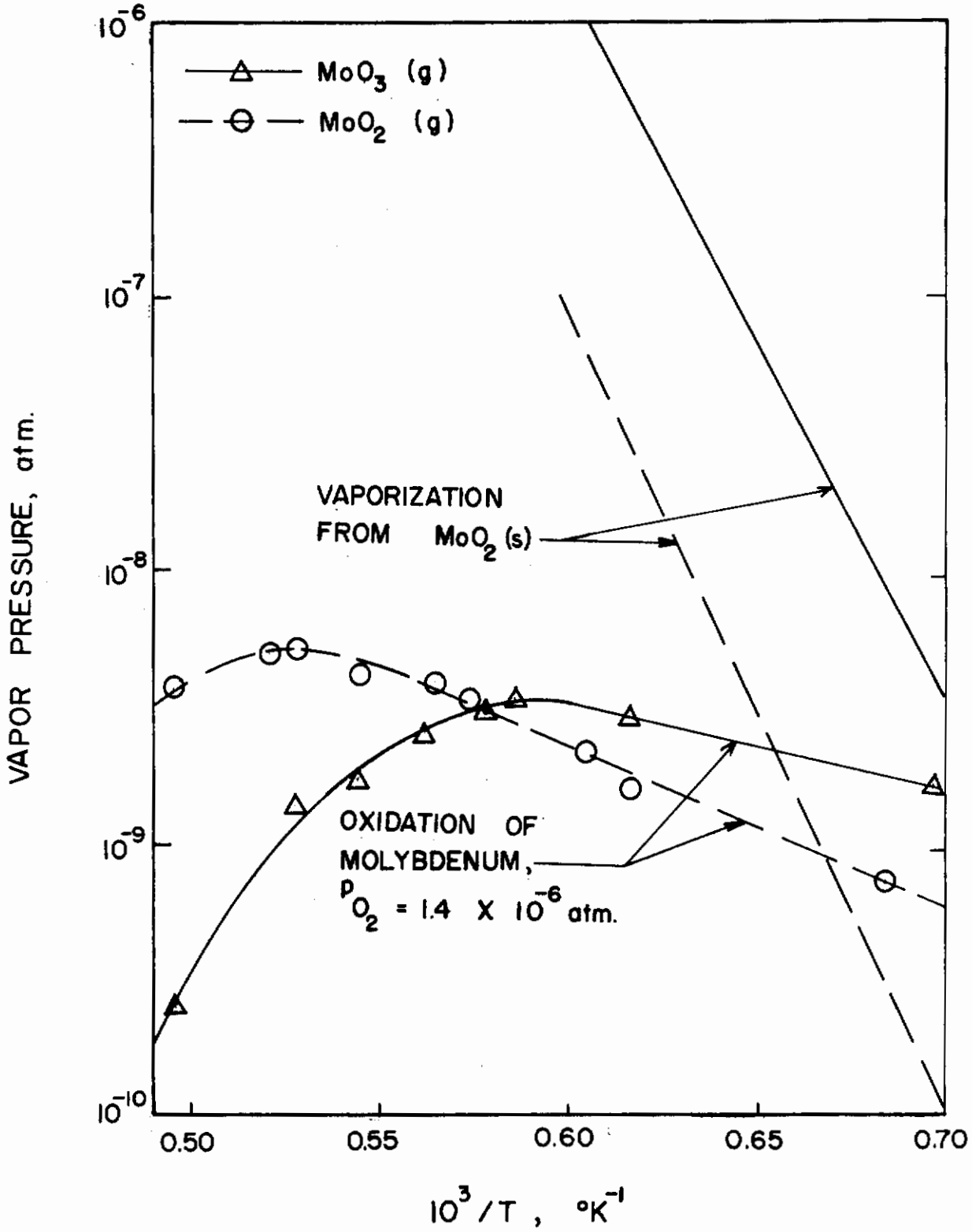

Figure 45. - Comparison of oxidation results (Run 3) to equilibrium vaporization from MoO_2(s).

Approved for Public Release

Contrails

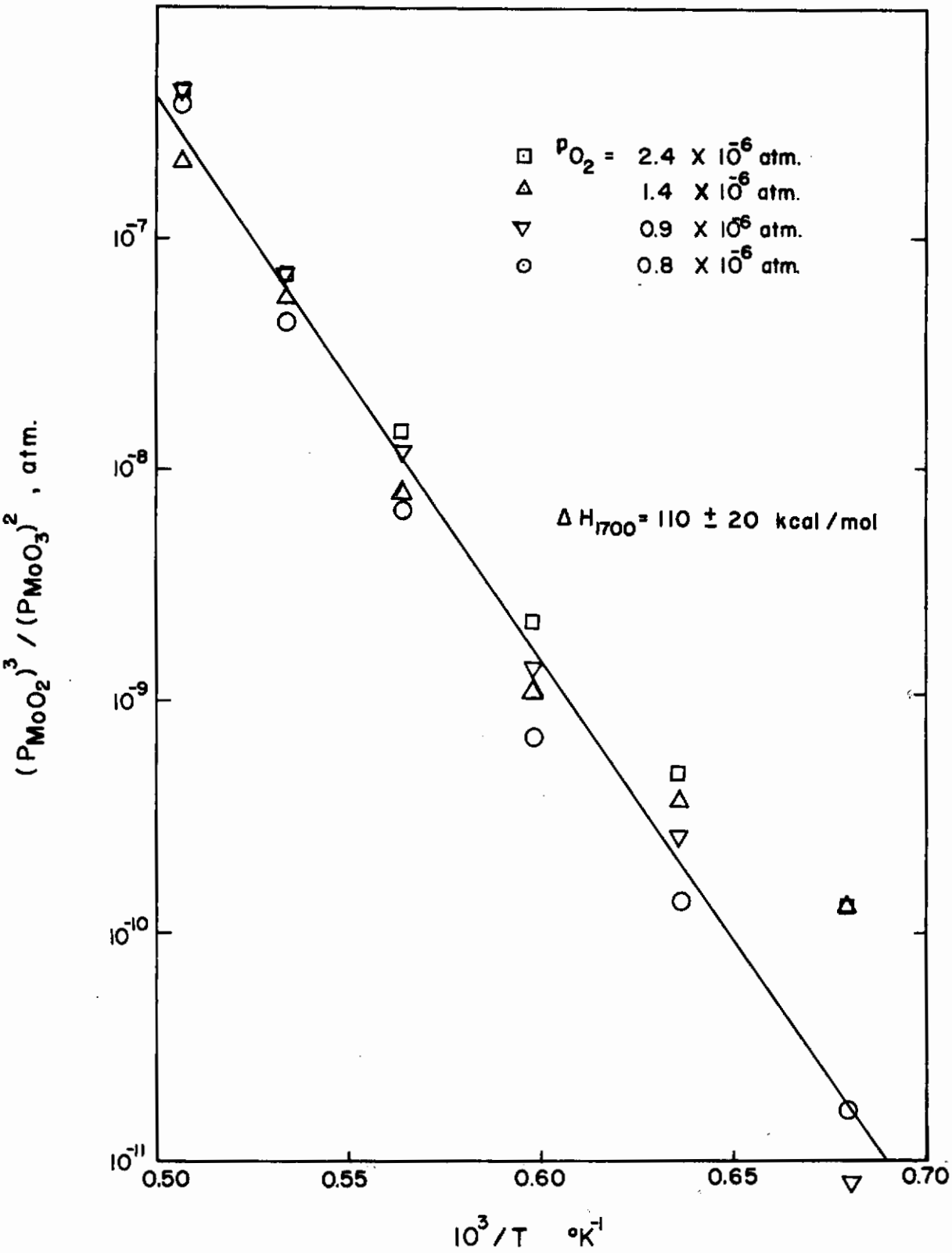

Figure 46. - Reciprocal temperature plot of equilibrium constant for the reaction $Mo(s) + 2\ MoO_3(g) = 3MoO_2(g)$.

Approved for Public Release

Contrails

from the data of Burns et al is 1.0×10^{-9} atm at 1700K compared with an average value of 2.0×10^{-9} atm for the oxidation results.

2. Kinetic Considerations

As was shown in the previous section, our results are consistent with rapid equilibration of MoO_2 and MoO_3 molecules on the surface. From the total concentration of combined molybdenum on the surface, Equation (3) permits one to derive the individual curves of MoO_3 and MoO_2 concentration as a function of temperature (which are obtained from the observed evaporation rates). What remains to be explained, however, is the process which determines the total concentration of molybdenum oxide species on the surface or, alternatively, the reason why only one molecule out of 400 hitting the surface reacts to form a volatile oxide. It must be assumed that the rate controlling step occurs before the equilibration process and that the concentration of the precursor is determined by the rate at which it is formed minus the rate at which the oxides volatilize.

When the molybdenum plate was heated, flash desorption of as many as 2×10^{16} MoO_2 and MoO_3 molecules/cm^2 were observed. Since it has been shown that the surface is free from condensed oxide this desorption must correspond to a change in the concentration of oxygen dissolved in the molybdenum, the change amounting to only 6×10^{-3} atomic per cent. In support of this view, the rate of approach to steady state discussed earlier is consistent with an estimated value of 10^{-6} cm^2/sec for the diffusion coefficient of oxygen in molybdenum at 1700K.

The first order dependence of the MoO_2 and MoO_3 vaporization rates on the oxygen pressure can be understood on the basis of a proportionality between the pressure and the concentration of chemisorbed oxygen atoms. The proportionality, as well as the absence of condensed phase oxidation, is most readily envisioned for a surface coverage of less than a monolayer.

All that is required to complete the reaction scheme is to postulate that the chemisorbed atoms react to form the precursor for the surface equilibration. In the following tentative reaction mechanism the precursor is assumed to be an adsorbed MoO molecule which forms when the chemisorbed oxygen reacts with a molybdenum atom of the metal lattice.

$$O_2(g) \longrightarrow 2\,O(ads) \qquad (4)$$

$$O(ads) \longrightarrow O(g) \qquad (5)$$

$$Mo(s) + O(ads) \longrightarrow MoO(ads) \qquad (6)$$

$$2MoO(ads) \rightleftarrows Mo(s) + MoO_2(ads) \qquad (7)$$

$$2MoO_2(ads) \rightleftarrows MoO(ads) + MoO_3(ads) \qquad (8)$$

$$MoO_2(ads) \longrightarrow MoO_2(g) \qquad (9)$$

$$MoO_3(ads) \longrightarrow MoO_3(g) \qquad (10)$$

Approved for Public Release

Contrails

The reverse of reaction 4 cannot contribute significantly to the reaction mechanism since it would imply an approach to equilibrium between gaseous and adsorbed oxygen. The latter situation in turn would require bulk oxidation of the molybdenum which is contrary to observations.

Since the probability for a bimolecular reaction is greater than that of a termolecular reaction two rapid equilibration steps (reactions 7 and 8) have been assumed. Reaction 3, which was shown to account for the variation of MoO_2 and MoO_3 evaporation rates, can be obtained by subtracting reaction 7 from two times reaction 8.

It must be emphasized that this mechanism, although consistent with the observations, is still tentative and that further work is required to refine the oxygen pressure dependence. The evaporation of oxygen as atoms or molecules should be verified and the rate of oxidation measured for the reaction with oxygen atoms.

In summary then, a kinetic mechanism is postulated for the oxidation of molybdenum at high temperature and low oxygen pressure in which the reaction of chemisorbed oxygen to form an active precursor is the rate controlling step. Rapid equilibration of adsorbed MoO_2 and MoO_3 has been shown to account for the observed vaporization rate of these species.

Approved for Public Release

Contrails

VIII. REFERENCE CITATIONS

1. M. Hansen and K. Anderko, "Constitution of Binary Alloys," McGraw-Hill, New York (1958).

2. E. K. Storms, LAMS 2674 Part I, "Selected Properties of Group 4a, 5a, and 6a Carbides," March 15, 1962.

3. R. V Sara and R. T. Dolloff (National Carbon Company, Parma, Ohio), WADD-TR-60-143 Part III, April 1962, under Contract AF 33(616)-6286.

   Also, WADD-TR-60-143 Part IV, February 1963, under Contract AF 33(657)-8025.

4. F. Benesovsky and E. Rudy, Plansee fur Pulvermet., 8, 66-71 (1960). See also C.A. 55, 1381 d.

5. D. S. Neel, C. D. Pears, and S. Oglesby, Jr. (Southern Research Institute), WADD-TR-60-924, February 1962, under Contract AF 33(616)6312. (ASTIA reference AD 275-536)

6. S. L. Bender. R E. Dreikorn et al (Research and Advance Development Division, Avco Corporation, Wilmington, Massachusetts), ASD-TR-61-260 Part I Vol. I, May 1962, under Contract AF 33(616)-7327. (ASTIA reference AD 278-633)

7. A. D. Mah and B. J. Boyle (Bureau of Mines, Berkeley, California), J.A.C.S. 77, 6512-6513 (1955).

8. C. H. Prescott, Jr., J.A.C.S. 49, 2744 (1927).

9. V. Kutsev, B. Ormont and V. Epelbaum, Doklady Akad. Nauk. S.S.S.R. 104, 567 (1955). See also C.A. 50, 16295 c.

10. B. D. Pollock (Atomics International, Canoga Park, California), J. Phys. Chem. 65, 731 (1961).

11. G. L. Vidale (Space Sciences Laboratory, General Electric Company, Philadelphia), "The Measurement of the Vapor Pressure of Atomic Species from Spectrophotometric Measurements of the Absorption of Resonance Lines. V The Free Energy of Formation of TiC and ZrC," August 1961. (ASTIA reference AD 263-336)

12. NYO 9625 (Pennsylvania University, Philadelphia), "Thermodynamic Properties of Metal Carbides at High Temperatures," 1960. See also NSA 15, 5374.

13. J. A. Coffman, G. M. Kebler et al (General Electric Company, Cincinnati, Ohio), Progress Reports under Contract AF 33(616)-6841.

Approved for Public Release

Contrails

14. A. S. Bolgar, T S Verkoglyadova, and G. V. Samsonov, Izvest. Akad. Nauk. S.S.S.R., Otdel Tekh. Nauk., Met. i Toplivo, No. 1, p. 142-145 (1961). See also NSA 15, 17344.

15. V. M. Zhelankin, V. S. Kutsev, and B. F. Ormont, Zh. Fiz. Khim 35 2608 (1961) and 33 1988 (1959). See also C.A. 57, 14689 i and 54, 13823 g.

16. E. F. Westrum, reported in "Thermodynamics and Kinetic Studies for a Refractory Materials Program," ASD-TDR-62-204 Part I, by L. A. McClaine, April 1962.

17. George Feick, reported in "Thermodynamics and Kinetic Studies for a Refractory Materials Program," ASD-TDR-62-204 Part I, by L. A. McClaine, April 1962.

18. D. Barnes, R. Mezaki, E Tilleux, and J. Margrave, Proc. International Symposium on Thermodynamics of Nuclear Materials, Paper SM-26/48, Vienna, Austria, May 21, 1962, p. 775.

19. JANAF Thermochemical Tables, Quarterly Supplement No. 5, Dow Chemical Co., September 30, 1962.

20. L. Kaufman, "Investigation of Boride Compounds for Very High Temperature Applications," Semiannual Report No. 1 for Aeronautical Systems Division on Contract AF 33(657)-8635, October 1962.

21. E. J. Huber, E. L. Head and C. E. Holley, unpublished work quoted by Leitnaker, et al. (See reference 25.)

22. V. A. Epelbaum and M. I. Starostina, Bor, Trudy Konf. Khim. Bora i Ego Soedinenii, p. 97 (1955) published 1958.

23. Private communication from Elliot Greenberg and Ward Hubbard, Argonne National Laboratory, 1962.

24. O. C. Trulson and H. W. Goldstein, reported in "Research on Physical and Chemical Principles Affecting High Temperature Materials for Rocket Nozzles," Quarterly Progress Report dated September 30, 1962, under Contract DA-30-069-ORD-2787, pp. III 35 to 37.

25. J. M. Leitnaker, M. G. Bowman, and P. W. Gilles, J. Chem. Phys. 36, 350 (1962).

26. J. M. Leitnaker, personal communication.

27. J. L. Margrave, this report, Appendix B.

28. Pitzer and Brewer revision of Lewis and Randall, "Thermodynamics," McGraw-Hill, New York (1961).

29. G. Verhaegen and J. Drowart, J. Chem. Phys. 37, 1367 (1962).

Approved for Public Release

Contrails

30. E. G. Wolff and C. B. Alcock, Trans. British Ceram. Soc. 61, 667 (1962).

31. M. S. Linevsky in "Refractory Materials Research," Contract AF 33(616)-6841, Ninth Quarterly Progress Report, December 31, 1962, General Electric Applied Research Operation, Cincinnati, Ohio.

32. M. C. Krupka, "High Temperature Vaporization Behavior and Thermodynamic Properties of Hafnium Diboride," Los Alamos Scientific Laboratory Report LA-2611, April 16, 1962.

33. Southern Research Institute (ASD-TR-62-765), August 1962.

34. T. F. Lyon, General Electric Applied Research Operation, Cincinnati, Ohio, reported at the International Symposium on Condensation and Evaporation held in Dayton, Ohio, September 1962.

35. M. B. Parrish and Liane Reif, J. Chem. Phys. 38, 253 (1963).

36. Yu. B. Paderno, "Preparation and Some Properties of HfB_2," Tsvetnye Metally 11, 48 (1959) D.S.I. Translation no. 614.

37. Glaser and Post, Trans. AIME 197, 1117-1118 (1953).

38. Glaser, Moskowitz, and Post, Trans. AIME 197, 1119-1120 (1953).

39. Eckstein and Forman, J. Appl. Phys. 33, 82 (1962).

40. F. H. Brown, Jr., Progress Report No. 20-252, Jet Propulsion Laboratory, Pasadena, California, February 25, 1955.

41. G. A Meyerson, G V. Samsonov, R. B. Kotelnikov, M. S. Voyonova, I. P. Yerterjera and S. D. Krasnenkova, Akad. Nauk. S.S.S.R. Zh. Neorgancheskoy Khimii, from Konferenskiya Po Khimii Bora I Yego Soyedineii 1955, 577 (1960).

42. J. B. Berkowitz-Mattuck, "Kinetics of Oxidation of Refractory Metals and Alloys at 1000°-2000°C," ASD-TR-62-203 Part II, January 1963.

43. W. D. Kingery, J. Pappis, M. E. Doty and D. C. Hill, J. Amer. Ceram. Soc. 42, 393 (1959).

44. R. W. Bartlett (University of Utah, 1961) Dissertation Abstr. 22 (11), 3973 (1961-62).

45. W. Watt, G. H. Cockett, and A. R. Hall, Metaux 28, 222 (1953).

46. F. Hund, Z. Physik. Chem. 199, 142-151 (1952).

47. Von E. Kauer, O. E. Klinger and H. Rabenau, Z. Electrochem. 63, 927-936 (1959).

48. December 1962 at Aeronautical Research Laboratories, Wright-Patterson Air Force Base, Ohio.

Approved for Public Release

Contrails

49. R. P. Burns, G. DeMaria, J. Drowart, and R. T. Grimley, J. Chem. Phys. 32, 1363 (1960).

50. J. Berkowitz-Mattuck, A. Buchler, and S. Goldstein, "Stability of Ceramic Materials to 2000C," Progress Report No. 7 to ASD, Contract AF 33(616)-6154, September 25, 1961.

51. D. R. Stull and G C. Sinke, "Thermodynamic Properties of the Elements," No. 18 of the Advances in Chemistry Series, American Chemical Society (1956).

52. N. Shönberg, Acta. Chem. Scand. 8, 617 (1954).

53. E. G. King, W. W. Weller and A. U. Christensen, "Thermodynamics of Some Oxides of Molybdenum and Tungsten," Bureau of Mines Report of Investigations 5664 (1960).

54. Leo Brewer and G. M. Rosenblatt, "Dissociation Energies of the Gaseous Metal Oxides," Chem. Rev., 61, 257 (1961).

55. G. DeMaria, R. Burns, J. Drowart and M. G. Inghram, J. Chem. Phys. 32, 1373 (1960).

56. D. L. Douglass, pp. 223-255 in "Corrosion of Reactor Materials," International Atomic Energy Agency, Vienna (1962).

57. Y. Oishi and W. D. Kingery, J. Chem. Phys. 33, 905-906 (1960).

58. Y. Oishi and W. D. Kingery, J. Chem. Phys. 33, 480-486 (1960).

Approved for Public Release

Contrails

Appendix A

THERMODYNAMIC PROPERTIES OF ZIRCONIUM AND HAFNIUM HALIDES*

Robert D. Freeman
Oklahoma State University, Stillwater, Oklahoma

Until this year, most of the efforts of this group had been devoted to development of experimental techniques with which to study the disproportionation of the zirconium and hafnium subhalides. In June, 1962, support for the development of these techniques was transferred to another source of funds (Contract No. AF 33(657)-8767). The results of those developments, in particular that of the inverted Knudsen technique, will be available, of course, for immediate use in these studies.

This report then covers work on these experimental techniques and the theoretical work on molecular flow for the period January through May only (items A, B, and C below). During the period June through December, efforts were directed toward sample procurement and preparation and toward design of calorimetric experiments and apparatus with which to obtain heats of formation of the solid subhalides.

A. ELECTRODYNAMOMETER

Testing of the electrodynamometer, as described in the previous report (ASD-TDR-62-204, Part I), has continued. The results can be summarized as follows:

1. With the electrodynamometer, a torque of 0.2 dyne-cm can be measured with a precision of 0.07% (average deviation from mean), and a torque of 0.01 dyne-cm with a precision of 0.5%. These values for the measured torque (0.2 - 0.01 dyne-cm) are typical of values expected when a molecular beam from a source at 10^{-6} - 10^{-3} atm impinges on a target attached to the electrodynamometer.

2. The greatest difficulty encountered in checking the performance of the electrodynamometer has been in calibrating the tungsten torsion wires. Despite the fact that the moments of inertia of the various weights used for calibration are presumably known (from mass and physical dimensions) within a few parts in 10^4 and that the period of oscillation of a given weight is reproducible within 5 parts in 10^4, the torsion constant calculated from the

* - Report on subcontracted study under Air Force Contract AF 33(616)-7472.

Approved for Public Release

Contrails

moments of inertia and periods of oscillation of any two weights may vary 1%-3% from that calculated from two other weights. These discrepancies appear to arise from inhomogeneous distribution of mass within the volume of the weight and from coupling of slight oscillations about the horizontal plane to the torsional oscillation about the vertical axis. These difficulties are being investigated in some detail; the results are applicable not only to the electrodynamometer, but should be of particular interest to those using the torsion-effusion technique.

B. MOLECULAR FLOW

The method proposed for solving the integral equations for molecular flow through conical orifices (cf. ASD-TDR-62-204, Part I) gave valid results over a portion of the range of orifice dimensions of interest, but poor results for relatively long orifices. A new and considerably more clear-cut method has been proposed and a computer program written. This program is in the final stages of "debugging"; results should be obtained within the month.

(It should perhaps be noted here that the solution of the integral equations which describe both total flow and angular distribution of molecules from conical orifices has been completed. The results are discussed in detail in the First and Second Quarterly Progress Reports submitted to Aeronautical Systems Division, ASRCPT-1, under Contract AF 33(657)-8767.)

C. INVERTED KNUDSEN TECHNIQUE

The inverted Knudsen technique involves suspending a Knudsen effusion cell, orifice downward, from a vacuum microbalance and determining both rate of evaporation and recoil force with the microbalance. The technique is, in principle, equivalent to the torsion-effusion technique, but, by providing for measurement of both rate of evaporation and recoil force with the same device, promises to eliminate many of the difficulties which have frustrated users of the torsion-effusion method.

We have designed and built a vacuum microbalance for use with this technique. The design is based on balances described by Honig and Czanderna[1] and by Gerritsen and Damon[2], except that the tungsten-pivot, quartz-cup bearing used by these workers has been replaced by a diamond pivot in a sapphire cup. The control circuitry is a combination of that described by Cochran[3] and by Pope[4].

---

(1) J. Honig and A. Czanderna, Anal. Chem., 29, 1206 (1957).

(2) A. N. Gerritsen and D. H. Damon, Rev. Sci. Instr., 33, 301 (1962).

(3) C. N. Cochran, in "Vacuum Microbalance Technique," Vol. 1 (M. J. Katz, ed.), Plenum Press, N.Y., 1961

(4) M. I. Pope, J. Sci. Instr., 34, 229 (1957).

Approved for Public Release

Contrails

The balance has been installed in a vacuum system with provision for the sample cell to hang in the center of a split-graphite heating element, which is energized by low-voltage ac current.

Tests of the balance as originally constructed indicated adequate sensitivity (in the range of 10^{-7} g) but inadequate mass range, i.e., maximum variation of current through the compensating solenoids was equivalent to a mass change deemed too small. Relatively minor redesign of the solenoids and associated circuitry is now in progress and should eliminate this difficulty. Testing and calibration of the balance will then be completed.

(In continuation of this work under AF 33(657)-8767 the solenoids have been redesigned to provide, with the 90 ma available from the present power supply, for compensation of a total weight loss of 13 mg, and to eliminate the problem of overheating which was encountered with the original solenoids. The range of compensation can fairly easily be doubled if that becomes desirable. The performance of the balance has been tested by measuring the rate of vaporization of silver and the recoil force produced by the effusion of silver. Qualitatively the results are good, but refinements in the automatic control circuitry are needed before the technique can be quantitatively evaluated. It is expected that this technique will be ready for application to the zirconium subhalide disproportionation studies in the near future.)

D. SAMPLE PROCUREMENT AND PREPARATION

Samples of $ZrCl_4$ and ZrF_4 which have high purity and low hafnium content have been obtained. A sample of $ZrCl_2$, prepared by reaction of stoichiometric quantities of high-purity $ZrCl_4$ and Zr metal but of unknown actual purity and stoichiometry, has been obtained through the generosity of Dr. Orville Frampton, Research Division, U. S. Industrial Chemicals Co., Cincinnati. Wah Chang Corporation indicated at one time that after 1 October 1962 it would have available "high-purity" hafnium ingot and powder with a zirconium content around 200 ppm. This material is not yet available but is expected in the near future.

It appears that of the methods for preparing $ZrCl_3$ the one most likely to give a high-purity, stoichiometric product is that devised by Newnham.[5] Design and construction of the apparatus needed for this method is under way (also see below). Preparation of high-purity $ZrCl_2$ is a more difficult problem. The two most reasonable approaches appear to be direct combination of stoichiometric quantities of $ZrCl_4$ and Zr metal, and a modification of the Newnham technique[5] to accomplish reduction of $ZrCl_3$ to $ZrCl_2$. Since the Newnham apparatus is being built for preparation of $ZrCl_3$, it will also be used to attempt the reduction of $ZrCl_3$ to $ZrCl_2$, although the disproportionation of $ZrCl_3$ may present insurmountable difficulties.

---

(5) I. E. Newnham and J. A. Watts, J. Am. Chem. Soc., 82, 2113 (1960).

Approved for Public Release

Contrails

E. CALORIMETRY

Because the zirconium, and presumably hafnium, subchlorides react so vigorously with water to give products with inaccurately known compositions, their heats of formation cannot be determined by the straightforward aqueous-solution calorimetry used by MacWood et al.[6] for the titanium compounds. There appear to be two reasonable alternate approaches. One is to construct a "chlorine bomb" calorimeter in which the energy of direct chlorination of $ZrCl_3$ and of $ZrCl_2$ to $ZrCl_4$ could be measured. The other is to find a solvent system in which the necessary enthalpies of solution can be measured.

A suitable solvent system must satisfy the following requirements: (1) $ZrCl_4$ must be readily soluble; (2) an oxidizing agent for the subchlorides and its reduced form (e.g., $FeCl_3$ - $FeCl_2$) must be readily soluble; and (3) the solvent system must be inert to the subchlorides which are very strong reducing agents, i.e., $ZrCl_3$ and $ZrCl_2$ must react with the oxidizing agent only. After reviewing the available information[7], in particular the results of solvent extraction studies of various chlorides including $ZrCl_4$, we have concluded that a 5 - 10 percent solution of a long-chain aliphatic tertiary amine (e.g., tridecylamine) in a saturated hydrocarbon (e.g., cyclohexane) will probably be a satisfactory medium for solution calorimetry.

Calorimetry in such a medium, with requirements for the strict exclusion of moisture, will present a number of difficulties, but these appear to be fewer in number and smaller in magnitude than those to be expected in chlorine-bomb calorimetry. Accordingly, we have proceeded with design and construction of a solution calorimeter and assembly of the necessary auxillary equipment for calorimetric measurements. Since this decision was made rather late in the year, there is little else to report at present. We expect the calorimeter and associated equipment to be in operation within two-three months.

---

(6) G. E. MacWood et al. Technical Reports No. 1, 2, and 3, Project NR037-024, Office of Naval Research, Washington. (Department of Chemistry, Ohio State University).

(7) Abstracts of Papers, Solvent Extraction Chemistry Symposium, Gatlinburg, Tennessee, October, 1963.

Approved for Public Release

Contrails

Appendix B

HIGH TEMPERATURE PROPERTIES OF REFRACTORY ZIRCONIUM AND HAFNIUM COMPOUNDS*

John L. Margrave et al
University of Wisconsin, Madison, Wisconsin

1. The High Temperature Heat Content of Zirconium Diboride

Robert H. Valentine, Thomas F. Jambois,
and John L. Margrave

A. BACKGROUND

Five sets of high temperature thermodynamic data[1-5] and a single low temperature study[6] have previously been available for ZrB_2 samples of 95-99% purity, but large positive and negative discrepancies (10-20% or more) have been observed even though all the calorimeters have been calibrated in standard ways. In a cross-check of data, Pears et al[7] made runs on the same ZrB_2 used by Barnes et al[3] and reproduced the results of Barnes et al within a few per cent, which indicates that the reported large differences between samples are real and not measurement errors. The AVCO results are pulse-type heat capacity measurements[4] over the temperature range 2000 to 2500K, but seem to differ drastically from conventional extrapolations of the lower temperature results, as do the results of Prophet[5].

* - Report on subcontracted studies under Air Force Contract AF 33(616)-7472.

(1) A. N. Krestovnikov et al, Izvest. Vysshikh Ucheb. Zavedenii, Razvedoch Tsvetnoya Met., No. 1, 73-75 (1958); also, Chem. Abstr. 53, 19552C (1959).

(2) D. Neel, C. Pears and S. Oglesby, Southern Research Institute Report No. ASD-TDR-62-765 to Wright Air Development Division, August 1962.

(3) D. Barnes, R. Mezaki, E. Tilleux and J. Margrave, Proc. International Symposium on Thermodynamics of Nuclear Materials, Paper SM-26/48, Vienna, Austria, May 21, 1962, p.775.

(4) R. Barriault et al, Thermodynamics of Refractory Compounds, Avco Reports to Wright-Patterson Air Force Base under Contract No. AF 33(616)-7327, ASO-TR-61-260, Vol. I, pp. 350, 378-80 (1961) and Vol. II (1962).

(5) H. Prophet, unpublished work cited in the JANAF Tables, edited by D. R. Stull, Dow Chemical Company, Midland, Michigan.

(6) E. F. Westrum and G. Feick, submitted for publication in J. Chem. Eng. Data. Also presented in ASD-TDR-62-204, Part I.

(7) C. D. Pears, Private Communication, May 21, 1962.

Approved for Public Release

Contrails

This report presents high temperature measurements on a sample of ZrB_2 prepared by Feick[8] which is from the same batch as the sample used by Westrum and Feick[6] for their low-temperature studies.

B. EXPERIMENTAL

The calorimeter used in this work has been described previously[9] and the samples were contained in platinum-rhodium capsules under an argon atmosphere. Temperature measurements were made with a Pt vs. Pt-10% Rh thermocouple calibrated against a reference which had been recently calibrated at the National Bureau of Standards. The reliability of the calorimeter was checked by re-running a standard sample of synthetic sapphire. The heat content for the empty Pt capsules was measured at several temperatures and found to check well with the equation of Kelley[10] while the heat content of the Pt-10% Rh capsule was calculated from Kelley's data on the elements.

According to Feick,[8] the samples used (Bar. No. 80) had been zone-refined and had the stoichiometry $ZrB_{1.97}$. Representative impurities in such bars are: O, 52 ppm; C, 215 ppm; N, 134 ppm; Si, 100-1000 ppm; Hf and Fe, 10-1000 ppm; Mg, 10-100 ppm; and Ag, Ca, Cu, Ti, V, Cr, and Mn, 10 ppm. There is also some possibility of ZrB being present originally,[6] although it probably annealed out during the heating cycles.

C. RESULTS

Two sets of data were obtained. The first set, covering the range 410-773K, was terminated when the capsule sprang a leak and allowed oxidation of the ZrB_2 as detected by a large, sudden weight gain in the next run attempted after 773°K. The second series covered the range 450-1126K and no weight changes were observed. The results were processed on a CDC-1604 high-speed computer to yield the data in Table B-I. These data were then used for obtaining a least squares fit and a Kelley equation[9] for $(H_T - H_{298})$ over the range 260-1126K by considering the higher temperature results of Westrum and Feick.[6] The equations derived are:

$$(H_T - H_{298}) = \left(14.23T + 1.554 \times 10^{-3}T^2 + \frac{2.725\times10^{-7}}{T} - 5296\right) \pm 64 \text{ calories mole}^{-1}$$

and

$$C_p = 14.23 + 3.108 \times 10^{-3}T - \frac{2.725\times10^{-7}}{T^2} \text{ cal deg}^{-1} \text{ mole}^{-1}$$

where $260K < T < 1126K$, but extrapolations above or below these limits must be made cautiously because of the empirical nature of the equation.

---

(8) G. Feick, Arthur D. Little, Inc., see ASD-TDR-62-204 Part I.

(9) R. T. Grimley and J. L. Margrave, J. Phys. Chem. 62, 1436 (1958); 63, 1505 (1959).

(10) K. K. Kelley, U. S. Bureau of Mines, Bulletin 584 (1960).

Approved for Public Release

Contrails

TABLE B-I

EXPERIMENTAL HEAT CONTENTS OF ZrB_2

T (°K)	T_{cal} (°K)	$H_T - H_{T_{cal}}$ (cal $mole^{-1}$)
410.46	298.60	1510
463.46	298.69	2204
553.76	298.93	3564
598.66	298.81	4288
711.06	298.89	5926
773.06	298.97	7114
450.02	297.88	1998
514.25	298.92	3017
724.16	299.44	6031
888.46	299.26	8782
986.46	299.02	10626
1123.46	299.17	12781
1125.62	299.17	13000

Approved for Public Release

Contrails

Thermodynamic functions based on the smoothed experimental points up to 1200K and the extrapolated equation for $(H_T - H_{298})$ in the range above 1200K are presented in Table B-II. For comparison, high temperature heat capacities based on all the available measurements on ZrB_2 samples are tabulated in Table B-III. The discrepancies clearly show the need for further high temperature studies on well-characterized samples of ZrB_2.

D. ACKNOWLEDGMENTS

This work was supported financially by the U. S. Air Force under Contract No. AF 33(616)-7472, administered for Arthur D. Little, Inc., by Dr. Leslie McClaine, and by the Wisconsin Alumni Research Foundation. The assistance of the staff of the University of Wisconsin Numerical Analysis Laboratory is also gratefully recognized.

Approved for Public Release

Contrails

TABLE B-II

SMOOTHED THERMODYNAMIC FUNCTIONS FOR ZrB_2*

T	$H_T^o - H_{298.15}^o$	C_p^o	S_T^o	$-\left(\frac{G_T^o - H_{298.15}^o}{T}\right)$
(°K)	(cal mole^{-1})	(cal deg^{-1} mole^{-1})	(cal deg^{-1} mole^{-1})	
0	- 1590	0	0	∞
50	- 1585	0.503	0.142	31.83
100	- 1503	2.870	1.177	16.21
150	- 1296	5.410	2.820	11.46
200	- 964	7.840	4.716	9.53
250	- 518	9.919	6.696	8.77
298.15	0	11.53	8.59	8.59
300	21	11.59	8.66	8.60
350	635	12.88	10.55	8.74
400	1327	13.77	12.41	9.09
500	2754	14.70	15.59	10.08
600	4258	15.34	18.33	11.23
700	5818	15.85	20.73	12.42
800	7426	16.29	22.88	13.60
900	9075	16.69	24.82	14.74
1000	10764	17.07	26.60	15.84
1100	12489	17.43	28.24	16.89
1200	14249	17.77	29.77	17.90
1300	16043	18.11	31.21	18.87
1400	17871	18.45	32.56	19.80
1500	19732	18.77	33.85	20.70
1600	21626	19.10	35.07	21.55
1700	23552	19.42	36.24	22.39
1800	25510	19.74	37.36	23.19
1900	27501	20.06	38.43	23.96
2000	29523	20.38	39.47	24.71

* - Data from 0-350K based on ref. 6; from 350-1200K based on this work; above 1200K extrapolated.

Approved for Public Release

TABLE B-III

A COMPARISON OF REPORTED HIGH TEMPERATURE HEAT CAPACITIES FOR ZrB_2

	C_p in cal deg^{-1} $mole^{-1}$						
T^oK	Krestovnikov[1]	SRI[2]	Barnes et al[3]	AVCO[4]	Prophet[5]	Westrum[6]	This Work
298.15	(14.41)	-	(13.1)	-	(10.55)	11.53	(11.53)
500	15.77	11.52	16.50	-	(14.06)	-	14.70
1000	17.74	19.36	19.66	-	(20.22)	-	17.07
1500	17.70	21.50	-	-	24.38	-	(18.77)
2000	(15.64)	23.50	-	38.37*	27.32	-	(20.38)
2500	-	25.20	-	41.76*	(29.41)	-	-

( ) - Indicates extrapolated values, usually beyond reliable limits of equations used.

* - These excessively high results could arise because no correction for sublimation of the sample was made.

Approved for Public Release

Contrails

2. The High Temperature Heat Contents of Zirconium Carbide and Tantalum Carbide

Reiji Mezaki, Thomas F. Jambois,
Arun K. Gangopadhyay, and John L. Margrave

A. BACKGROUND

Reliable high temperature thermodynamic data for non-oxide refractories have been scarce, although Kelley reported the low temperature specific heat of TaC in 1940.[11] Westrum and Feick[12] have recently published measurements of the heat capacity of ZrC at low temperatures. This paper reports supplementary high temperature measurements over the range 400-1200K for both TaC and ZrC. In addition, Pears et al[2] have recently reported high temperature heat content data on both TaC and ZrC.

B. EXPERIMENTAL TECHNIQUES

The calorimeter used in this work has been described previously.[9] Samples of powdered TaC and ZrC from The Carborundum Company and a zone-refined sample of ZrC from the batch used by Westrum and Feick[12] were utilized in these experiments without further treatment. Gold container capsules were used and no reactions or changes in weight were observed during the runs.

C. RESULTS AND DISCUSSION

The results of the calorimetric experiments are summarized in Tables B-IV and B-V. Such data may be fitted by the method of least squares to either a 3- or 4-constant equation of the type used by Kelley[10] and others for tabulating high temperature thermodynamic data. The following equations were derived:

$$(H_T - H_{298})_{TaC} = 8.69\ T + 2.60 \times 10^{-3}\ T^2 - 2{,}823 \text{ cal mole}^{-1}$$

$$C_p(TaC) = 8.69 + 5.20 \times 10^{-3}\ T \text{ cal mole}^{-1} \text{ deg}^{-1}$$

for the temperature range: $476^\circ < T < 1113^\circ K$

$$(H_T - H_{298})^{\text{powdered}}_{ZrC} = 11.40\ T + 0.71 \times 10^{-3}\ T^2 + 1.87 \times 10^{5}\ T^{-1} - 4{,}087 \text{ cal mole}^{-1}$$

$$C_p(ZrC) = 11.40 + 1.42 \times 10^{-3}\ T - 1.87 \times 10^{5}\ T^{-2} \text{ cal mole}^{-1} \text{ deg}^{-1}$$

for the temperature range: $470^\circ < T < 1174^\circ K$.

---

(11) K. K. Kelley, J. Am. Chem. Soc. 62, 818 (1940).

(12) E. F. Westrum and G. Feick, submitted for publication in J. Chem. Engr. Data. See also Appendix C of this report.

Approved for Public Release

Contrails

TABLE B-IV

EXPERIMENTAL HEAT CONTENT DATA FOR POWDERED TaC

$\frac{T}{(^{o}K)}$	$\frac{T_{cal}}{(^{o}K)}$	$\frac{H_T - H_{T_{cal}}}{(cal\ mole^{-1})}$
476.4	298.79	1,887
587.3	298.87	3,159
728.2	298.87	4,899
851.2	299.04	6,451
978.9	298.84	8,181
1,113.2	298.97	10,062

Approved for Public Release

Contrails

TABLE B-V

EXPERIMENTAL HEAT CONTENT DATA FOR ZrC

(a) Powdered Sample from The Carborundum Company

T (^{o}K)	T_{cal} (^{o}K)	$H_T - H_{T_{cal}}$ (cal $mole^{-1}$)
470.80	298.81	1,833
603.40	299.00	3,337
735.40	298.98	4,881
863.00	299.00	6,446
973.00	299.16	7,875
1,174.40	299.16	10,381

(b) Zone-refined Sample from Arthur D. Little, Inc.

Data for 21 temperatures over the range 366-1212K are now being processed.

Approved for Public Release

Contrails

An alternative approach for representation of the data is the use of theoretically sound Debye and Einstein functions fitted to the experimental points. This allows extrapolation to high temperatures with somewhat more confidence than with the empirical Kelley equation. From a survey of 3200 possible combinations of Debye and Einstein functions with a program written for the CDC-1604 computer, one selects the following best fits:

(1) C_p (ZrC) = D(550/T) + E(650/T) + 1.014 x 10^{-3} T cal deg^{-1} $mole^{-1}$ which gives $(H_T - H_{298})$ to $\pm$24 cal $mole^{-1}$ over the range 0-1174K and gives S^o_{298} = 7.45$\pm$0.5 cal deg^{-1} $mole^{-1}$ which compares well with the experimental entropy at 298K of 7.90 cal deg^{-1} $mole^{-1}$ reported by Westrum and Feick.[12]

(2) C_p (TaC) = D(330/T) + E(950/T) + 2.287 x 10^{-3} T cal deg^{-1} $mole^{-1}$ which gives $(H_T - H_{298})$ to $\pm$24 cal $mole^{-1}$ over the range 0-1113K and indicates S^o_{298} = 9.81$\pm$0.5 cal deg^{-1} $mole^{-1}$ while Kelley[11] reported 10.1$\pm$0.1 cal deg^{-1} $mole^{-1}$.

Studies of the zone-refined sample of ZrC are now in progress and the data are being processed. Additional data on TaC and ZrC from the work at the Southern Research Institute will be compared with these data when present measurements are completed.

Derived thermodynamic functions for TaC are presented in Table B-VI and for ZrC in Table B-VII based on the measurements with the powdered samples only, and extrapolated with the selected Debye-Einstein functions.

D. ACKNOWLEDGMENTS

The authors are pleased to acknowledge the financial support of this work by the United States Air Force under Contract No. AF 33(616)-7472 administered by Dr. Leslie McClaine for Arthur D. Little, Inc., and by the Wisconsin Alumni Research Foundation. The powdered samples were generously provided by Dr. Peter Schaffer of The Carborundum Company, Niagara Fall, New York.

Approved for Public Release

Contrails

TABLE B-VI

HIGH TEMPERATURE THERMODYNAMIC FUNCTIONS FOR TaC*

T	$H_T - H_{298}$		C_p		$S_T - S_{298}$		$-\left(\frac{F_T - H_{298}}{T}\right)$
(^oK)	(cal $mole^{-1}$)		(cal deg^{-1} $mole^{-1}$)		(cal deg^{-1} $mole^{-1}$)		(cal deg^{-1} $mole^{-1}$)
0	--	(-1542)	0	(0)	-10.1	(-9.81)	∞
100	-1356	(-1361)	--	(4.22)	--	(-7.02)	16.7
200	- 765	(- 794)	--	(6.98)	--	(-3.20)	10.9
250	- 406	(- 415)	--	(8.14)	--	(-1.51)	10.3
298.15	0	(0)	--	(9.07)	0	(0)	10.1
300	18	(17)	10.25	(9.11)	0.06	(0.06)	10.1
400	1070	(1003)	10.77	(10.51)	3.08	(2.99)	10.7
500	2174	(2104)	11.29	(11.45)	5.54	(5.34)	11.4
600	3329	(3284)	11.82	(12.12)	7.65	(7.49)	12.3
700	4537	(4523)	12.34	(12.63)	9.51	(9.40)	13.2
800	5796	(5808)	12.86	(13.06)	11.19	(11.11)	14.0
900	7108	(7132)	13.38	(13.42)	12.74	(12.67)	14.9
1000	8472	(8492)	13.90	(13.75)	14.17	(14.10)	15.8
1100	10,032	(9882)	14.47	(14.06)	15.65	(15.43)	16.8
1200	11,355	(11303)	14.94	(14.35)	16.80	(16.67)	17.5
1300	(12,750)		(14.6)		(17.8)		(18.1)
1400	(14,230)		(14.9)		(18.9)		(18.8)
1500	(15,730)		(15.2)		(20.0)		(19.6)
1600	(17,260)		(15.4)		(20.9)		(20.3)
1700	(18,810)		(15.7)		(21.9)		(20.9)
1800	(20,390)		(15.9)		(22.8)		(21.5)
1900	(21,990)		(16.1)		(23.7)		(22.2)
2000	(23,610)		(16.4)		(24.5)		(22.8)

( ) - Based on machine-selected fit $C_p = D(300/T) + E(950/T) + 2.287 \times 10^{-3} T$.

* - Data for 0-300K from Kelley;[11] for 300-1200K from the empirical fit of the data in Table B-IV and above 1200K from the extrapolation of the Debye-Einstein equation.

Approved for Public Release

Contrails

TABLE B-VII

HIGH TEMPERATURE THERMODYNAMIC FUNCTIONS FOR ZrC*

T	$H_T - H_{298}$		C_p		$S_T - S_{298}$		$-\left(\frac{F_T - H_{298}}{T}\right)$
(°K)	(cal mole^{-1})		(cal deg^{-1} mole^{-1})		(cal deg^{-1} mole^{-1})		(cal deg^{-1} mole^{-1})
0	-1401	(-1378)	0	(0)	-7.96	(-7.45)	
100	-1300	(-1310)	3.06	(2.35)	-6.57	(-6.50)	14.39
200	- 791	(-823)	6.86	(7.05)	-3.19	(-3.32)	8.89
250	- 414	(-433)	8.14	(8.48)	-1.51	(-1.58)	8.18
298.15	0	(0)	9.06	(9.43)	0	(0)	7.96
300	17.5	(17)	9.09	(9.46)	0.06	(0.06)	7.96
400	1052	(1029)	10.80	(10.65)	3.03	(2.96)	8.42
500	2162	(2130)	11.36	(11.31)	5.50	(5.41)	9.14
600	3317	(3284)	11.73	(11.74)	7.61	(7.52)	10.04
700	4504	(4474)	12.01	(12.04)	9.44	(9.35)	10.97
800	5717	(5690)	12.24	(12.28)	11.06	(10.98)	11.87
900	6951	(6928)	12.44	(12.47)	12.51	(12.43)	12.75
1000	8205	(8184)	12.63	(12.64)	13.83	(13.76)	13.58
1100	9476	(9456)	12.80	(12.79)	15.04	(14.97)	14.39
1200	10,764	(10743)	12.97	(12.93)	16.16	(16.09)	15.15
1300	(12,040)		(13.01)		(17.1)		(15.8)
1400	(13,360)		(13.2)		(18.1)		(16.6)
1500	(14,680)		(13.3)		(19.0)		(17.2)
1600	(16,020)		(13.4)		(19.9)		(17.8)
1700	(17,370)		(13.5)		(20.7)		(18.5)
1800	(18,730)		(13.7)		(21.5)		(19.0)
1900	(20,100)		(13.8)		(22.2)		(19.6)
2000	(21,480)		(13.9)		(22.9)		(20.2)

( ) - Based on machine-selected fit $C_p = D(550/T) + E(650/T) + 1.014 \times 10^{-3} T$.

* - Data for 0-350K from Westrum and Feick;[12] for 350-1200K from the empirical fit of the data in Table B-V; and above 1200K from the extrapolation of the Debye-Einstein equation.

Approved for Public Release

Contrails

3. The Oxidation of Zirconium Diboride and Zirconium Carbide at High Temperatures

A. K. Kuriakose and J. L. Margrave

A. INTRODUCTION

Because of the very refractory nature, hardness and high tensile strength, in general, of the borides, carbides and nitrides of the refractory metals, they are highly promising materials in many high temperature applications. The relatively low density of the zirconium compounds makes them all the more attractive for space vehicle applications. A knowledge of the oxidation kinetics of these materials is essential for such technical uses and hence the present investigation of the high temperature oxidation kinetics for zirconium diboride and zirconium carbide was undertaken. Work in this topic is also under way by Berkowitz[13] who has examined the oxidation of ZrC and ZrB_2 at temperatures of 1100-2200K with an oxygen partial pressure around 10 mm. in helium, following the extent of reaction by measuring the amount of oxygen reacted, by a thermal conductivity method. However, our investigation is at temperatures 554-652C for ZrC and 945-1256C for ZrB_2 at oxygen pressures of up to 1 atmosphere and estimating the progress of reaction by observing directly the weight gained by the samples with time.

B. APPARATUS AND EXPERIMENTAL PROCEDURE

The schematic diagram of the apparatus used (Figure B-1) is self-explanatory. The inset in Figure B-1 is a view of the combustion furnace and accessories. The Mullite combustion tube, A, is 15" long and 1-1/2" wide and is mounted vertically and heated by two concentric furnace windings, C, of Kanthal wire. The inner winding is on the Mullite itself. Standard Pyrex ground-glass joints are sealed on to the Mullite tube at both ends. An inlet tube, J, for the reacting gas, and a chromel-alumel thermocouple, F, are attached from the bottom portion, and two outlets are provided at the top, one for evacuating the system and the other for the gases to escape into the hood. A helical quartz spring, D, calibrated for load vs extension is suspended vertically as shown in the figure and the sample to be examined is attached to the lower hook of the spring by means of 0.007" nickel wire, G, and a piece of quartz fiber, E, so that the sample, S, is only about 1 cm above the thermocouple bead. The proximity of the sample to the thermocouple insures accurate temperature measurement of the sample. The temperature of the heating furnace is regulated to $\pm$2C. The extension of the spring is measured by means of a cathetometer. A change in weight by 0.2 mgm could be determined.

---

(13) See Chapter V of this report.

Approved for Public Release

Contrails

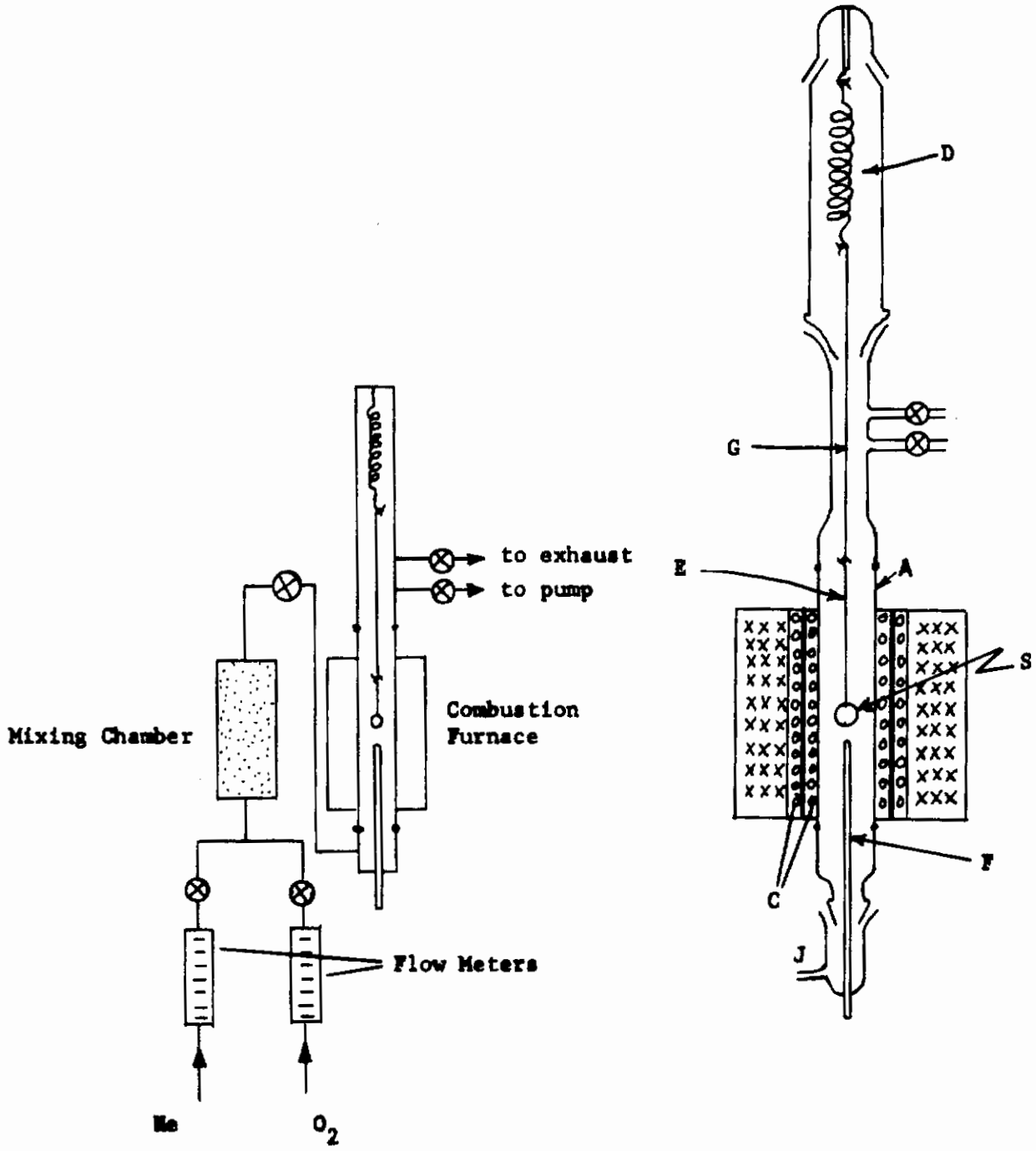

Figure B-1. - Schematic diagram of the apparatus used for studying high temperature oxidation kinetics.

Approved for Public Release

Contrails

All the experiments were done at a total pressure of 1 atm and various partial pressures for the O_2 were obtained by mixing it with purified helium gas. The sample was initially heated in an atmosphere of helium to the desired temperature and the zero-reading on the cathetometer taken against a fixed point (end) on the suspension wire. The system was then evacuated, O_2 gas was suddenly admitted and the flow-rate slowly adjusted. The time when oxygen was introduced was taken as zero. The readings of the cathetometer at suitable intervals of time were recorded and each run was continued until a sufficient number of points was obtained to determine the kinetics of the process.

The zirconium diboride used had a composition $ZrB_{1.95}$ with 1.7% of Hf and a carbon content of about 200 ppm. Circular pieces of the material weighing about 0.5-0.8 gm were cut from a cylindrical bar and polished by grinding with fine abrasive powder. They were thoroughly washed with water and dried in air. The areas of the samples were determined to the nearest 1 mm^2. A similar procedure was used for the zirconium carbide samples.

The oxide film on the oxidized samples was removed by micro sand blasting and repolished by grinding again. Thus, the same piece could be used several times. This method, apparently, did not affect the nature of the surface of the material, since identical rates of oxidation within experimental error were observed (cf. section on prerun treatment).

C. OXIDATION OF ZIRCONIUM DIBORIDE: RESULTS AND DISCUSSION

From the extension of the spring at various intervals of time, the weight gain of the samples in milligrams/cm^2 at the respective time intervals were evaluated. A plot of the weight increase in mgm/cm^2 vs time yielded parabolic curves as shown in Figure B-2. Straight lines were obtained by plotting (wt. gain/cm^2)^2 vs the time (Figure B-3) which shows that the oxidation of ZrB_2 follows a parabolic rate law, and rate constants were obtained from the slopes of the straight lines.

The prerun treatment was varied in a few runs and the parabolic rate constants obtained in each case are recorded in Table B-VIII. It may be seen from Table B-VIII that there is no significant change in the rate of oxidation of ZrB_2 when the sample is preheated or when the oxidized material is repolished and used without preheating, although when a fresh piece is used without preheating the rate constant is higher. Hence, in all the other runs the fresh sample was either preheated for 1/2 hour, or the oxidized surface was repolished and used with no preheating.

Three runs were done with O_2 flow rates of 100, 50, and 20 ml/min, at 1056C in order to determine the affect of flow rate on the reaction, and the rate constants (parabolic) obtained in these cases are reported in Table B-IX. It is evident from this table that the rate of oxidation of ZrB_2 is independent of the flow rate of O_2 in the system in the range studied, within experimental error.

Figure B-4 represents the parabolic plot of the results obtained at various O_2 partial pressures (102-744 mm of mercury, mixed with helium gas) on the

Approved for Public Release

Contrails

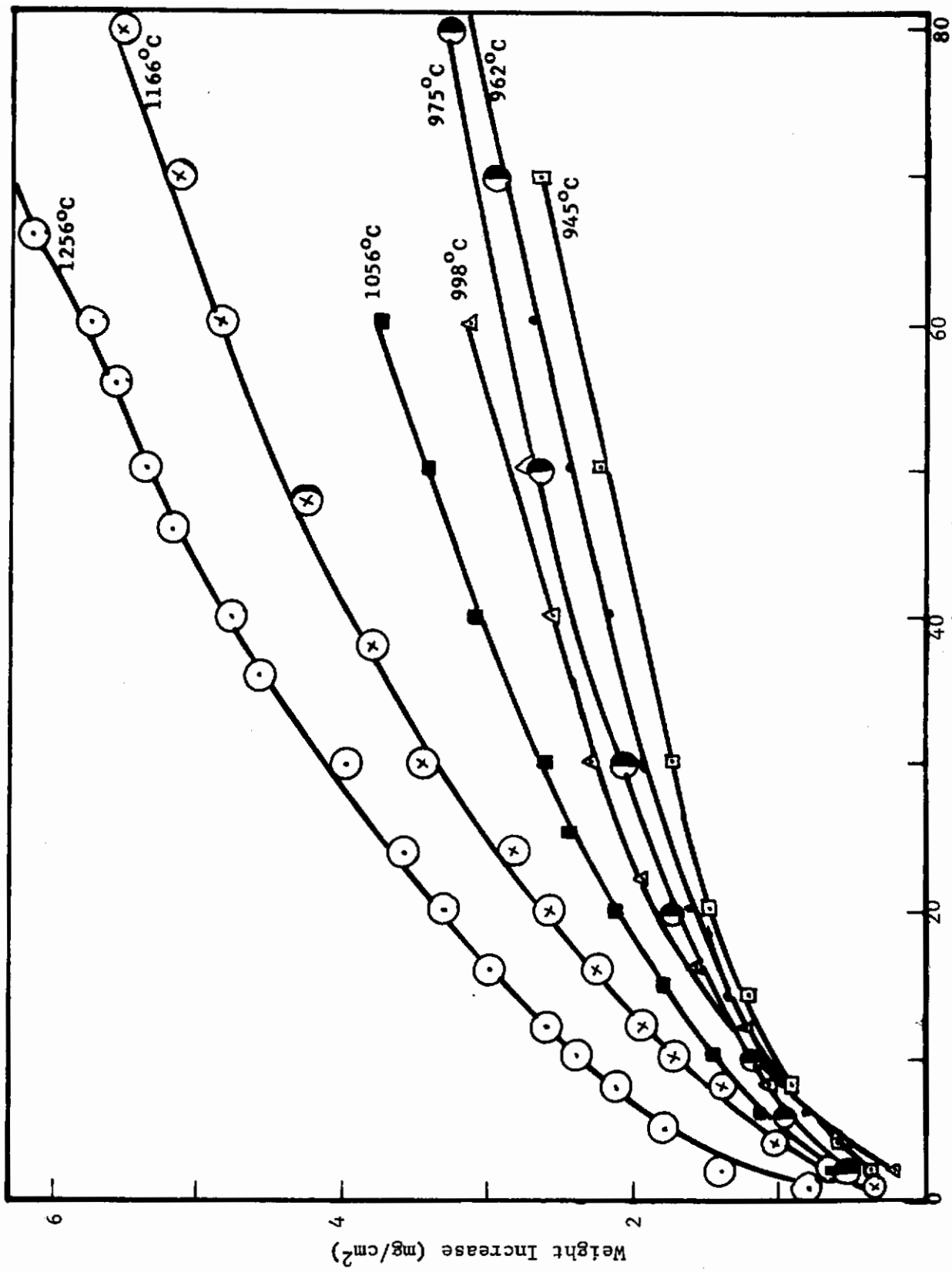

Figure B-2. - Linear plot for the oxidation of ZrB_2 in pure oxygen (oxygen pressure, 1 atm)

Approved for Public Release

Contrails

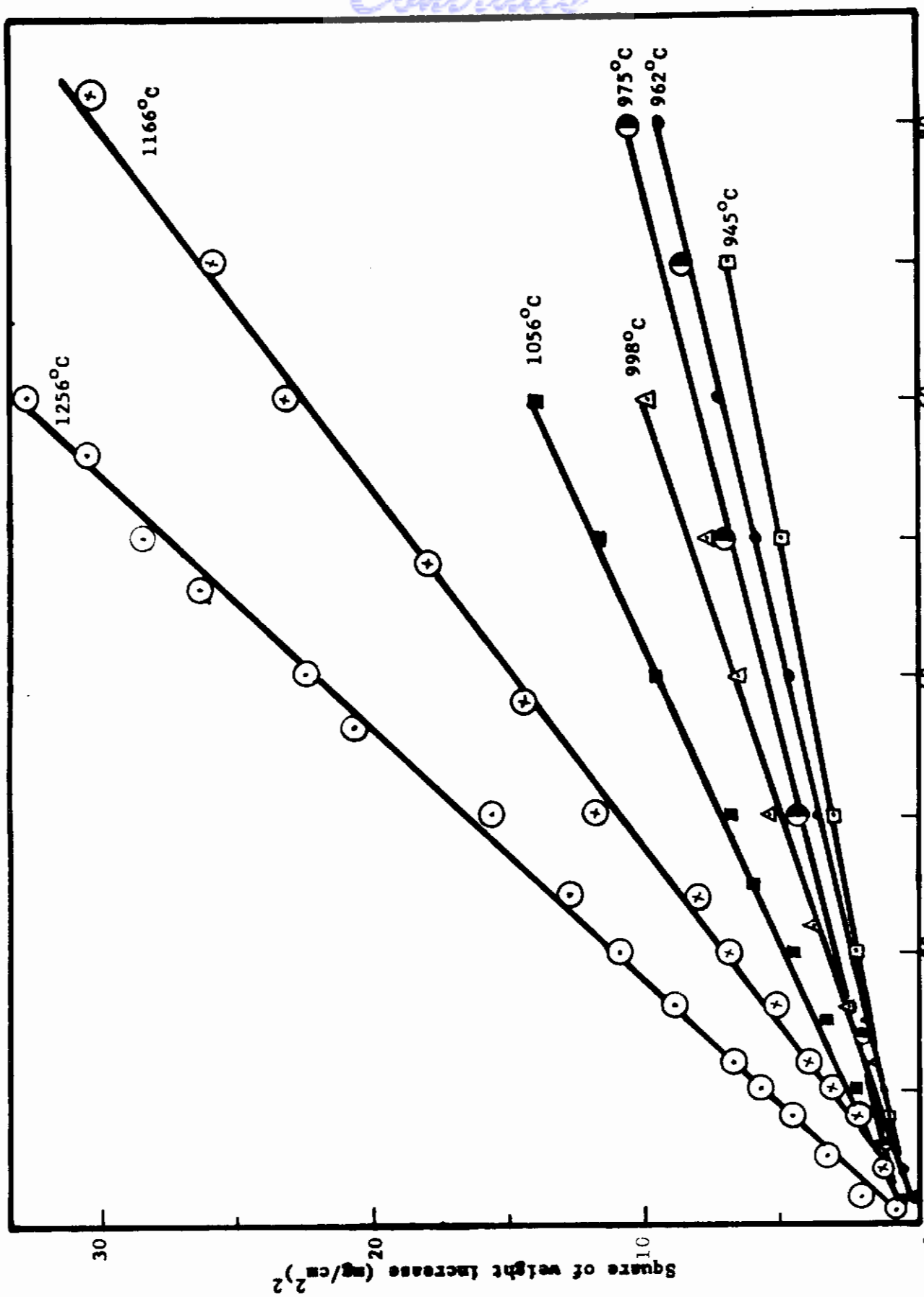

Figure B-3. - Parabolic plot for the oxidation of ZrB_2 in pure oxygen (oxygen pressure, 1 atm)

Approved for Public Release

Contrails

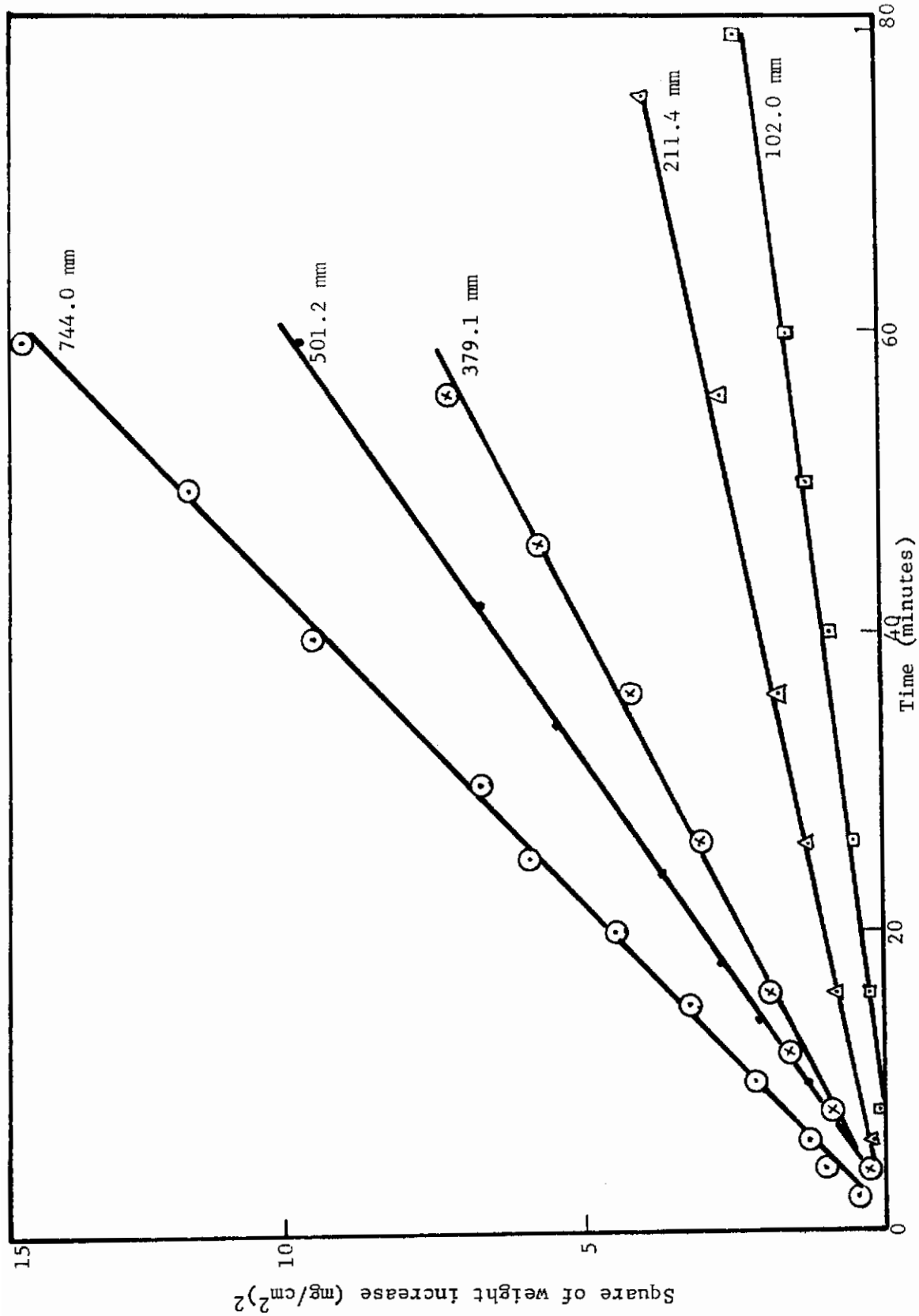

Figure B-4. - Parabolic plot for the oxidation of ZrB_2 at various oxygen partial pressures. (Temperature 1056C)

Approved for Public Release

Contrails

TABLE B-VIII

PARABOLIC RATE CONSTANTS FOR
THE OXIDATION OF ZrB_2 UNDER VARIOUS PRERUN TREATMENTS

Run No.	Prerun Treatment	Parabolic Rate Constants ($(mgm/cm^2)^2/min$)
1	Preheated for 1/2 hr at the temperature of the experiment	0.2368
2	Oxidized sample repolished and no preheating	0.2459
3	Fresh sample with no preheating	0.3000

TABLE B-IX

PARABOLIC RATE CONSTANTS FOR
THE OXIDATION OF ZrB_2 WITH VARIOUS FLOW RATES OF O_2

Flow Rate (ml/min)	Rate Constant, k_p ($(mgm/cm^2)^2/min$)
20	0.2206
50	0.2612
100	0.2459

Approved for Public Release

Contrails

oxidation of ZrB_2. The oxidation rate increases with increasing partial pressure of O_2, and the increase in the parabolic rate constant is directly proportional to the partial pressure of O_2 as indicated by Figure B-5 which is a plot of the rate constants against the partial pressure.

In order to obtain the activation energy for the reaction between ZrB_2 and O_2, experiments were carried out at various temperatures ranging from 945 to 1256C at a pressure of 1 atm and flow rate of O_2 = 100 ml/min. The parabolic rate constants calculated in each case are listed in Table B-X. The Arrhenius plot of the results (Figure B-6) is linear with an activation energy of 19.8±1.0 kcal/mole, calculated by a least square method. Considering the volatility of boron oxide, one would expect the rate constant to fall off from the log k vs 1/T plot at higher temperatures. This is apparently not the case, possibly because the loss in weight by evaporation of B_2O_3 is compensated for by an increased oxidation due to lower thickness in the protective film of oxides.

In one of the experiments, oxygen was bubbled through distilled water and passed into the combustion tube containing ZrB_2 at 1056C, for studying the effect of moist oxygen on the reaction. A parabolic reaction rate was observed and the rate constant in this run was lower ($0.20(mgm/cm^2)^2/min$) than that for dry oxygen under similar conditions, ($0.24(mgm/cm^2)^2/min$). The decrease in the rate might be attributed to two reasons: (1) a reduction in the partial pressure of oxygen from 744 to 719 mm due to the presence of saturated water vapor and (2) the formation of boric acid which is more volatile than B_2O_3, causing further apparent decrease in the observed rate of weight gain. Glistening white crystals of boric acid were observed on the cooler parts of the combustion tube. It was further noticed, unlike in the other cases, that the ZrB_2 became very brittle after being exposed to moist oxygen.

D. OXIDATION OF ZIRCONIUM CARBIDE: RESULTS AND DISCUSSION

Unlike zirconium diboride, zirconium carbide is more susceptible to oxidation and at lower temperatures. Pieces of zirconium carbide were found to break up immediately in contact with O_2 at 1000C or even lower. Berkowitz[13] also has observed the same phenomenon. It may be mentioned here that Gangler[14] found excessive oxidation of ZrC in air at 980C. In order to find a workable temperature range for studying the oxidation kinetics, a piece of ZrC was heated slowly from room temperature in an atmosphere of oxygen. The sample began to crumble at about 700C and broke up into several pieces at about 850C, so that the maximum workable temperature was about 650C. Even at this temperature, samples started crumbling after about an hour of oxidation. A porous film of zirconium oxide was formed on the sample. The results of the successful runs at 554-652C are presented graphically in Figure B-7. It is clear that the reaction follows a linear rate law at 1 atm pressure of O_2 and a flow rate of 100 ml/min. The linear rate constants at various temperatures are given in Table B-XI. The activation energy calculated in this case from the Arrhenius plot (Figure B-8) is 16.7±1.7 kcal/mole.

---

(14) J. J. Gangler, Am. Ceramic Soc. 52nd Annual Meeting, preprint (1950) (as cited in P. Schwartzkopf and R. Kieffer, Refractory Hard Metals, MacMillan Publishing Co., New York, (1953)).

Approved for Public Release

Approved for Public Release

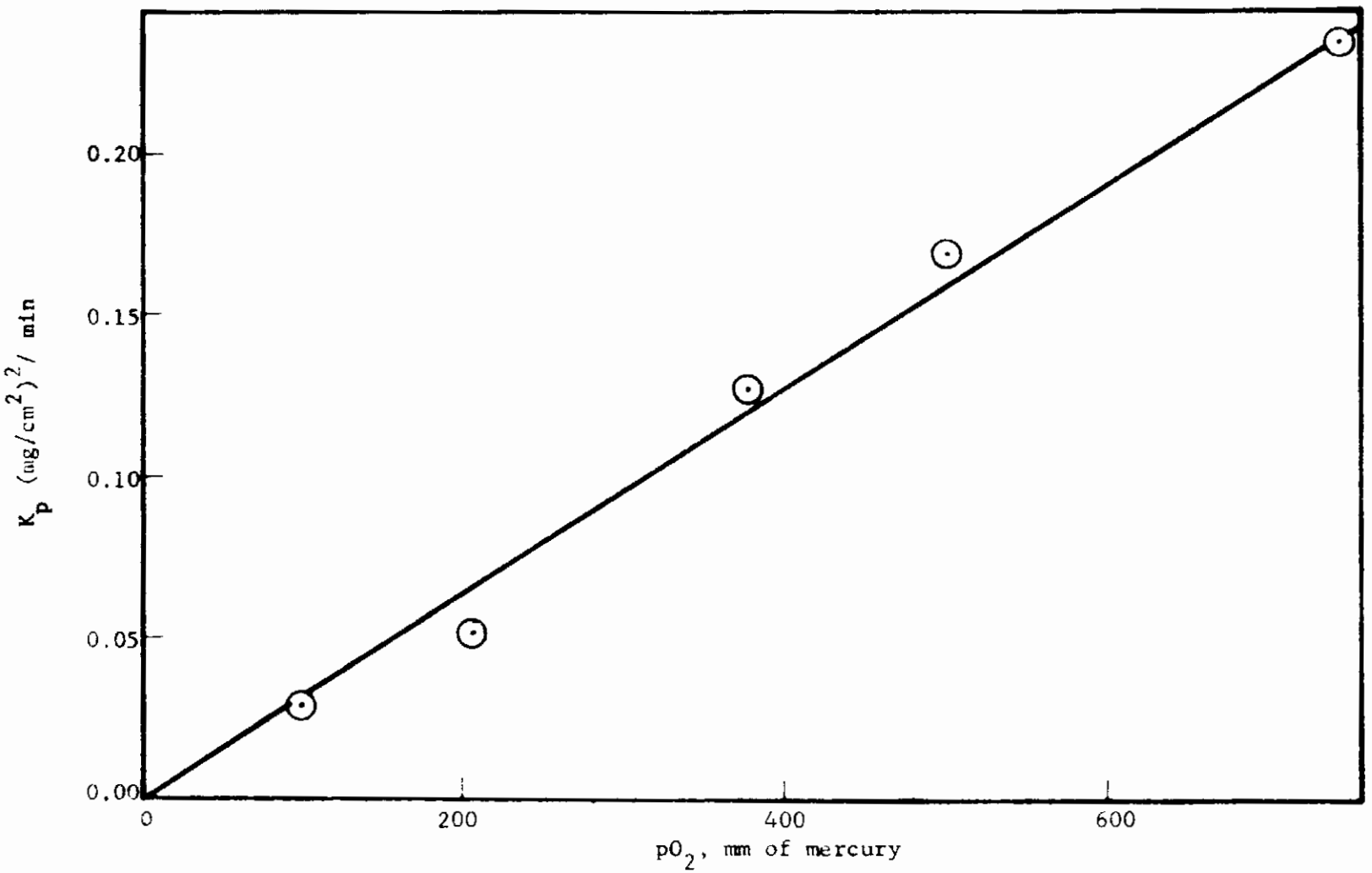

Figure B-5. - The effect of oxygen partial pressure on the oxidation of ZrB_2.
(Temperature 1056C)

Contrails

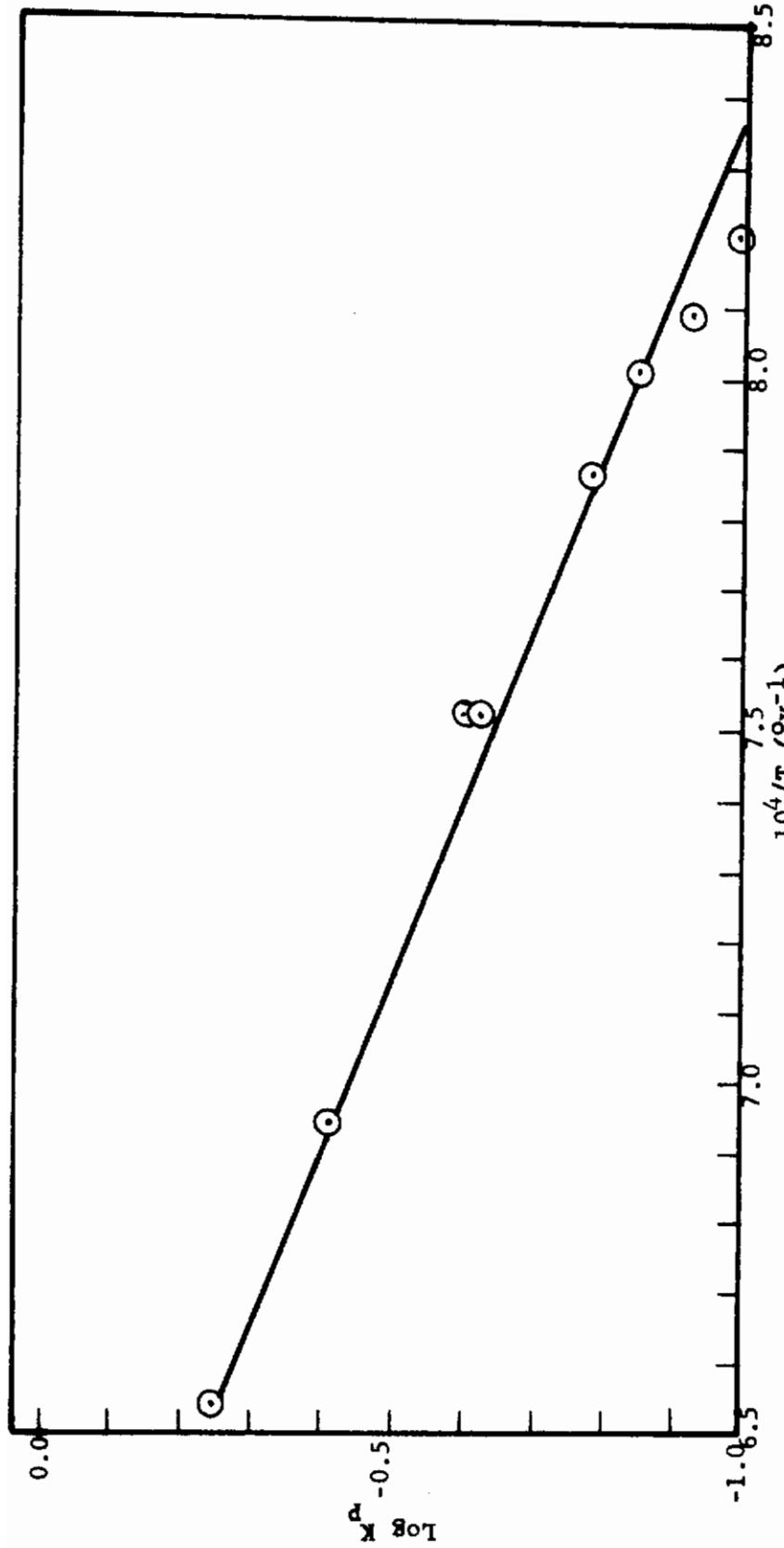

Figure B-6. - Arrhenius plot for the oxidation of ZrB_2
(oxygen pressure, 1 atm)

Approved for Public Release

Contrails

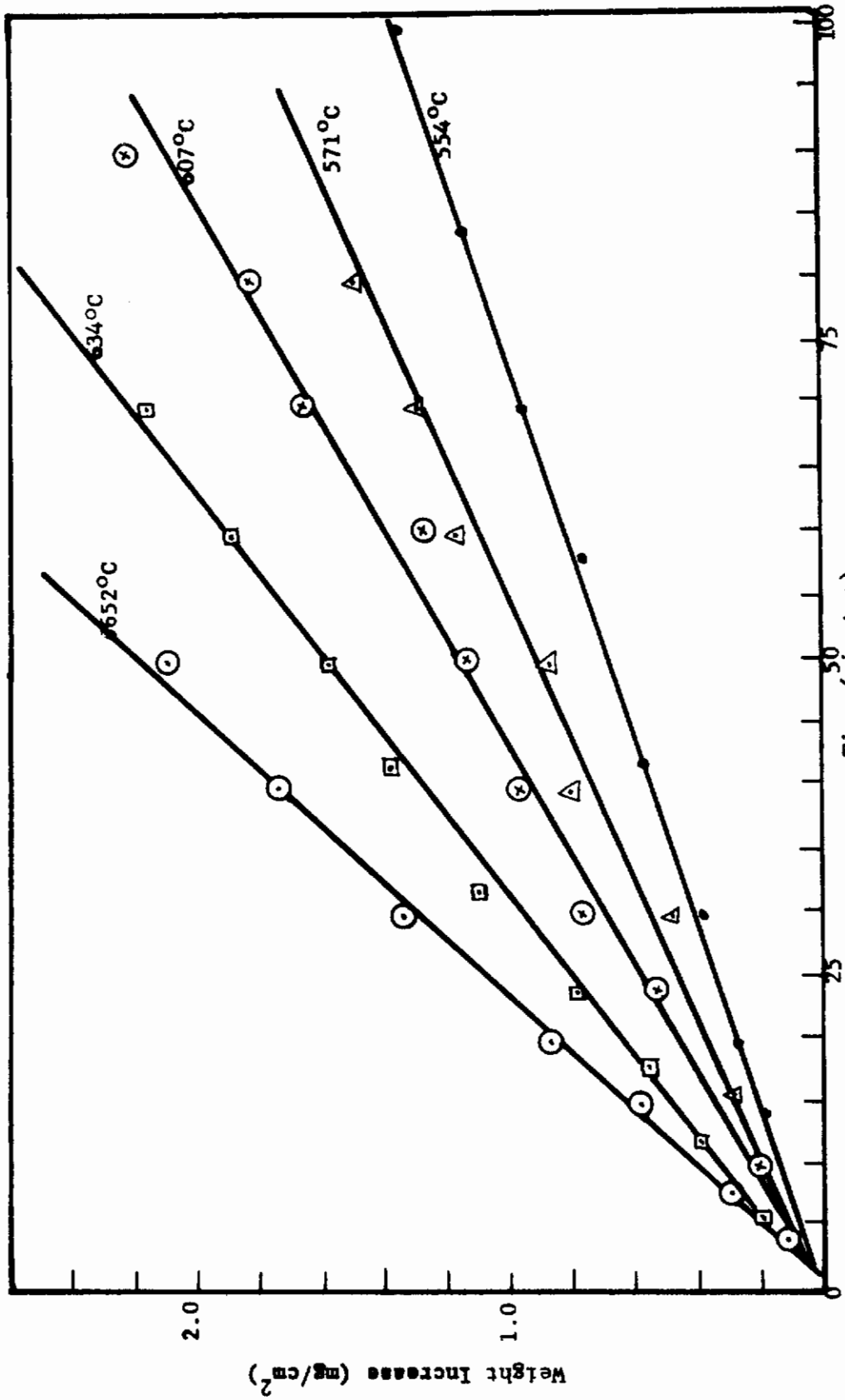

Figure B-7. - Linear plot for the oxidation of ZrC at various temperatures.
(oxygen pressure, 1 atm; oxygen flow rate 100 ml/min)

Approved for Public Release

Contrails

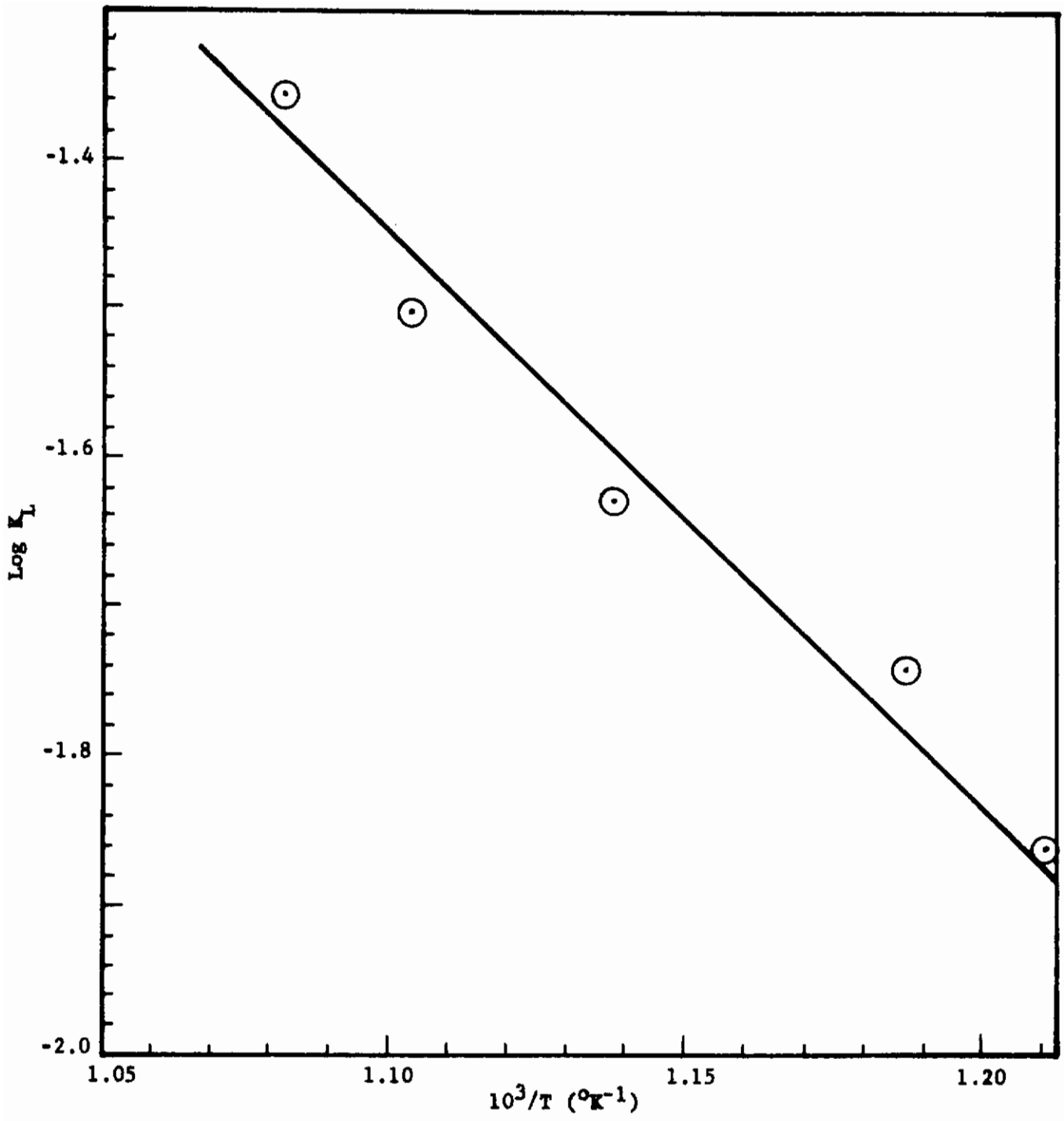

Figure B-8. - Arrhenius plot for the oxidation of ZrC (oxygen pressure, 1 atm)

Approved for Public Release

Contrails

TABLE B-X

THE EFFECT OF TEMPERATURE ON THE OXIDATION OF ZrB_2

O_2 Pressure, 1 atm
Flow Rate, 100 ml/min

Temperature (^oC)	Parabolic Rate Constant $((mg/cm^2)^2/min)$
945	0.1019
962	0.1190
975	0.1435
998	0.1653
1056	0.2459
1056	0.2368
1166	0.3889
1256	0.5625

$\Delta E_a = 19.8 \pm 1.0$ kcal/mole

TABLE B-XI

THE EFFECT OF TEMPERATURE ON THE OXIDATION OF ZrC

O_2 Pressure, 1 atm

Temperature (^oC)	Linear Rate Constant, k_1 $(mg/cm^2/min)$
554	0.01371
571	0.01818
607	0.02320
634	0.03153
652	0.04444

$\Delta E_a = 16.7 \pm 1.7$ kcal/mole

Approved for Public Release

Contrails

E. CONCLUSIONS

1. The oxidation of zirconium diboride between the temperatures 945 and 1256C follows a parabolic rate law over the first hour of oxidation.

2. The flow rate of oxygen in the system has practically no effect on the rate of oxidation from 20-100 ml/min at 1056C.

3. The parabolic rate of oxidation of ZrB_2 increases directly with the partial pressure of O_2 (mixed with helium).

4. The Arrhenius plot is linear for the oxidation of ZrB_2 between 945 and 1256C and gives an activation energy of 19.8 kcal/mole.

5. The oxidation products from ZrB_2 seem to be the oxides of Zr and boron, with the boron oxide present as a molten layer on the surface of the ZrB_2. Part of the boron oxide slowly vaporizes at high temperatures as indicated by a white deposit on the cooler parts of the combustion tube after several runs.

6. The oxidation of zirconium carbide follows a linear rate law at 554-652C, and at higher temperatures a destructive oxidation of the material takes place in pure O_2. The activation energy for the oxidation of ZrC based on data at 554-652C is 16.7 kcal/mole.

Approved for Public Release

Contrails

4. Kinetics of the Reaction of Elemental Fluorine with Zirconium Carbide and Zirconium Diboride at High Temperatures

A. K. Kuriakose and J. L. Margrave

A. INTRODUCTION

Although there have been extensive studies of oxidation and nitridation rates for metals and compounds, there have been very few studies of reaction rates with fluorine. The kinetics of the reactions between fluorine and ZrC and ZrB_2 is complicated because of the variety of possible solid reaction products--a mixture of zirconium fluorides with the tetrafluoride being the most stable. The other products (carbon tetrafluoride or boron trifluoride) are both gases at normal temperatures and one predicts that these should leave a rather porous layer of ZrF_4 as the reaction takes place at the carbide-fluoride or the boride-fluoride interface. Thus, the reaction would obey a linear rate law and not be diffusion controlled. On the other hand, because of the large volume ratio of fluoride to carbide or fluoride to boride of zirconium, one might expect some degree of protection if the fluoride layer is adhesive. The actual state of affairs is complicated by the fact that ZrF_4 sublimes readily at moderately high temperatures and decomposes at higher temperatures. Volatilization and decomposition data for ZrF_4 are therefore required for a complete explanation of the fluorination kinetics of zirconium and its compounds.

B. EXPERIMENTAL

A detailed description of the apparatus used has been given previously.[15] Slight modifications were effected for sending a slow stream of dry nitrogen from the top of the helical spring chamber in order to exclude any fluorine from the spring-compartment. Proper changes were also made in the furnace windings for attaining high temperatures rapidly and in the flow meter systems for obtaining low fluorine partial pressures.

In order to check the variability of the apparatus for fluorination studies in general, observations were first made on the reaction between electrolytic copper foil and fluorine as a standard, since this is the only system for which the kinetics of reaction with fluorine have been worked out in any detail.[16, 17]

---

(15) T. C. M. Pillay and J. L. Margrave, Technical Documentary Report No. ASD-TDR-62-204 Part I, April 1962, pp. 77-79.

(16) P. M. O'Donnell and A. E. Spakowski, NASA Technical Note D-768, April 1961.

(17) P. E. Brown, J. M. Crabtree and J. F Duncan, J Inorg. and Nuclear Chem. 1, 202 (1955).

Approved for Public Release

Contrails

Before commencing the reaction, the nickel furnace tube was passivated by reacting it with fluorine at 500C. Nickel is known to form a protective coating of nickel fluoride at high temperature in fluorine.[18] The process was carried out during a period of three days, intermittently admitting fluorine for two or three hours each time. Also, before starting any run, a mixture of fluorine and helium was passed through the already passivated furnace tube, heated at the desired temperature for nearly half an hour to one hour as required, until fluorine was detected coming out of the exit from the combustion tube in large amounts, as indicated by use of KI paper. After passivation at the required temperature, the system was evacuated and flushed with helium several times and the sample to be fluorinated was suspended from the helical spring by means of a 0.007" nickel wire, in the atmosphere of flowing helium gas. After about 10 minutes, fluorine was also admitted, along with the helium and a timer started simultaneously. The partial pressure of fluorine was calculated from the individual flow rates of fluorine and helium at atmospheric pressure. Any reaction of the fluorine with the nickel suspension wire was neglected on the grounds that the surface area of the nickel wire exposed to the hot zone of the furnace was negligibly small compared to the relatively large area of the specimen. The change in extension of the spring was observed by means of a cathetometer and the smallest measurable weight change was 0.05 mg. Readings were taken at suitable intervals of time. The silica spring was protected from attack by fluorine by having a blanket of dry nitrogen in the form of a slow, steady stream sent from the top of the system. At the conclusion of the run, the fluorine was cut off and helium and nitrogen continued to flow until the exit gas was free from fluorine.

The copper foil was cleaned with dilute HNO_3 and washed with water and subsequently with acetone and benzene and dried. The ZrC and ZrB_2 samples in the form of small pellets weighing about 0.2 to 0.4 gm were polished by grinding with abrasive powder. The ZrB_2 had a shining mirror-like appearance while the ZrC had a dark gray color. Surface areas of the specimens were determined to the nearest 0.01 cm^2.

C. RESULTS AND DISCUSSION

Reaction between fluorine and copper: The fluorination study on copper was carried out at 500C under various fluorine partial pressures ranging from 23-740 mm of Hg. Parabolic plots of the results indicated an initial fast reaction during the first five minutes followed by a slower reaction for a period of approximately an hour and a half until the runs were stopped. In a diffusion-controlled surface reaction, deviations from a parabolic law may be expected in the early stages of the reaction, when the thickness of the product layer is small, since other factors are operative. Parabolic rate constants for the reactions, shown in Table B-XII, were, therefore, computed taking into consideration only the values after the initial fast reactions. It is clear from Table B-XII that the partial pressure of fluorine does not influence the rate of fluorination of copper to any great extent; the rate of increase of the rate constant is roughly proportional to the fourth root of fluorine partial pressure between 23 and 167 mm and thereafter being almost independent of the same up to 1 atm. The reaction product in all the cases is an

(18) M. J. Steindler and R. C. Vogel, ANL-5662, Argonne Nat. Lab., January 1957.

Approved for Public Release

Contrails

TABLE B-XII

PARABOLIC RATE CONSTANTS FOR FLUORINATION OF COPPER UNDER VARIOUS FLUORINE PARTIAL PRESSURES AT 500C

F_2 Partial Pressure (mm of Hg)	Parabolic Rate Constant, k_p $((mg/cm^2)^2/min \times 10^3)$
23.3	8.00
45.3	9.27
144.0	12.00
167.0	12.57
740.0	13.07

Approved for Public Release

Contrails

adherent layer of red cuprous fluoride beginning to darken on the outside possibly due to the formation of small amounts of cupric fluoride.

It may be mentioned that Brown et al[17] observed no change in the rate of fluorination of copper with changes in the fluorine partial pressures over the range 6-60 mm of Hg and at temperatures below 250C whereas the present investigation shows a slight enhancement of the reaction rate with increase of fluorine partial pressure. In general, the role of the partial pressure of the reacting gas in diffusion-controlled gas-solid reactions is not clearly understood in the sense that the pressure dependence of rates of reaction changes from one system to another.

Fluorination of ZrC and ZrB_2: Zirconium carbide is known to be readily decomposed by halogens and oxidizing agents,[19] in general, and hence a rather vigorous reaction is to be expected with fluorine. A preliminary examination showed that ZrC would burn in fluorine or in an atmosphere rich in fluorine, at about 250-300C. On the other hand, ZrB_2 did not catch fire in pure fluorine at a pressure of 1 atm, but broke into several bits at about the same temperature. The fluorination of these materials was examined at low fluorine partial pressures where the reactions could be effectively controlled.

Reaction between ZrC and Fluorine: Initial experiments with ZrC and F_2 under low partial pressure of F_2 (31 mm of Hg) indicated that the reaction was rather smooth at about 300C with a regular increase in weight. The reproducibility of the results was checked at 300C and found to be within 15-20%. With the same fluorine partial pressure, the reaction was conducted at various temperatures ranging from 278 to 410C. Above 410 the reaction became too fast to be measured. The weight increase per unit area of ZrC with time at the various temperatures is illustrated in Figure B-9. There is no question regarding the linearity of the reaction with time. Abrupt breaks at and above 334C indicate the crumbling of part of the fluoride layer formed on the ZrC. Thick scales of ash-gray zirconium tetrafluoride were observed on the surface of the ZrC after reaction. The adhesion of the scales was very poor and the material was soft and fluffy. The reacted samples had a sandwich appearance and their volumes had increased markedly because of the fluffiness of the ZrF_4 formed. The scales were apparently uniform and there were no visible cracks on them except at the edges, where the inner core was practically naked. Viewed under a microscope, the layers were made up of fine sugar-like crystals uniformly formed without any cracks. It is possible that the unreacted ZrC was in direct contact with the fluorine atmosphere outside the fluoride coating through the corners and thus could show a linear rate of reaction. It is intended to study the fluorination of ZrC in the form of a sphere or a piece with rounded edges in order to check this possibility.

---

(19) P. Schwarzkopf and R. Kieffer in Refractory Hard Metals, MacMillan Publishing Co., New York, 1953, p. 95.

Approved for Public Release

Contrails

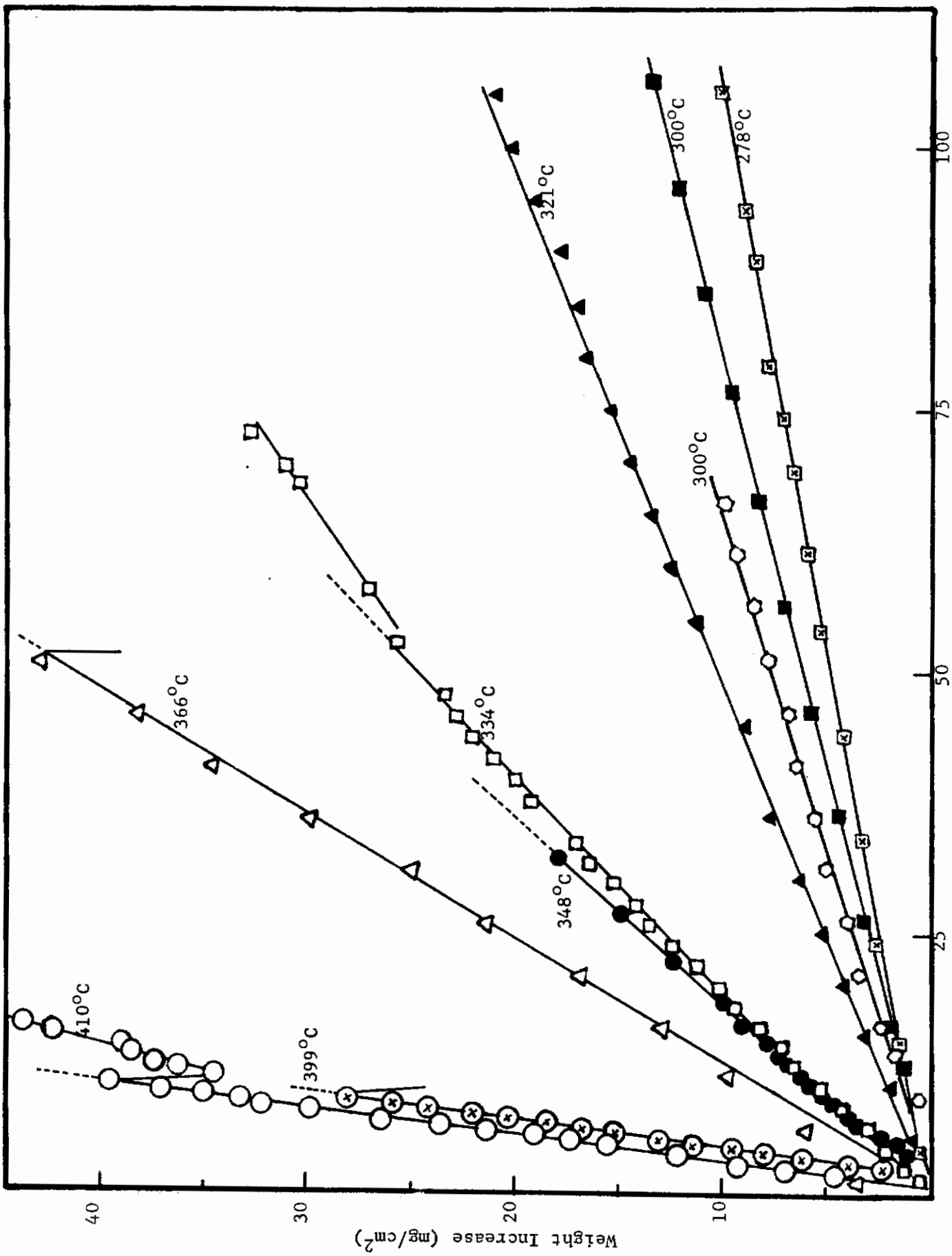

Figure B-9. - Linear plot for the ZrC-F_2 reaction.
(fluorine partial pressure, 31 mm)

Approved for Public Release

Contrails

It is not possible to say whether zirconium or carbon in the system is preferentially attacked by fluorine, since the gaseous products were not analyzed. X-ray analysis of the inner core and the outer layer might show some evidence regarding this question. The fact that the inner core is rough when once the fluoride scales are removed indicates that possibly one of the elements is reacted faster than the other.

From the slopes of the straight lines in Figure B-9, the linear rate constants for the reactions were estimated, not taking into account the volatile products. The activation energy computed by a least squares method is 22.1±1.6 kcal/mole.

Further work is in progress with regard to the effect of variation of the fluorine partial pressure on the reaction and the possibility of studying the reaction at higher temperatures with very low fluorine partial pressures.

Fluorination of ZrB_2: For the conditions in which the fluorination kinetics of ZrC were investigated, ZrB_2 does not react with fluorine to any measurable extent. At 500C, however, a gain in weight is observed as ZrB_2 reacts with F_2 at a partial pressure of 3-4 mm of Hg. At about 600C, it begins to lose weight in presence of F_2. Specimens removed after fluorination above 600C have practically no coating of fluoride on the outside and the ZrB_2 had lost its lustre. This indicates that the fluorides formed were all volatilized, especially when the system was continuously flushed with about 600 ml of gas every minute. However, the loss in weight could be measured reproducibly for calculating the rate of the reactions. The reaction was studied at 600, 700, 800, and 900C and in all the cases the ZrB_2 was losing weight. An interesting point observed was that, out of these four temperatures, the corrosion rate was a maximum at 800C. At 900, the rate of the reaction was nearly equal to that at 700C. This abnormal behavior apparently shows that above 800C the ZrB_2-F_2 reaction has a negative temperature coefficient, which means that the reaction rate could be still slower at higher temperatures. This phenomenon might be explained as being due to the onset of the decomposition of ZrF_4 above 800 into its elements. However, these few experiments are not decisive and further work is needed before making any conclusions. The detailed values are, therefore, not reported herein.

It should also be mentioned that the ZrB_2-F_2 reaction obeys a linear rate law, except for a slight apparent decrease in the rate of reaction with time, due to the decrease in the surface area of the ZrB_2 with increasing extent of corrosion.

Approved for Public Release

Contrails

Appendix C

ZIRCONIUM CARBIDE: THE HEAT CAPACITY AND THERMODYNAMIC PROPERTIES FROM 5 TO 350°K.*

Edgar F. Westrum, Jr.
University of Michigan, Ann Arbor, Michigan

and

George Feick
Arthur D. Little, Inc., Cambridge, Massachusetts

A. INTRODUCTION

Previous studies providing values for thermodynamic properties of zirconium carbide (ZrC) have been performed by Mah and Boyle[1], by Krikorian[2], by Prescott[3], by Kutsev, Ormont, and Epel'baum[4], by Fujishiro and Gokcen[5], by Pollock[6], and by Margrave[7]. The enthalpy of combustion of zirconium carbide

* - Manuscript prepared for publication which includes subcontracted studies at University of Michigan under Air Force Contract AF 33(616)-7472.

(1) A. D. Mah, B. J. Boyle, J. Am. Chem. Soc., 77, 6512 (1955).

(2) O. H. Krikorian, "High Temperature Studies; 11. Thermodynamic Properties of the Carbides," University of California Radiation Laboratory Report 2888, 1955.

(3) C. H. Prescott, Jr., J. Am. Chem. Soc. 48, 2534 (1926).

(4) V. S. Kutsev, B. F. Ormont, V. A. Epel'baum, Doklady Akad. Nauk SSSR, 104, 567 (1955).

(5) S. Fujishiro, N. A. Gokcen, "Thermodynamic Properties of Zirconium Carbide at High Temperature," presented at the International Symposium on the Physical Chemistry of Process Metallurgy, April 27 - May 1, 1959.

(6) B. D. Pollock, J. Phys. Chem., 65, 731 (1961).

(7) J. L. Margrave reported in "Thermodynamic and Kinetic Studies for a Refractory Materials Program," Report No. C-63081 to Wright Air Development Division, by L. A. McClaine, July 1961, pp. 21-24.

Approved for Public Release

Contrails

was measured by Mah and Boyle who derived the value -44.1 ± 1.5 kcal. for the enthalpy of formation at 298.15°K. Krikorian reviewed the available data for the carbides and estimated the heat capacity and the entropy by assuming that the difference between the heat capacities of zirconium carbide and zirconium nitride was equal to that between titanium carbide and titanium nitride. Using the entropies of these compounds recommended by Kelley (cf. Kelley and King (8)) the entropy of zirconium carbide was estimated as 7.8 ± 0.5 cal. (g.f.m. °K.)$^{-1}$, and the heat capacity estimate was made by using the data of Coughlin and King (9) on zirconium nitride and the data of Naylor (10) on titanium carbide and titanium nitride. Kelley and King (8) recently estimated the entropy at 298.15°K. as 9.3 ± 0.3 cal. (g.f.m. °K.)$^{-1}$. Experimental enthalpy increments over the range 298 to 1174°K. have been reported by Margrave (7). The other investigations cited involve studies on the vaporization and equilibrium properties of systems involving zirconium carbide at high temperatures. The present investigations were made to provide a definitive value for the entropy and low temperature chemical thermodynamic properties.

B. EXPERIMENTAL

1. Cryostat and Calorimeter

Measurements were made in the Mark II adiabatic vacuum cryostat, which is similar to one previously described (11) but modified and improved to provide an instrument of greater efficiency, mechanical rigidity, and operating convenience. The metal cryostat is provided with a heat exchanger which utilizes the enthalpy of the effluent helium gas to provide a thermal dam for the conduction of heat by the bundle of electrical leads and thus minimize vaporization of the liquid helium from the lowest temperature reservoir. The calorimeter itself is surrounded by a cylindrical adiabatic shield, the three portions of which are individually controlled by separate channels of automatic regulation which provide a.c. power to the several separate heaters. Copper-Constantan thermocouples monitor the temperature difference between calorimeter and shield and between shield and the ring used to temper the gradient in the bundle of leads. Three separate channels of recording electronic circuitry provided with proportional, rate, and reset control actions are used in preference to manual shield control above 50°K. and provide control of temperature to within approximately a millidegree over the temperature range to 350°K., thereby reducing the energy exchange between the calorimeter and the surroundings so that it is negligible in comparison with other

(8) K. K. Kelley, E. G. King, "Contributions to the Data on Theoretical Metallurgy, XIV. Entropies of the Elements and Inorganic Compounds," Bureau of Mines Bulletin 592, 1961.

(9) J. P. Coughlin, E. G. King, J. Am. Chem. Soc. 72, 2262 (1950).

(10) B. F. Naylor, J. Am. Chem. Soc. 68, 370 (1946).

(11) E. F. Westrum, Jr., J. B. Hatcher, D. W. Osborne, J. Chem. Phys. 21, 419 (1953).

Approved for Public Release

Contrails

sources of error. The adiabatic method of operation has been described elsewhere (11).

The copper calorimeter of laboratory designation W-31, a gold-plated vessel with a capacity of 50 cc., has an offset thermometer well which projects through the bottom of the calorimeter for approximately a centimeter, but no thermal conduction vanes. The heat capacity of the empty calorimeter was determined in a separate series of measurements in which identical amounts of indium-tin solder for sealing the calorimeter and Apiezon-T grease for thermal contact with the heater-thermometer-calorimeter assembly were used. At the lowest temperatures the heat capacity of the sample represented 30% of the total. This increased to 50% at 55°K., to 70% at 170°K., and to 76% by 350°K. and hence was a favorable fraction of the total over most of the range. The mass of the calorimetric sample was 125.948 g. (in vacuo). Buoyancy corrections were made by using a density of 6.73 g. $cm.^{-3}$ for zirconium carbide. A pressure of 13.6 cm. of helium at 300°K. was used to facilitate thermal conduction in the sample space.

Temperatures were determined with a capsule-type, strain-free, platinum-resistance thermometer (laboratory designation A-5) contained within an entrant well in the calorimeter. Temperatures are considered to accord with the thermodynamic temperature scale to within 0.03° from 10 to 90°K. and within 0.04° from 90 to 350°K. The temperature increments may be determined with more precision and are probably correct to a few tenths of a millidegree after correction for quasi-adiabatic drift. All measurements of mass, resistance, potential, temperature, and time are referred to calibrations made by the National Bureau of Standards.

2. Preparation and Characterization of the Sample

The zirconium carbide was obtained from the Carborundum Company in powder form having the following analysis: 88.16% Zr; 11.45% C; 0.05% O; 0.15% N; 0.12% Fe. In order to reduce the surface area and impurity level of this material it was sintered into bars about 1 cm. dia. by 18 cm. long and melted in an argon atmosphere containing 5% of hydrogen using the vertical floating-zone method with induction heating. Details of the apparatus and method have been presented elsewhere (12).

About 1% of free carbon in the form of high-purity graphite was added to the powder before sintering in order to correct the carbon deficiency and to make up for expected losses in melting.

The zone-refined product was obtained in the form of dense, macrocrystalline rods about 6 to 8 mm. dia. A slight surface film was removed by etching with hot,

---

(12) G. Feick reported in Technical Documentary Report No. ASD-TDR-62-204, Part I, Aeronautical Systems Division, Wright-Patterson Air Force Base, Ohio, April, 1962.

Approved for Public Release

Contrails

conc. aq. HF. The average carbon content of four separate rods was 11.22 ± 0.07% by weight corresponding to a deficiency of 3.5% from the stoichiometric value of 11.63%. This deficiency could probably have been prevented by the addition of more carbon to the sintered rods before melting. Analysis of a single sample for zirconium gave 89.27% (theoretical, 88.37%) which, together with its carbon content of 11.20%, yielded a total of 100.47%. The carbon analysis is considered to be more reliable than that for zirconium. The oxygen content of the zone-refined product was 0.005% and the nitrogen content was 0.067%. Quantitative spectrographic analysis gave: 0.12% Ti; 0.07% each B and Fe; 0.01% each Al and Sn; 0.001 to 0.01% Mg; and 0.001% each Ca, Mn, Cu, Mo, Ag, Si, Hf, and Pb, all by weight. Metallographic examination showed the presence of a very small amount of a second phase, possibly ZrB_2, in some samples but not in others.

The proximate composition of the sample by weight may be represented as follows: 96.5% ZrC; 2.4% excess Zr; 0.5% ZrN; 0.4% ZrB_2 and 0.15% TiC. In interpreting these figures, however, it should be borne in mind that the ZrN, TiC, and excess Zr are probably all in solid solution in the ZrC. The actual structure is probably best represented as a ZrC lattice with 3.5% of the carbon sites vacant and with nitrogen and titanium substituted in some of the C and Zr sites, respectively.

C. RESULTS

The experimental heat capacities are presented in chronological order at the mean temperatures of the determinations in Table C-I. These data are based upon a defined thermochemical calorie equal to 4.1840 abs. j., an ice point of 273.15°K., and a gram formula mass (g.f.m.) of 103.231 for zirconium carbide. These data have been corrected for curvature, i.e., for the difference between the $\Delta H/\Delta T$ and the corresponding derivative. The approximate values of ΔT used in the heat capacity determinations can usually be inferred from the increments between adjacent mean temperatures shown in Table C-I. Precision reflected by probable errors decreasing from about 5% at 5°K. to 1% at 10°K., and to less than 0.1% above 50°K. is considered to characterize these data.

The heat capacities and thermodynamic functions at selected temperatures, as presented in Table C-II, are obtained from the heat capacity data by a least-squares-fitted curve through the experimental points (carefully compared with a large-scale plot of the data) or by the integration thereof. Both the fitting and quadrature are performed by high-speed digital computers using programs previously described (13). The thermodynamic functions are considered to have a

(13) B. H. Justice, "Calculation of Heat Capacities and Derived Thermodynamic Functions from Thermal Data with an IBM 704 Digital Computer," U.S. Atomic Energy Commission Report TID-6206, June, 1960; revised and modified in the Appendix to "Thermodynamic Properties and Electronic Energy Levels of Eight Rare Earth Sesquioxides," Ph.D. Dissertation, University of Michigan, 1961.

Approved for Public Release

Contrails

Table C-I. Heat Capacity of Zirconium Carbide

ZrC: g.f.m. = 103.23 Units: cal. (g.f.m. $^{o}K.)^{-1}$

T, $^{o}K.$	C_p	T, $^{o}K.$	C_p	T, $^{o}K.$	C_p
Series I		258.94	8.330	14.83	0.0118
		267.76	8.502	16.52	0.0159
71.02	1.659	276.48	8.678	18.44	0.0219
77.48	1.978	292.81	8.973	20.59	0.0311
84.53	2.333	301.41	9.105	22.95	0.0447
92.01	2.688	336.31	9.604	25.57	0.0654
99.71	3.039	345.16	9.721	28.44	0.0955
107.56	3.392			31.45	0.1383
115.66	3.748	Series II		34.62	0.1975
123.93	4.107			37.91	0.2747
132.58	4.475	313.69	9.297	41.60	0.3783
141.47	4.831	322.55	9.427	45.97	0.5227
150.35	5.182	331.36	9.556	50.94	0.7166
159.30	5.514			56.46	0.9557
168.31	5.839	Series III		62.43	1.2391
177.30	6.146			68.86	1.549
186.29	6.442	5.59	0.0011	75.78	1.890
195.30	6.721	6.75	0.0016	201.94	6.914
222.32	7.476	7.85	0.0024	205.90	7.033
231.69	7.712	9.11	0.0034	209.81	7.136
240.94	7.937	10.43	0.0048	213.67	7.240
250.03	8.138	11.81	0.0064	217.49	7.346
		13.30	0.0087		

Approved for Public Release

Contrails

precision corresponding to a probable error of less than 0.1% above 100°K. Additional digits beyond those significant are given in Table C-II for internal consistency and to permit interpolation and differentiation. The entropies and Gibbs energies have not been adjusted for nuclear spin and isotope mixing contributions and hence are practical values for use in chemical thermodynamic calculations.

D. DISCUSSION

Assuming the sample to have the proximate composition indicated with impurities of partial molal heat capacities equal to those for the bulk phases tabulated by Kelley and King (8), the heat capacity of pure zirconium carbide corrected for the impurities would have values of 0.62 cal. (g.f.m. °K.)$^{-1}$ at 50°K., 3.01 at 100°K., 5.15 at 150°K., 6.89 at 200°K., and 9.13 at 298.15°K. Corresponding adjustment of the thermodynamic functions at 298.15°K. yields estimates of 7.90 cal. (g.f.m. °K.)$^{-1}$ for the entropy, -3.20 cal. (g.f.m. °K.)$^{-1}$ for the Gibbs energy function, and 1400 cal. (g.f.m.)$^{-1}$ for the enthalpy increment of pure zirconium carbide.

E. ACKNOWLEDGMENT

The authors acknowledge with thanks the experimental assistance of Ray Radebaugh in the cryogenic measurements and of Wilson Menashi and Gerald Clay in the sample preparation. The authors also express their appreciation to the United States Air Force Aeronautical Systems Division under Contract AF 33(616)-7472 for partial support and permission to publish these data.

Approved for Public Release

Contrails

Table C-II. Thermodynamic Properties of Zirconium Carbide

ZrC: g.f.m. = 103.23 Units: cal., g.f.m., °K.

T, °K	C_p	S°	$H^\circ - H^\circ_0$	$-\frac{(G^\circ - H^\circ_0)}{T}$
5	0.0008	0.0003	0.001	0.0001
10	0.0043	0.0017	0.012	0.0005
15	0.0121	0.0047	0.041	0.0013
20	0.0282	0.0101	0.147	0.0028
25	0.0600	0.0194	0.359	0.0051
30	0.1167	0.0349	0.788	0.0087
35	0.2057	0.0592	1.579	0.0140
40	0.3307	0.0944	2.905	0.0218
45	0.4899	0.1422	4.944	0.0324
50	0.6777	0.2033	7.852	0.0463
60	1.1229	0.3652	16.80	0.0852
70	1.609	0.5746	30.44	0.1397
80	2.102	0.8217	49.00	0.2091
90	2.586	1.0974	72.46	0.2923
100	3.055	1.3943	100.68	0.3875
110	3.507	1.7067	133.50	0.4931
120	3.943	2.0307	170.8	0.6077
130	4.365	2.3631	212.3	0.7299
140	4.771	2.7015	258.0	0.8586
150	5.163	3.0441	307.7	0.9929
160	5.539	3.3894	361.2	1.1318
170	5.897	3.7361	418.4	1.2748
180	6.237	4.0828	479.1	1.4212
190	6.558	4.429	543.1	1.570
200	6.861	4.773	610.2	1.722
210	7.147	5.115	680.3	1.875
220	7.415	5.453	753.1	2.030
230	7.669	5.789	828.5	2.186
240	7.908	6.120	906.4	2.344
250	8.135	6.448	986.6	2.501

Approved for Public Release

Contrails

260	8.350	6.771	1069.7	2.659
270	8.552	7.090	1153.6	2.817
280	8.743	7.404	1240.1	2.976
290	8.922	7.714	1328.4	3.134
300	9.088	8.020	1418.5	3.291
310	9.244	8.320	1510.1	3.449
320	9.390	8.616	1603.3	3.606
330	9.528	8.907	1697.9	3.762
340	9.658	9.194	1793.8	3.918
350	9.778	9.475	1891.0	4.072
273.15	8.614	7.189	1181	2.867
298.15	9.058	7.964	1401	3.262

Approved for Public Release

Contrails

Appendix D

SPECTROSCOPY OF HIGH TEMPERATURE SPECIES BY MATRIX ISOLATION*

Otto Schnepp
Technion Research and Development Foundation
Haifa, Israel

A. EXPERIMENTAL

During this report period the spectral studies in the infrared have been extended to the cesium bromide region, i.e., out to 35 microns. The cryostat used in the earlier studies was fitted with a cesium bromide deposition window which replaced the sodium chloride window used in the earlier part of this investigation. All other windows in the optical path were likewise replaced by cesium bromide. The Perkin-Elmer 21 Infrared Spectrophotometer was fitted with a cesium bromide prism unit. The infrared spectra of vaporization products of lithium fluoride and lithium chloride trapped in solid argon, krypton, xenon and nitrogen matrices were studied. The deposition window was cooled to liquid helium or liquid hydrogen temperature. For these experiments resistance heated tantalum and stainless steel effusion cells were used. Temperatures up to about 1000°C could be obtained with this equipment.

One experiment for lithium fluoride was carried out with a high resolution prism-grating spectrometer (Perkin-Elmer, model 112-G).

An electron bombardment furnace fitted with a graphite crucible has been tested. This furnace attained a temperature of 1800°C and further modifications are being completed in order to reach temperatures above 2000°C. These modifications involve mainly the addition of further radiation shields. The furnace is suitable for use with the cryostat employed for the matrix isolation studies and is exchangeable with the resistance heated furnace in use at present.

B. RESULTS

The experimental results for lithium fluoride are summarized in Table D-I, together with the tentative assignments. The experiments were first carried out using liquid helium as coolant and great care was taken that the temperature of the deposition window was below 10°K. For this purpose a copper-constantan ther-

* - Report on subcontracted study under Air Force Contract AF 33(616)-7472.

Approved for Public Release

Contrails

mocouple soldered with Woods metal into a hole drilled through the salt window was used, the emf of this thermocouple being compared to that of a similar thermocouple immersed in liquid helium. Subsequently, experiments were carried out using liquid hydrogen as coolant and identical results were obtained.

Table D-II summarizes the results obtained for lithium chloride, again with tentative assignments indicated. The measurements were made at liquid hydrogen temperature.

The absorption of lithium fluoride in solid argon at 843-838cm^{-1} was examined with a high dispersion spectrometer. This absorption was assigned to the lithium fluoride monomer and consists of a doublet, when observed with a conventional prism spectrometer. No further structure was observed with the high dispersion instrument. The spectral slit width was 1cm^{-1}.

C. DISCUSSION

The monomer frequencies of LiF and LiCl have been reported at 900cm^{-1} and 641cm^{-1} respectively[1,2] for the gas phase. For both these molecules the shift of the absorption from gas to argon matrix is about 60cm^{-1} to lower energies, and the shifts for the other matrices are larger. Theoretical treatment of these shifts is needed.

The alkali halide dimers are expected to have three infrared active vibrational fundamentals[3]. The results for LiCl leave little doubt that two of these have been observed here although the assignment is still subject to confirmation on the basis of isotopic substitution. The interpretation of the spectra of the LiF vaporization species has recently been discussed by Linevsky[4] who has applied isotopic substitution techniques to this case. He interpreted the bands at 621 and 538cm^{-1} as dimer bands. The interpretation of the band at 720cm^{-1} in solid argon must be considered as of uncertain origin at present.

Dimer bands of lithium fluoride in the vapor phase have been reported[5] at 640cm^{-1} and 460cm^{-1} and of lithium chloride at 460cm^{-1} and 335cm^{-1}. The vapor to matrix shifts for the dimers may be expected to be smaller than for the mon-

---

(1) G. Vidale, J. Phys. Chem., 64,314 (1960).

(2) W. Klemperer, W. G. Norris and A. Buechler, J. Chem. Phys., 33, 1534 (1960).

(3) J. Berkowitz, J. Chem. Phys., 32, 1519 (1960).

(4) M. J. Linevsky, Unpublished.

(5) W. Klemperer and W. G. Norris, J. Chem. Phys., 34, 1071 (1961).

Approved for Public Release

Contrails

omer in view of the fact that the dimers are not believed to have a dipole moment. This prediction is born out by the lithium chloride bands but only by one of the lithium fluoride bands, whereas the other is apparently shifted by 80cm^{-1} and to higher energy. Such a shift is highly unlikely and it is probable that the gas phase measurement is inaccurate owing to the great line widths encountered in these experiments.

The occurrence of closely spaced doublets or triplets both in the LiF and LiCl spectra is assumed to be due to different trapping sites in the matrix.

It is concluded from the studies completed to date that the matrix isolation method is highly promising for the study of the infrared spectra of high temperature molecular species. It has proved already most useful for the investigation of the alkali halide dimers and will, no doubt, contribute greatly to this field in the future. However, several further studies are required before it may be said with certainty that the vaporization species can be trapped quantitatively. Such studies must include double oven experiments such as have been recently employed in mass spectrometric studies.[6]

D. ACKNOWLEDGMENT

The work reported here was carried out by Mrs. S. Schlick.

---

(6) J. Berkowitz, H. A. Tasman and W. A. Chupka, J. Chem. Phys., 36, 2170 (1962).

Approved for Public Release

Contrails

TABLE D-I

The infrared absorption bands of LiF vaporization species. (Frequencies in cm^{-1}. The most prominent band in each group is underlined.)

Matrix Material				Molecular Species
Argon	Krypton	Xenon	Nitrogen	
841 836	831	821	776	Monomer
720	717	715	696	Uncertain
621	618	612	599 608	Dimer
547 538	542	544 534	548	Dimer

TABLE D-II

The infrared absorption bands of LiCl vaporization species. (Frequencies in cm^{-1}. The most prominent band in each group is underlined.)

Matrix Material			Molecular Species
Argon	Krypton	Xenon	
580 569	568 556	573 558 545	Monomer
488 480	481 472	482 472 465	Dimer
352	344	348 338	Dimer

Approved for Public Release

Contrails

Appendix E

INVESTIGATION OF STRUCTURES OF METAL HALIDE AND METAL OXIDE SYSTEMS BY ELECTRON DIFFRACTION AND SPECTROSCOPIC TECHNIQUES*

Four postdoctorates and one predoctoral student comprised the group working this past year on electron diffraction and associated structural problems. These were sponsored by various organizations, one postdoctorate being sponsored by this Air Force program. Members of the group were Dr. Katsumi Kimura, Dr. Kinya Katada, Dr. Kjell Hjortaas, Dr. Michio Kawano, and Mr. Robert Bohn.

A. EQUIPMENT

During the year shop work continued on the construction of the new electron diffraction apparatus which has been specifically designed for operation with low density samples. The apparatus is being constructed with considerable care, so that one can not only obtain useful patterns from low density samples but also quantitative electron diffraction data of high precision. The cost of this apparatus has been covered mainly by two NSF grants. At the present time the apparatus is ready for an over-all vacuum test; all portions have been individually leak tested. The new high voltage power supply and the precision voltmeter have been checked out and are in use with the old electron diffraction unit. There are still some troublesome parts in the camera which require reworking. The major incompleted items are the sector, rotor, and vacuum drive. The apparatus will soon be installed in a remodeled, air-conditioned laboratory.

In addition to the above, an all-metal, high-speed vacuum system for the preparation of pure samples of MX_4 salts was constructed. A variety of MX_4 salts were obtained from the suppliers. However, it was determined that none of these was really pure, and much time was devoted to purifying the salts by successive sublimations to obtain reliable samples.

About two months operating time was lost last spring because the laboratory in which the old electron diffraction apparatus was situated had to be completely renovated. The old unit was moved to a temporary location. By midyear it was set up and in operation and test electron diffraction photographs of new materials were being taken.

---

* - Prepared from reports submitted by Professor S. H. Bauer and Professor R. F. Porter, Cornell University, Ithaca, New York. A subcontracted study under Contract AF 33(616)7472.

Approved for Public Release

Contrails

The Department of Chemistry has purchased for this project a special model 23-100 Jarrell Ash recording microdensitometer. This unit is being further modified to permit the rotation of the electron diffraction photographs about their centers while they are being scanned, in order to reduce the effect of grain in the emulsion and to average over asymmetries in the diffraction pattern.

Finally, much time was spent in the process of designing, constructing and testing a high temperature sample holder and nozzle suitable for the study of MX_4 salt vapors and for operation between 50C and about 450C. The new nozzle is made of Inconel and platinum and has an externally operated valve. It can be loaded in a dry box to prevent reaction of the sample with the atmosphere. This new nozzle and sample holder has been vacuum tested and will be in use during the coming month.

B. COMPUTATIONAL PROGRAM

Dr. Kimura has formulated a computational program for machine reduction of electron diffraction data. A sequence of four stages is being programmed for the Datatron 200. Each of these stages is set up for independent operation, so that various portions could be used advantageously as needed. So far, two of the stages have been completed and are being utilized in our current data reduction work. The other two parts appear to be more difficult and have yet to be fully developed. This is taking longer than anticipated because of the rather limited time that our programmers can devote to this effort. As a peripheral problem, Dr. Katada is testing proper data reduction methods for radial distribution computations of powder diffraction patterns.

C. ELECTRON DIFFRACTION STUDIES

The old electron diffraction apparatus has been utilized in current studies on a variety of compounds. Initial attempts to obtain electron diffraction photographs of hafnium tetrachloride and zirconium tetrabromide, which are of interest to this Air Force sponsored program, were not successful. The difficulties may have been due to two factors. The samples were used as supplied, and it is now recognized that these were far from having the indicated purity. Secondly, the high temperature nozzle which was used in these experiments was of a rudimentary design. In addition, the vapors of these compounds reacted with the O-rings, greases, and metals of the vacuum system under conditions for which it was believed there should be no reaction; this was probably caused by water vapor which entered the system upon opening to the atmosphere.

It became evident from these and other experiences that purity control is essential for the electron diffraction as well as spectroscopic studies. As a result, extensive purification of the metal tetrahalides by repeated sublimations was undertaken.

Approved for Public Release

Contrails

It also became evident from our studies on the halides and other compounds that no single high temperature sample and nozzle system would be adequate for the variety of substances under study. Dr. Katada and Mr. Bohn spent a considerable fraction of their time in devising a high temperature nozzle suitable for working with samples up to about 450C. The limitation appeared to be the lack of a reliable valve which would withstand corrosive effects as well as high temperatures. The new nozzle construction is completed and will be utilized in the study of the metal tetrahalide compounds which have vapor pressures in the range of 1 to 5 mm Hg.

D. SPECTROSCOPIC STUDIES

Dr. Kawano has spent most of his tenure at Cornell attempting to obtain infrared and raman spectra of the alkali metal halide dimers and of several metal tetrahalides. With regard to the latter, solvents were sought with the hope of recording metal halide spectra in solution. He discovered at this stage that while the metal tetrahalide samples as obtained from the supplier showed some solubility in noncomplexing solvents, when fully purified these samples did not dissolve appreciably in such solvents. As a result, he studied the spectra of the purified solids in the form of mulls and KBr pellets. Dr. Kawano has prepared a draft of a report on his spectroscopic studies of zirconium and hafnium tetrahalides. His work proved most revealing with regard to purity of available sample material and led to the development of facilities for preparation of relatively pure metal tetrahalide samples.

Approved for Public Release